INFORMATION TO USERS

This manuscript has been reproduced from the microfilm master. UMI films the text directly from the original or copy submitted. Thus, some thesis and dissertation copies are in typewriter face, while others may be from any type of computer printer.

The quality of this reproduction is dependent upon the quality of the copy submitted. Broken or indistinct print, colored or poor quality illustrations and photographs, print bleedthrough, substandard margins, and improper alignment can adversely affect reproduction.

In the unlikely event that the author did not send UMI a complete manuscript and there are missing pages, these will be noted. Also, if unauthorized copyright material had to be removed, a note will indicate the deletion.

Oversize materials (e.g., maps, drawings, charts) are reproduced by sectioning the original, beginning at the upper left-hand corner and continuing from left to right in equal sections with small overlaps.

Photographs included in the original manuscript have been reproduced xerographically in this copy. Higher quality 6" x 9" black and white photographic prints are available for any photographs or illustrations appearing in this copy for an additional charge. Contact UMI directly to order.

ProQuest Information and Learning
300 North Zeeb Road, Ann Arbor, MI 48106-1346 USA
800-521-0600

Isolation and Characterization of Calmodulin-Binding Centrosome Components Related to *Saccharomyces cerevisiae* Spc110p from the Fission Yeast *Schizosaccharomyces pombe* and Humans

Mark Randall Flory

A dissertation submitted in partial fulfillment of the requirements for the degree of

Doctor of Philosophy

University of Washington

2001

Program Authorized to Offer Degree: Molecular and Cellular Biology Program

UMI Number: 3014069

Bell & Howell Information and Learning Company
300 North Zeeb Road
P.O. Box 1346
Ann Arbor, MI 48106-1346

In presenting this dissertation in partial fulfillment of the requirements for the Doctoral degree at the University of Washington, I agree that the Library shall make its copies freely available for inspection. I further agree that extensive copying of the dissertation is allowable only for scholarly purposes, consistent with "fair use" as prescribed in the U.S. Copyright Law. Requests for copying or reproduction of this dissertation may be referred to Bell and Howell Information and Learning, 300 North Zeeb Road, Ann Arbor, MI 48106-1346, to whom the author has granted "the right to reproduce and sell (a) copies of the manuscript in microform and/or (b) printed copies of the manuscript made from microform."

Signature Mark R. Plug

Date 3/15/2001

University of Washington

Graduate School

This is to certify that I have examined this copy of a doctoral dissertation by

Mark Randall Flory

and have found that it is complete and satisfactory in all respects,
and that any and all revisions required by the final
examining committee have been made.

Chair of Supervisory Committee:

Trisha Davis

Reading Committee:

Trisha Davis

Breck Byers

Joe Howard

Date: 3/15/2001

University of Washington

Abstract

Isolation and Characterization of Calmodulin-Binding Centrosome Components Related to *Saccharomyces cerevisiae* Spc110p from the Fission Yeast *Schizosaccharomyces pombe* and Humans

Mark Randall Flory

Chairperson of the Supervisory Committee:
Associate Professor Trisha N. Davis
Department of Biochemistry

Accurate segregation of chromosomes during eukaryotic cell division depends on the integrity of the mitotic spindle apparatus. Nucleation of mitotic spindle microtubules is a highly regulated process that requires linking the soluble γ-tubulin complex to the centrosome. In the budding yeast *Saccharomyces cerevisiae*, the calmodulin-binding protein Spc110p links the γ-tubulin complex to the spindle pole body (SPB), a centrosome equivalent.

To complement work on Spc110p I examined whether centrosomal calmodulin targets might exist in divergent organisms. The localization of calmodulin to the SPB of the fission yeast *Schizosaccharomyces pombe* and the mitotic defects exhibited by a fission yeast calmodulin mutant suggested that a calmodulin-binding Spc110p homologue is present in fission yeast.

I identified a calmodulin-binding fission yeast Spc110p homologue based on its homology with a related protein in the filamentous fungus *Aspergillus nidulans*. I named this fission yeast protein Pcp1p for pole target

of calmodulin in *S. pombe*. A fusion of Pcp1p to GFP localizes to the SPB throughout the cell cycle. Overexpression of Pcp1p in *S. pombe* cells causes abnormal SPB aggregates, ectopic and broken mitotic spindles, and DNA missegregation. Localization of Pcp1p to the SPB, and to abnormal SPB aggregates in *S. pombe* cells overexpressing Pcp1p, was confirmed by immunoelectron microscopy.

I subsequently used the calmodulin-binding site sequences of these fungal homologues to identify kendrin as the human orthologue of Spc110p. Kendrin is a large centrosomal protein with a predicted central coiled-coil region and a C-terminal calmodulin-binding domain and localizes specifically to centrosomes throughout the cell cycle. In mitotic human breast carcinoma cells containing abundant centrosome-like structures, kendrin is found only at centrosomes associated with microtubules. Kendrin shares striking sequence homology with mouse pericentrin, a centrosome component known to interact with γ-tubulin. Kendrin additionally contains a unique calmodulin-binding C-terminal domain not found in mouse pericentrin.

Analysis of public sequence data indicates that the human and mouse genomic regions encoding kendrin and pericentrin, respectively, share synteny, revealing that kendrin and pericentrin are direct homologues. Together my data demonstrate the conservation from yeast to vertebrates of Spc110p-related molecules that bind calmodulin and localize to the SPB/centrosome.

TABLE OF CONTENTS

Page

List of Figures..... ii

Chapter I: Introduction..... 1

Calmodulin..... 1

The Yeast Spindle Pole Body..... 4

The Vertebrate Centrosome..... 8

Chapter II: Calmodulin Function in *Schizosaccharomyces pombe*..... 12

Introduction..... 12

Results..... 14

Discussion..... 20

Chapter III: The *Schizosaccharomyces pombe* Spc110p Homologue 26

Introduction..... 26

Results..... 28

Discussion..... 36

Materials and Methods..... 41

Chapter IV: A Human Centrosomal Calmodulin-Binding Protein that Shares Homology with Pericentrin..... 58

Introduction..... 58

Results and Discussion..... 60

Chapter V: Relationship Between Human and Mouse Pericentrin..... 68

Introduction..... 68

Results and Discussion..... 69

Chapter VI: Future Directions..... 75

Bibliography..... 80

Appendix A: Calmodulin Localizes to the Spindle Pole Body of *Schizosaccharomyces pombe* and Performs an Essential Function in Chromosome Segregation..... 97

Appendix B: Identification of a Human Centrosomal Calmodulin-Binding Protein that Shares Homology with Pericentrin..... 106

LIST OF FIGURES

Number *Page*

Figure III.1 Analysis of fungal calmodulin-binding domains..... 51

Figure III.2 Fluorescence microscopy of Pcp1p:GFP..... 52

Figure III.3 Immunoelectron microscopy of Pcp1p:GFP..... 53

Figure III.4 Fluorescence microscopy of overexpressed GFP:Pcp1p..... 54

Figure III.5 Immunoelectron microscopy of overexpressed GFP:Pcp1p... 55

Figure III.6 Wild-type fission yeast tubulin morphology..... 56

Figure III.7 Tubulin morphology with overexpressed GFP:Pcp1p..... 57

Figure V.1 Synteny between human and mouse pericentrin 74

ACKNOWLEDGEMENTS

I sincerely thank Trisha N. Davis for all of her support, enthusiasm and guidance, and for her commitment to careful and thorough scientific analysis. I also thank Mike Moser for his friendship and for serving as a mentor to me with creative ideas on technical and strategic approaches to scientific problems. I thank Susan Francis for stimulating conversations about science and music and for making our lab section a pleasant work environment. I thank Linda Breeden, Breck Byers, Joe Howard, Adam Geballe and Sue Biggins for serving on my advisory committee. I am indebted to Trisha, Breck, and Joe for reading my dissertation. Finally, my graduate training was greatly enriched by collaborations with Mike Moser and Ray Monnat at the University of Washington, Jim Joseph and Tony Means at Duke University, and Mary Morphew and Dick McIntosh at the University of Colorado at Boulder. I extend a sincere thanks to our collaborators for sharing their invaluable insight and advice that greatly facilitated both my experiments and my growth as a developing scientist.

DEDICATION

I dedicate this dissertation to my parents, Randall and Patricia Flory. Their unconditional support made completion of my studies possible. I will always be grateful for their commitment to me as devoted parents to whom I can always turn for advice and encouragement.

CHAPTER I

INTRODUCTION

Calmodulin

Calmodulin is a small eukaryotic protein that reversibly binds Ca^{2+}. Study of calmodulin in genetically tractable organisms has yielded many insights into calmodulin function. Calmodulin is essential for proliferation in fungi, including the yeasts *Saccharomyces cerevisiae* (Davis et al., 1986) and *Schizosaccharomyces pombe* (Takeda and Yamamoto, 1987) as well as the filamentous fungus *Aspergillus nidulans* (Rasmussen et al., 1990). The function of calmodulin has been extensively studied in *S. cerevisiae* with appreciable work also performed in *A. nidulans*. Although both species are fungi, the relative importance of the Ca^{2+}-dependent functions for calmodulin differ markedly.

In *S. cerevisiae*, the Ca^{2+}-binding function of calmodulin is dispensable for cell growth and division. Mutant calmodulins in which the Ca^{2+}-binding sites are inactivated support growth (Geiser et al., 1991). Furthermore, neither the Ca^{2+}-calmodulin-dependent protein kinase nor the Ca^{2+}-calmodulin-dependent phosphatase calcineurin are required for growth (Cyert et al., 1991; Cyert and Thorner, 1992; Moser et al., 1995; Ohya et al., 1991; Pausch et al., 1991). However, Ca^{2+}-calmodulin and the Ca^{2+}-calmodulin dependent enzymes are required for survival in mating pheromone

and for maintaining ion homeostasis (Cunningham and Fink, 1996; Moser et al., 1995; Pozos et al., 1996). Thus, the conservation of the Ca^{2+}-binding sites in calmodulin throughout evolution is readily explained.

Diverse techniques have identified two essential Ca^{2+}-independent functions for calmodulin during the *S. cerevisiae* cell cycle. First, calmodulin is required to bind Spc110p, a coiled-coil protein that connects the inner and central layers of the spindle pole body (SPB), the yeast mitotic microtubule organizing center (Geiser et al., 1993; Kilmartin et al., 1993; Stirling et al., 1994). Calmodulin localizes to the SPB and this localization is dependent on the calmodulin-binding site in Spc110p (Spang et al., 1996). This interaction is essential for proper assembly of spindle pole components because mutations in the C-terminal calmodulin-binding site of Spc110p result in the formation of large electron-dense structures that appear to nucleate microtubules (Sundberg et al., 1996). The presence of calmodulin at the SPB is also required for proper function of the spindle during mitosis (Davis, 1992; Kilmartin and Goh, 1996; Stirling et al., 1996; Sun et al., 1992; Sundberg et al., 1996).

Calmodulin is also important for polarized growth in *S. cerevisiae* (Davis, 1992; Ohya and Botstein, 1994). The polarized growth function of budding yeast calmodulin is mediated by interaction with an unconventional type V myosin, Myo2p (Brockerhoff et al., 1994). Calmodulin binds in a Ca^{2+}-independent manner in vitro to a region of Myo2p containing IQ sites

(Brockerhoff et al., 1994). This binding is responsible for the co-localization of calmodulin and Myo2p throughout the cell cycle (Brockerhoff et al., 1992; Brockerhoff et al., 1994; Lillie and Brown, 1994; Sun et al., 1992).

In striking contrast to *S. cerevisiae*, *A. nidulans* requires Ca^{2+}-calmodulin for cell cycle progression. *A. nidulans* calmodulins mutated in the Ca^{2+}-binding sites do not support growth and division. Calmodulin appears to function at two points in the *A. nidulans* cell cycle (Rasmussen et al., 1992). Deletion of the gene encoding the calcineurin A subunit causes *A. nidulans* to arrest early in the cell cycle, suggesting an essential role for Ca^{2+}-calmodulin at the G1 to S phase transition (Rasmussen et al., 1994). Later in the cell cycle, depletion of calmodulin blocks the ability of *A. nidulans* to progress from a *nimT* block between G2 and M (Lu et al., 1993). The unique gene encoding *A. nidulans* Ca^{2+}-calmodulin-dependent protein kinase is also essential (Means, 1994). Thus, *A. nidulans* requires Ca^{2+}-calmodulin during cell cycle progression to activate both calcineurin and Ca^{2+}-calmodulin-dependent protein kinase. If calmodulin functions at the SPB or at sites of polarized growth and whether these putative functions are Ca^{2+}-dependent in *A. nidulans* is not known.

S. pombe requires at least one intact Ca^{2+}-binding site for growth (Moser et al., 1995). Thus, like *A. nidulans*, *S. pombe* appears to require Ca^{2+}-calmodulin for some aspect of cellular proliferation. The importance of

Ca^{2+}-binding to calmodulin in fission yeast suggests that Ca^{2+}-dependent calmodulin targets that are essential in *A. nidulans* might also be essential in *S. pombe* . However, the only Ca^{2+}-dependent calmodulin binding protein found so far in *S. pombe*, calcineurin, is not essential for growth although over-expression of calcineurin does affect SPB and nuclear positioning (Yoshida et al., 1994). Essential Ca^{2+}-calmodulin dependent enzymes may yet be found in *S. pombe*. Alternatively, the essential Ca^{2+}-independent SPB and polarized growth functions of calmodulin found in *S. cerevisiae* might also exist in *S. pombe*, but they may be Ca^{2+}-dependent.

The Yeast Spindle Pole Body

The spindle pole body (SPB) serves as the principal microtubule-organizing center in fungi. The SPB of budding yeast is a laminar structure composed of three disk-shaped plaques that are embedded in the nuclear envelope throughout the cell cycle. The central plaque interfaces with the nuclear envelope, the outer plaque faces the cytoplasm, and the inner plaque is contiguous with the nucleoplasm. During vegetative growth, the outer plaque of the SPB nucleates cytoplasmic microtubules, while nuclear spindle microtubules emanate from the inner plaque (Byers and Goetsch, 1975). The budding yeast SPB also contains a lateral extension known as the half-bridge that serves as the initiation site for formation of a daughter SPB during the duplication process (Byers and Goetsch, 1975). In addition to functioning as the microtubule-organizing center in budding yeast cells, the SPB also plays

roles in both karyogamy, nuclear fusion during sexual conjugation of haploid cells, and in formation of the spore wall during meiosis (Winey and Byers, 1993).

A combination of mass spectrometry, completion of the *S. cerevisiae* genome database and genetic power facilitated rapid identification of many constituent proteins of the budding yeast SPB (Wigge et al., 1998). Nucleation from the budding yeast SPB requires the γ-tubulin complex, a multiprotein complex of γ-tubulin (Tub4p) and two related proteins, Spc97p and Spc98p. The budding yeast γ-tubulin complex localizes to both the outer plaque and inner plaque of the SPB (Knop et al., 1997). The γ-tubulin complex is targeted to the outer plaque of the SPB by Spc72p as a precursor to nucleation of cytoplasmic microtubules (Knop and Schiebel, 1998). The central plaque, the core of the budding yeast SPB, is composed chiefly of of Spc42 and Spc29p (Adams and Kilmartin, 1999; Bullitt et al., 1997; Elliott et al., 1999). The large coiled-coil protein Spc110p, which spans the space between the central and inner plaques (Kilmartin et al., 1993), facilitates nucleation of the mitotic spindle microtubules by anchoring the γ-tubulin complex to the inner plaque. The N-terminal region of Spc110p binds directly to the γ-tubulin complex, as shown by genetic analysis and the two-hybrid assay (Knop and Schiebel, 1997; Nguyen et al., 1998). The 70 kD coiled-coil central region of Spc110p acts as a spacer between the spindle microtubules and the core of the SPB (Kilmartin et al., 1993). The Spc110p C-terminal

region binds to the central plaque of the SPB, and this association is dependent on calmodulin binding to the Spc110p C-terminal calmodulin-binding site (Kilmartin and Goh, 1996; Stirling et al., 1994; Sundberg et al., 1996).

In the divergent yeast *Schizosaccharomyces pombe*, which divides by medial fission, the mitotic spindle and SPB are distinguishable from those found in budding yeast. High-resolution analysis of the *S. pombe* mitotic spindle reveals that multiple (2-4) kinetochore microtubules terminate at each kinetochore (Ding et al., 1993), wherease in *S. cerevisiae* the mitotic spindle contains only one microtubule per kinetochore (Winey et al., 1995). Also unlike the budding yeast mitotic spindle (Winey et al., 1995), the fission yeast spindle loses all continuous interpolar microtubules as the spindle apparatus elongates (Ding et al., 1993). The fission yeast SPB also demonstrates unique properties. First, the fission yeast SPB lacks the distinct laminar structure of the budding yeast SPB and appears as a largely amorphous ellipsoid by electron microscopy. Second, the *S. pombe* SPB exhibits cell-cycle related changes in localization (Ding et al., 1997). During interphase, the fission yeast SPB localizes to the cytoplasm on the periphery of the nuclear envelope. Following SPB duplication and as cells enter mitosis, a small hole or "fenestra" opens in the nuclear envelope into which the duplicated, side-by-side SPBs insert. The SPBs initiate microtubule nucleation and subsequently move apart within the nuclear envelope as mitotic spindle formation proceeds.

At the completion of mitosis, the SPBs move back into the cytoplasm just outside the nuclear envelope. Most γ-tubulin in the interphase fission yeast cell is found inside the nucleus just below the future site of the fenestra which will allow insertion of the SPB (Ding et al., 1997). Similar to budding yeast γ-tubulin, fission yeast γ-tubulin exists in complex with homologues of *S. cerevisiae* Spc97 (Alp4p) and Spc98 (Alp6p) (Vardy and Toda, 2000). Microtubule nucleation is initiated just as the SPB inserts into the nuclear envelope (Ding et al., 1997), bringing the SPB into the nucleus and into proximity of the fission yeast γ-tubulin complex. Given that budding yeast Spc110p recruits the γ-tubulin complex to the inner plaque of the budding yeast SPB (Knop and Schiebel, 1998), microtubule nucleation in *S. pombe* may be initiated when the SPB is brought into contact with the nuclear pool of γ-tubulin by SPB insertion.

The mechanism underlying insertion of the fission yeast SPB is not well understood, but the fission yeast proteins Cut11p and Sad1p may be involved. Cut11p, a transmembrane domain-containing component of both the fission yeast SPB and nuclear pore complex, is proposed to anchor the SPB to the nuclear envelope (West et al., 1998). The budding yeast homologue of Cut11p, Ndc1p, also localizes to both SPBs and nuclear pores and may facilitate permanent attachment of the budding yeast SPB to the nuclear envelope (Chial et al., 1998). Sad1p, identified in a visual screen for fission yeast cells containing abnormal mitotic spindles, contains multiple

proposed transmembrane domains and may facilitate the interaction between the SPB and nuclear envelope. In addition to attaching the SPB to the nuclear envelope, Sad1p may also anchor microtubule motor proteins to the SPB (Hagan and Yanagida, 1995). In budding yeast, Spc110p may also function to anchor the SPB in the nuclear envelope, as mutations that block calmodulin binding to Spc110p result in the formation of abnormal microtubule-associated aggregates of SPB components that localize apart from the nuclear envelope in the nucleoplasm (Sundberg et al., 1996). Together these data suggest that a fission yeast Spc110p homologue might have multiple roles at the SPB affecting both mitotic spindle formation and assembly of the SPB into the nuclear envelope.

The Higher Eukaryotic Centrosome

The centrosome serves as the principal microtubule-organizing center in higher eukaryotic cells. Given the importance of the centrosome in promoting mitotic spindle assembly, attention has focused on the fundamental mechanisms underlying centrosomal-dependent microtubule nucleation. Clinical interest in the centrosome also exists given that centrosomal abnormalities, including supernumerary and hypertrophic centrosomes, occur in variety of cancer tissues and cell lines (Lingle et al., 1998; Lingle and Salisbury, 1999; Pihan et al., 1998). These observations support the long-standing hypothesis that defects in centrosome function facilitate cancerous growth (Brinkley and Goepfert, 1998).

Quite distinct from the structure of the SPB, the vertebrate centrosome is composed of two cylindrical centrioles surrounded by a dense layer of fibrous pericentriolar material from which microtubules emanate (Kellogg et al., 1994). Despite their differences in overall structure, the vertebrate centrosome and fungal SPB share similar functional roles and contain many homologous proteins. Like the fungal SPB, the higher eukaryotic centrosome is the principal microtubule-organizing center in higher eukaryotes and facilitates nucleation of stable microtubules that compose the higher eukaryotic mitotic spindle apparatus (Kellogg et al., 1994). Despite the low abundance of centrosomal proteins (Kellogg et al., 1994), recent studies aimed at understanding mechanisms underlying centrosomal function have identified and characterized several centrosomal proteins that share homology with proteins of the fungal SPB.

One such centrosomal protein with a key role in microtubule nucleation is γ-tubulin. In higher eukaryotic cells, γ-tubulin is rapidly recruited to the centrosome during mitosis (Khodjakov and Rieder, 1999), and recruitment and attachment of the vertebrate γ-tubulin complex to the centrosome appears essential for microtubule nucleation (Moritz et al., 1998; Schnackenberg et al., 1998). In a variety of higher organisms, including *Drosophila melanogaster*, *Xenopus laevis* and humans, γ-tubulin is found in a complex with approximately seven other proteins. These large γ-tubulin complexes are composed of smaller subcomplexes containing homologues of

the budding yeast γ-tubulin complex proteins Spc97 and Spc98 (Martin et al., 1998; Murphy et al., 1998; Oegema et al., 1999; Tassin et al., 1998). Immuno-electron microscopic tomography of purified centrosomes indicates that γ-tubulin complexes (γ-TURCs) form ring-shaped structures that localize to centrosomal pericentriolar material. These ring structures associate with the minus ends of microtubules during *in vitro* nucleation from purified centrosomes (Moritz et al., 1995; Zheng et al., 1995). Based on these data it is hypothesized that γ-tubulin ring structures serve as a template for nucleating microtubules (Moritz et al., 1995; Zheng et al., 1995), and several recent studies using high-resolution immunolocalization methods support this model (Keating and Borisy, 2000; Moritz et al., 2000; Wiese and Zheng, 2000). An alternative model exists in which γ-tubulin and associated proteins form a short protofilament that catalyzes microtubule formation (Erickson, 2000).

Given that SPB anchoring proteins such as Spc110p and Spc72p determine the attachment sites and likely govern microtubule nucleation capacity of the γ-tubulin complex in budding yeast cells (Knop and Schiebel, 1998), a key point of regulation for the γ-tubulin complex in higher eukaryotes will likely be the mechanism by which they are recruited to and attached to the centrosomal core. Recruitment of the γ-tubulin complex to the centrosome is facilitated by pericentrin, a centrosomal protein that interacts with both γ-tubulin (Dictenberg et al., 1998) and the motor protein dynein (Purohit et al., 1999). The centrosomal proteins that subsequently anchor the γ-tubulin

complex to the centrosome have not yet been identified, but *in vitro* fractionation of purified centrosomes indicates that one or more salt-insoluble centrosomal proteins of the centrosomal core, or "centromatrix," are essential for nucleation. These centromatrix proteins may serve as anchors for the γ-tubulin complex during nucleation (Moritz et al., 1998; Schnackenberg et al., 1998). The conservation of both calmodulin (Li et al., 1999; Willingham et al., 1983; Zavortink et al., 1983) and Spc110p epitopes (Tassin et al., 1997) in mammalian centrosomes suggested the existence of a calmodulin-binding orthologue of yeast Spc110p, but the striking structural differences between the yeast spindle pole body and the centrosome cast doubt that the protein or proteins conferring anchoring activity in higher eukaryotic cells would bear any resemblance to yeast Spc110p. However, as described here I identified and characterized Spc110p-related homologues from the fission yeast *Schizosaccharomyces pombe* and humans. This work reinforces the similarities between the fungal SPB and the vertebrate centrosome and demonstrates the remarkable conservation of Spc110p-related proteins at fungal SPBs and vertebrate centrosomes. We predict completion of the human genome project will reveal additional components in the human centrosome that share homology with components of the yeast SPB, and that a composite understanding of these proteins will shed light on conserved mechanisms of centrosomal function.

CHAPTER II

ANALYSIS OF CALMODULIN FUNCTION IN SCHIZOSACCHAHAROMYCES POMBE

Introduction

Calmodulin is essential for proliferation in lower eukaryotic organisms, including the yeasts *Saccharomyces cerevisiae* (Davis et al., 1986), and *Schizosaccharomyces pombe* (Takeda and Yamamoto, 1987), as well as the filamentous fungi *Aspergillus nidulans* (Rasmussen et al., 1990). Diverse techniques have identified two essential Ca^{2+}-independent functions for calmodulin during the *S. cerevisiae* cell cycle. First, calmodulin is required to bind Spc110p, a coiled-coil protein that connects the inner and central layers of the spindle pole body (SPB), the yeast mitotic microtubule organizing center (Geiser et al., 1993; Kilmartin et al., 1993; Stirling et al., 1994). This interaction is essential for proper assembly of spindle pole components (Sundberg et al., 1996) and for proper function of the spindle during mitosis (Davis, 1992; Kilmartin and Goh, 1996; Stirling and Stark, 1996; Sun et al., 1992; Sundberg et al., 1996). Calmodulin is also important for polarized growth in *S. cerevisiae* (Davis, 1992; Ohya and Botstein, 1994). The polarized growth function of budding yeast calmodulin is mediated by interaction with an unconventional type V myosin, Myo2p (Brockerhoff et al., 1994).

When I entered the lab in 1994, attention focused on understanding the functional roles of Spc110p at the budding yeast SPB. In order to complement work in budding yeast, I sought to identify Spc110p homologues in the divergent yeast *Schizosaccharomyces pombe* (fission yeast), and perhaps in higher eukaryotic organisms. To determine if a calmodulin-binding protein like Spc110p might exist in fission yeast, I collaborated with a more senior graduate student, M. Moser, to examine the subcellular localization of calmodulin in live *S. pombe* cells. We used a fusion between the green fluorescent protein (GFP) and fission yeast calmodulin to examine calmodulin localization in live cells. We confirmed our findings by performing immunofluorescence microscopy on fixed fission yeast cells. Similar to GFP-calmodulin in budding yeast, fission yeast calmodulin localizes to both the SPB and to areas of polarized growth. We subsequently generated and characterized a conditional *S. pombe* calmodulin mutant that exhibits mitotic defects, including abnormalities in mitotic spindle architecture and DNA segregation, at the restrictive temperature. Our results revealed striking similarities for calmodulin function in two divergent yeasts, and suggested the existence of a Spc110p homologue in fission yeast. This work has been published and appears in Appendix A.

Results

Localization of calmodulin fusions to green fluorescent protein (GFP)

S. cerevisiae-Indirect immunofluorescence previously showed that calmodulin localizes to two different regions in the budding yeast cell. First calmodulin localizes to sites of cell growth and overlaps the location of actin patches in buds (Brockerhoff et al., 1992; Sun et al., 1992). Second, calmodulin localizes to the spindle pole body (Geiser et al., 1993; Stirling et al., 1994). The presence of calmodulin at both these sites has been confirmed by immunoelectron microscopy (Spang et al., 1996; Sundberg et al., 1996) (H. Sundberg and T. N. Davis, unpublished results). Using the previous techniques, calmodulin was not seen at both subcellular locations at the same time, because fixation procedures that preserved the sites of cell growth did not allow visualization at the SPB and vice versa. Therefore, we extended our experiments in *S. cerevisiae* to living cells by visualizing the location of a fusion between S65T-GFP and the N-terminus of budding yeast calmodulin. A gene encoding the GFP-Cmd1p fusion protein expressed under control of the *CMD1* promoter and terminator was integrated in place of the wild-type *CMD1* gene. The fluorescent GFP-Cmd1p in living cells shows a pattern consistent with a location at both the SPB and at areas of polarized growth. Unbudded cells and cells with small buds each contain one dot of fluorescence as expected for either a single SPB or for two SPBs in the side-by-side configuration. These cells also have a bright patch of fluorescence at the

nascent bud site or the small bud (Appendix A, Figure 1A). Cells with a medium bud contain two small fluorescent dots near the neck region of the cell as expected for a protein at the poles of the short spindle (Appendix A, Figure 1B). In addition patches of fluorescence appear in the bud similar to the pattern seen for the actin capping protein, Cap2p (Waddle et al., 1996). In a large budded cell, both mother and daughter contain a dot of GFP-Cmd1p presumably corresponding to their single SPB (Appendix A, Figure 1C). In addition a bright ring appears at the neck (Appendix A, Figure 1C). Importantly, the Ca^{2+}-binding mutant GFP-Cmd1-6p fusion had a pattern of localization identical to that of the wild-type fusion protein (Appendix A, Figure 1D-F). This is the first demonstration that a mutant calmodulin defective in binding Ca^{2+} localizes to the SPB in addition to sites of cell growth.

S. pombe-The localization of calmodulin in *S. pombe* cells was determined using fusions of *S. pombe* calmodulin to GFP. A gene encoding a fusion of wild-type GFP to the N-terminus of wild-type *S. pombe* calmodulin expressed under the control of the *cam1*$^+$ promoter and terminator was integrated in place of the *cam1*$^+$ gene. Because we were examining living cells, the behavior of the GFP-Cam1p in single cells could be observed over a period of time. GFP-calmodulin displayed two distinct patterns of localization. First, small fluorescent dots behaved exactly as previously demonstrated for both the budding and fission yeast SPBs (Byers and

Goetsch, 1975; Hagan and Hyams, 1988; McCully and Robinow, 1971) (Appendix A, Fig. 2A-D). In cells early in the cell cycle as judged by their small size, a single spot of fluorescence was observed at the edge of the nucleus (Appendix A, Figure 2A). The dot of fluorescence elongated and eventually divided (Appendix A, Figure 2B). Later the separation between the dots increased (Appendix A, Figure 2C) with one spot of the pair eventually being distributed to each new daughter cell following mitosis and cytokinesis (Appendix A, Figure 2D). Notably, calmodulin was not seen at the additional MTOCs that nucleate microtubules near the septum in *S. pombe* cells following mitosis.

We observed a second pattern of fluorescence indicating that GFP-Cam1p localized at regions of the fission yeast cell undergoing polarized growth (Appendix A, Figure 3A-D). In cells undergoing septation and cytokinesis, bright fluorescence was found on both sides of the growing septum dividing the cell (Appendix A, Figure 3A). In a newly divided cell immediately following cytokinesis, fluorescence was seen to move from the septum to the opposite or 'old' end of the cell (Appendix A, Figure 3B,C). The old end corresponds to the former end of the mother cell and is in opposition to the end directly created by septation. *S. pombe* cells are known to only grow from the old end just after division (Mitchison and Nurse, 1985). Later the fluorescence redistributed to both ends of the lengthening cell (Appendix A, Figure 3D). This bipolar localization coincides with an event in

the *S. pombe* cell cycle known as NETO, or new end take off, the time when both ends of the cell begin to grow (Mitchison and Nurse, 1985). A strain containing an integrated fusion of S65T-GFP to *cam1+* was found to have a fluorescence pattern that was identical to that observed with the fusion to wild-type GFP except that the fluorescence was much easier to detect (data not shown).

Indirect immunofluorescence of *S. pombe* calmodulin

Indirect immunofluorescence using antiserum to fission yeast calmodulin gave a pattern very similar to that seen with GFP-Cam1p. The growing ends and the septum as well as what appeared to be the SPB all were stained by the antiserum. The presence of fission yeast calmodulin at the SPB was confirmed by comparing the localization of calmodulin to that of Sad1p. Sad1p is a recognized component of the *S. pombe* SPB and remains permanently associated with the SPB throughout the cell cycle (Hagan and Hyams, 1988). Attempts were made to localize Sad1p in cells containing GFP-calmodulin fusions, but the combined aldehyde fixation procedures necessary for tubulin immunofluorescence were found to eliminate GFP fluorescence. Instead we found that the localization of calmodulin, tubulin and DNA matched that of Sad1p, tubulin and DNA in cells processed in parallel (Appendix A, Figure 4). Tubulin staining, representing the elongating spindle, was observed between the two dots of calmodulin staining. Sad1p dots similarly localized to the ends of the spindle. The localization of Sad1p,

in relation to tubulin and DNA, is identical to that previously described (Hagan and Yanagida, 1995).

Analysis of a temperature-sensitive *S. pombe* calmodulin mutant

When the Ca^{2+}-binding-site mutant *cam1-E14* allele is carried on a plasmid it does not confer temperature-sensitivity (Moser et al., 1995). However, when *cam1-E14* is integrated as a single copy in place of the wild-type *cam1*$^+$ gene, fission yeast cannot form colonies at temperatures above 32°C. Calmodulin mutant and wild-type fission yeast were arrested in S phase with hydroxyurea at a temperature permissive for growth and then released from arrest and shifted to restrictive temperature. The wild-type culture completed S phase and proceeded normally through mitosis and then cytokinesis. The septation index peaked 80 minutes after the shift to 37°C and the number of viable cells began to increase 100 minutes after the shift (Appendix A, Figure 5). In contrast, 80 minutes after the shift to 37°C cells in the mutant culture began to lose viability (Appendix A, Figure 5). Cytokinesis in the mutant culture was delayed and asynchronous although most of the cells did eventually form a septum.

The calmodulin localization and cell-cycle timing studies suggested that mitotic defects might underlie the loss of viability in the calmodulin mutant strain. Therefore, an analysis of DNA and spindle morphology was performed on synchronized cultures of both the wild-type and calmodulin mutant following incubation at non-permissive temperature. DNA-specific

staining with DAPI in control cells revealed the chromatin as a brightly staining crescent with a faintly stained nucleolus completing the sphere of the nucleus. As the cells progressed through mitosis, the nucleus divided and the chromatin segregated to either end of the dividing cell. Two discrete nuclei formed, followed by septation.

Analysis of microtubule distribution by indirect immunofluorescence revealed the disappearance of cytoplasmic microtubules concomitant with formation of a mitotic spindle in cells undergoing mitotic transit. As previously described (Hagan and Hyams, 1988), early short spindles aligned nearly perpendicular to the length of the cell and spanned the centrally-located chromosomal DNA mass (Appendix A, Fig. 6A). Later, spindle alignment became more parallel with the long axis of the elongating cell. The spindle midpoint corresponded with the midpoint of the cell. As well, chromatin segregating along medium to full-length spindles was always found near the two endpoints of the spindle (Appendix A, Figure 6B). At full spindle extension, the newly segregated chromosomal masses were observed at the two ends of the cell (Appendix A, Figure 6C). Following mitosis, spindle microtubules disappeared and post-anaphase arrays of cytoplasmic microtubules became apparent (Appendix A, Figure 6D). Cytokinesis resulted in two daughter cells each containing an equal mass of segregated chromosomal DNA.

The *cam1-E14* mutant cells exhibited several abnormal phenotypes. When the culture first began to lose viability (80 minutes), the chromosomal DNA appeared strikingly condensed in 20% of the cells (n=200). Metaphase plates with three pairs of discrete chromosomes could often be observed (Appendix A, Figure 7A). The DNA also frequently appeared to be broken or fragmented by improper distribution along the spindle (Appendix A, Figure 7B). For comparison only 2.5% of the wild-type cells contained abnormal DNA at that time point. Anti-tubulin immunofluorescent staining of mutant spindles was more diffuse and less uniform than wild-type. Perhaps the most striking cells were those that appeared to have broken mitotic spindles (Appendix A, Figure 7C).

At later times, mutant cells appeared with chromosomes that were missegregated. Some cells divided with two nuclei on one side of the septum while other cells divided with only one DAPI-staining mass that often appeared abnormally large. Cytoplasmic microtubules of normal morphology were found assembled in association with the mislocalized chromatin (Appendix A, Figure 7D). At 240 minutes after the shift, 27% of the mutant cells contained mislocalized DNA and 11% contained no apparent nuclear DNA.

Discussion

As a first step in probing the function of calmodulin in *Schizosaccharomyces pombe*, we used fluorescence microscopy in live and

fixed fission yeast cells to determine the subcellular localization of calmodulin. Antiserum to calmodulin appears at the end of the spindle in a pattern identical to Sad1p, a molecular marker whose localization has been previously defined with respect to SPB position (Hagan and Yanagida, 1995). A GFP-Cam1p fusion protein allowed examination of the SPB in living cells and demonstrated that in living cells the SPB went through the stages previously observed in fixed isolates (Hagan and Hyams, 1988; McCully and Robinow, 1971; Tanaka and Kanbe, 1986). Unlike a GFP fusion to Dis1p (Nabeshima et al., 1995), GFP-Cam1p is the first molecular marker for SPBs that can be seen in living *S. pombe* cells throughout the cell cycle. This integrated marker should allow monitoring of SPB behavior in mutant fission yeast cells.

Localization of calmodulin using both a green fluorescent protein fusion and indirect immunofluorescence also indicates an association between *S. pombe* calmodulin and areas of polarized growth. GFP-Cam1p was observed in the region of the septum as it formed, then at only one end of newly formed cells. Later fluorescence was seen at both ends of the growing cell. These behaviors are similar to those of known components of the polarized fission yeast actin cytoskeleton (Marks et al., 1986).

The SPB localization and the polarized localization of GFP-Cam1p can easily be differentiated using two criteria. First, the SPB fluorescence is best seen in a focal plane that bisects the center of the cell while the polarized

localization is more clearly seen when the focus is in a plane that is level with the surface of the cell. The second criterion can only be applied to live cells. The spot of SPB fluorescence remains relatively constant in location for several minutes. During this time interval, the fluorescence associated with cortical cytoskeleton can be seen to undergo extensive remodeling, as has been previously reported in *S. cerevisiae* (Waddle et al., 1996).

Subcellular localization of calmodulin to the SPB and the cortical cytoskeleton suggests roles for *S. pombe* calmodulin in mitosis and in polarized cell growth, respectively. Analysis of the restrictive-temperature phenotype of a temperature-sensitive calmodulin mutant further substantiates a mitotic function for *S. pombe* calmodulin and indicates a role for calmodulin in facilitating chromosome segregation. At the restrictive temperature, *S. pombe* cells containing a temperature-sensitive Ca^{2+}-binding-site calmodulin mutant begin to lose viability after DNA replication, at a time when wild-type cells are completing mitosis and initiating cytokinesis. Examination of the DNA of the mutant cell reveals abnormal chromatin and spindle morphologies that are consistent with a failure in chromosome segregation. First, at the time when the cells begin to lose viability, the chromatin appears to condense and fragment. The chromatin may appear as distinct chromosomes like that found in cold-sensitive fission yeast *nda3* mutants when incubated at non-permissive temperature (Hiraoka et al., 1984). The *nda3*$^+$ gene encodes β-tubulin, an essential component of the mitotic spindle apparatus. Consistent with a

presumed defect in spindle assembly, mutant cells were found that appear to contain broken spindles. However, while the tubulin defect in the *nda3* mutant is detected by a spindle checkpoint causing a reversible mitotic arrest at the restrictive temperature, the defect in the *cam1-E14* mutant cells does not cause arrest. The *cam1-E14* calmodulin mutant continues to divide, resulting in cells with DNA mislocalized on only one side of the septum and a significant number of cells containing no nuclear DNA. This observation suggests several, as yet untested hypotheses. Calmodulin may have a role in a mitotic checkpoint function. Alternatively, the calmodulin defect may simply not be detected by the checkpoint mechanism. Furthermore, the fact that the mutant cells can form a septum suggests that any defect the *cam1-E14* mutant may have in polarized growth is not severe enough to manifest itself before the lethal effects of mitotic failure.

In *S. cerevisiae*, GFP-calmodulin fusions are easily seen at the SPB and at sites of cell growth in living cells. This is the first demonstration of the presence of calmodulin at both structures at the same time. Previous methods employing fixation showed calmodulin at only one place or the other (Brockerhoff et al., 1992; Geiser et al., 1993; Stirling et al., 1994; Sun et al., 1992; Sundberg et al., 1996). Furthermore, although the *cmd1-6* Ca^{2+}-binding calmodulin mutant is viable (Geiser et al., 1991), immunofluorescence methods have not been able to detect the Cmd1-6p protein product at the SPB. The GFP-Cmd1-6p fusion provides the first cytological evidence that the

interaction between calmodulin and the budding yeast SPB is Ca^{2+}-independent. GFP-calmodulin serves as an excellent integrated marker for the SPB allowing the observation of SPB behavior in living cells. Our results are similar to those observed previously examining the location of Nuf2p-GFP, a protein that associates with the microtubules near the SPB (Kahana et al., 1995; Osborne et al., 1994).

Calmodulin appears to perform a similar mitotic function in both fission and budding yeasts. The subcellular localization pattern of calmodulin in both *S. cerevisiae* and *S. pombe* is quite similar. Calmodulin can be found at the SPB and at sites of cell growth associated with the polarized cortical cytoskeleton. The mitotic phenotypes of temperature-sensitive calmodulin mutants from both species are also related. Like the *cam1-E14* mutant, the *S. cerevisiae cmd1-1* mutant loses viability at non-permissive temperature during mitosis and accumulates cells with broken spindles and fragmented DNA (Davis, 1992). Calmodulin in *S. cerevisiae* is known to function in mitosis by direct interaction with the SPB component Spc110p. Therefore, we propose that calmodulin also performs an essential mitotic function via an interaction at the *S. pombe* SPB. Yet, unlike in *S. cerevisiae* (Geiser et al., 1991), in *S. pombe* at least one wild-type Ca^{2+}-binding-site in calmodulin is required to maintain viability (Moser et al., 1995). Thus, the essential interaction between *S. pombe* calmodulin and the SPB may be a Ca^{2+}-dependent process. However, any determination of the Ca^{2+}-dependence of the interaction

between calmodulin and centrosome components from *S. pombe* as well as from other species awaits their isolation and characterization.

Materials and Methods

Materials and Methods for Chapter II can be found in Appendix A.

CHAPTER III

THE SCHIZOSACCHAROMYCES POMBE SPC110P HOMOLOGUE

Introduction

The classic electron microscopy studies of B. Byers and L. Goetsch describe the morphology of the budding yeast centrosome, or spindle pole body (SPB), in exquisite detail (Byers and Goetsch, 1975). Over the subsequent twenty-five years, the combination of genetic manipulation and completion of the sequence of the *Saccharomyces cerevisiae* genome database facilitated description and analysis of many of the molecular subunits of the budding yeast SPB (Wigge et al., 1998). One critical budding yeast SPB component, the coiled-coil protein Spc110p, facilitates mitotic spindle assembly by anchoring the γ-tubulin complex to the inner plaque of the SPB. The N-terminal region of Spc110p binds directly to the γ-tubulin complex (Knop and Schiebel, 1997; Nguyen et al., 1998). The Spc110p C-terminal region binds to the core or central plaque of the SPB, and this association is dependent on calmodulin binding to the Spc110p C-terminal calmodulin-binding site (Kilmartin and Goh, 1996; Stirling et al., 1994; Sundberg et al., 1996). I sought to complement work on budding yeast Spc110p through isolation and characterization of Spc110p-related homologues from the divergent yeast *Schizosaccharomyces pombe*, which divides by medial fission.

Our work on fission yeast calmodulin described in Chapter I suggested the existence of a Spc110p homologue in *S. pombe*. Simultaneous electron

microscopy studies by R. Ding and coworkers in the laboratory of J. R. McIntosh revealed cell cycle-dependent changes in morphology and subcellular localization that distinguish the fission yeast SPB from the budding yeast SPB. While the budding yeast SPB remains uniform in shape and permanently embedded in the nuclear envelope throughout the cell cycle (Byers and Goetsch, 1975), the fission yeast SPB changes from a disk shape to a dumbbell shape and moves from the cytoplasm into a hole or "fenestra" in the nuclear envelope just prior to mitotic onset (Ding et al., 1997). Given the unique dynamic qualities of the fission yeast SPB, we predicted that isolation and characterization of the fission yeast Spc110p homologue would complement work on budding yeast Spc110p, and that composite sequence data from the two yeasts might additionally facilitate cloning of centrosomal calmodulin targets from higher eukaryotes.

I identified the fission yeast Spc110p homologue in the *S. pombe* genome database by virtue of its homology with a related calmodulin-binidng protein in the filamentous fungus *Aspergillus nidulans*. Like Spc110p, the predicted secondary structure of Pcp1p (*pcp1*$^+$, pole target of calmodulin in *S. pombe*) contains a central coiled-coil domain flanked by noncoiled ends. Also, Pcp1p and the *A. nidulans* Spc110p-related homologue each contain a functional C-terminal calmodulin-binding site similar to that found in the C-terminal region of Spc110p. Pcp1p localizes to the fission yeast SPB throughout the cell cycle as shown by both fluorescence microscopy of a

Pcp1p-GFP fusion in live cells and immunofluorescence microscopy of fixed fission yeast cells stained with antibodies. Higher resolution localization of Pcp1p by immunoelectron microscopy suggests a SPB assembly mechanism for Pcp1p distinct from that described for budding yeast Spc110p (Adams and Kilmartin, 1999). Overexpression of the *S. pombe* homologue in fission yeast cells produces multiple, abnormal SPB-like structures similar to the supernumerary centrosomes known to occur in many cancer lines. The work described in this chapter was done in collaboration with J. Joseph and A. R. Means (Duke University), who discovered and characterized the *A. nidulans* Spc110p homologue, and D. M. Morphew and J. R. McIntosh (University of Colorado, Boulder), who performed and analyzed results of immunoelectron microscopy.

Results

Identification of Spc110p homologues in the filamentous fungus *Aspergillus nidulans* and the fission yeast *Schizosaccharomyces pombe*

An expression cloning strategy was used to identify novel calmodulin-binding proteins in *A. nidulans* (Joseph and Means, 2000). Several positive phage plaques contained inserts that encoded a protein fragment predicted to contain a large coiled-coil domain followed by the putative calmodulin-binding region. This entire portion of the *A. nidulans* protein showed some sequence similarity to the equivalent region of Spc110p indicating a relationship between the two proteins. I used the *A. nidulans* partial cDNA

sequence to identify Spc110p-related proteins in *S. pombe* and found a single high-scoring match on cosmid c6G9 from *S. pombe* Chromosome I in the *S. pombe* genome database. This sequence mapped to an open reading frame predicted to encode a protein of 140 kD with a long central coiled-coil domain spanning residues residues 149-1085, with small gaps of predicted noncoiled sequence at 804-872, 904-916, and 1022-1029. This gene was subsequently named *pcp1*$^{+}$ for pole target of calmodulin in *S. pombe*. The protein sequences of Pcp1p and the *S. cerevisiae* spindle pole body component Spc110p share only 12% identity but are predicted to contain similar overall structures, including a long central coiled-coil domain flanked by noncoiled ends. We identified a calmodulin-binding site related to the Spc110p calmodulin-binding site in both the C-terminal region of Pcp1p that was also similar to the putative calmodulin-binding site in the C-terminal region of the protein predicted by the *A. nidulans* partial cDNA (Flory et al., 2000).

To determine if the predicted region of Pcp1p and the *A. nidulans* protein bind calmodulin, fragments of each protein were expressed in bacteria. As shown in Figure III.1A, a bacterially-expressed GST fusion to the C-terminal region of Pcp1p directly binds purified protein A-labeled fission yeast calmodulin (Protein A-Cam1p). A GST fusion to a truncated version of the Pcp1p C-terminal region that lacks the predicted calmodulin-binding site does not bind Protein A-Cam1p, nor does GST alone, even though these two proteins are overproduced (Figure III.1A). Protein A alone did not produce a

signal in control blots run in parallel (data not shown). Similarly, a hexahistidine-tagged *A. nidulans* C-terminal fragment isolated from *E. coli* bound purified protein A-conjugated *A. nidulans* calmodulin (Figure III.1B). A truncated *A. nidulans* C-terminal fragment lacking the predicted calmodulin-binding site does not bind calmodulin (Figure III.1B).

S. pombe pcp1$^+$ is an essential gene

To determine if *pcp1*$^+$ is essential for growth, we created a diploid *S. pombe* strain hemizygous for *pcp1*$^+$ in which one copy of the *pcp1*$^+$ ORF was precisely replaced with the nutritional marker *ura4*$^+$ by PCR-mediated gene deletion (see Materials and Methods). Deletion of *pcp1*$^+$ in this strain was confirmed by PCR and Southern blot analyses. The hemizygous diploid strain was sporulated, and the resultant spores were germinated on rich medium. Visual inspection of meiotic asci by light microscopy indicated that sporulation was disrupted, including the formation of two- and three-spore tetrads and ascus cases of abnormal morphology (data not shown). Of 170 resultant colonies tested, 169 (99.4%) were unable to grow on medium lacking uracil, indicating that spores carrying the *ura4*$^+$ nutritional marker were unable to undertake vegetative growth. These data indicate that *pcp1*$^+$ is an essential gene and that reduced levels of *pcp1*$^+$ impair sporulation.

Pcp1p localizes specifically to SPBs throughout the cell cycle

In order to examine the subcellular localization of Pcp1p throughout the cell cycle of *S. pombe*, we created a fusion of *pcp1*$^+$ and the green

fluorescent protein (GFP). GFP was integrated at the 3' end of the *pcp1*$^+$ ORF using PCR-mediated gene tagging (Bahler et al., 1998), resulting in strain MFP5 containing a single-copy GFP-tagged *pcp1*$^+$ allele under the control of the endogenous *pcp1*$^+$ promoter. We used similar methods to construct a strain MFP6 carrying a single-copy, integrated *pcp1*$^+$ allele in which GFP is fused to the 5' end of the *pcp1*$^+$ ORF and expression is controlled by the attenuated *nmt1* promoter (Bahler et al., 1998). These two strains demonstrate indistinguishable localization patterns by fluorescence microscopy. In live fission yeast cells, the pattern of punctate flourescence matched exactly that described for fission yeast SPBs (Hagan and Hyams, 1988; Moser et al., 1997) (Figure III.2). Interphase cells of smaller size demonstrated one dot of fluorescence at the nuclear periphery (Figure III.2 A and B). Cells entering mitosis contained a single bright dot of fluorescence that divided into two dots (Figure III.2 C and D), which subsequently migrated toward the ends of the cell along an axis roughly parallel to that of the cell body (Figure III.2 E and F). Dots approached the ends of the cell, and cytokinesis subsequently resulted in two daughter cells each containing one dot of fluorescence (Figure III.2 G and H).

In order to confirm localization of Pcp1p:GFP to the SPB, we fixed MFP5 (*pcp1*$^+$*:GFP*) cells in formaldehyde and stained with polyclonal antibodies against Sad1p, a recognized component of the fission yeast SPB (Hagan and Yanagida, 1995). In all cells examined, the Pcp1p:GFP signal

colocalized with Sad1p (Figure III.2 I-L). We also counterstaind strain MFP5 with a mouse monoclonal antibody against γ-tubulin (Sigma), a component of both fission yeast SPBs and also the two cytoplasmic MTOCs (microtubule-organizing centers) that appear near the septum following mitosis (Hagan and Hyams, 1988; Horio et al., 1991). Cells in interphase or early mitosis demonstrated colocalization of γ-tubulin with Pcp1p at the SPBs (data not shown). Following mitosis, two additional dots of γ-tubulin staining representing the cytoplasmic MTOCs became evident, but Pcp1p was never observed to colocalize with these structures (Figure III.2 M vs. N).

As an additional confirmation of this localization pattern, we demonstrated that endogenous Pcp1p C-terminally tagged with 13XMyc colocalizes with the ends of the mitotic spindle. In interphase cells, a single dot of Myc staining was observed in a pattern matching that seen with the GFP fusions (data not shown). In mitotic cells, two dots of Myc staining always flanked the ends of the linear mitotic spindle visualized with antibodies against alpha-tubulin (Figure III.2 O-Q).

Pcp1p associates with the SPB both prior to and after mitotic insertion of the SPB into the nuclear envelope

We used immunoelectron microscopy with anti-GFP antibodies (see Materials and Methods) to confirm and extend our findings regarding the localization of Pcp1p at the fission yeast SPB. In interphase MFP5 cells containing a SPB in the cytoplasm near the nuclear periphery immunogold

staining was detected throughout the SPB (Figure III.3A). Similarly, cells containing SPBs in the process of duplication but prior to insertion into the nuclear envelope reveal immunogold staining on both the mother and daughter SPB structures (Figure III.3B). In mitotic cells containing inserted SPBs associated with the ends of the mitotic spindle, the immunogold staining is present on SPBs in the nuclear envelope (Figure III.3 C and D).

Overexpression of GFP:Pcp1p results in the formation of ectopic SPB-like structures, mitotic spindle defects, and DNA missegregation

To further examine the function of Pcp1p, we evaluated the effects of moderately overexpressing GFP:Pcp1p. The strain MFP19 contains a single-copy GFP-tagged *pcp1*$^{+}$ allele under the control of the wild-type *nmt1* promoter. When cultured in the presence of excess thiamine, which partially represses expression from the *nmt1* (*n*o *m*essage in *t*hiamine) promoter, MFP19 still overexpresses GFP:Pcp1p at least 5-fold relative to strain MFP6. MFP6 expresses GFP:Pcp1p from the attenuated *nmt1* promoter and produces GFP:Pcp1p at wild-type levels, as indicated by quantitative western blotting (data not shown). Our measurement of 5-fold overexpression for MFP19 is in approximate agreement with levels of mRNA transcript expression reported for wild-type and attenuated *nmt1* promoters in the presence of thiamine (Forsburg, 1993). We therefore examined the phenotype of strain MFP19 cultured in rich medium, which contains excess thiamine. This strategy allowed us to examine the effects of moderate, constitutive overexpression of

GFP:Pcp1p on aspects of cell division, particularly mitotic functions such as spindle formation and DNA segregation, without lengthy induction times and extreme overexpression levels.

Assessed by fluorescence microscopy MFP19 cells often contained more than two dots of GFP fluorescence (43/232, 19%, Figure III.4 A, D, G, J; see also Figure III.7 E, I, M, Q). The number of foci per cell ranged from one to eight. These foci were observed in both mitotic and interphase cells. We further confirmed the presence of abnormal structures containing GFP:Pcp1p in strain MFP19 using immunoelectron microscopy. We observed clusters of immunogold staining at both the SPB and extra structures (ES) in the cytoplasm (Figure III.5 A and B). These structures were often located near the SPB (Figure III.5C). To determine if these extra foci contained other known components of the SPB, we fixed cells in formaldehyde and separately counterstained MFP19 cells for the known fission yeast SPB components Sad1p (Hagan and Yanagida, 1995) and γ-tubulin (Horio et al., 1991). Many cells containing more than two dots of GFP fluorescence also contained more than two dots of Sad1p staining (27/55, 49%, Fig. 4 B and E). Similarly, a monoclonal antibody against γ-tubulin also recognized more than two structures in cells containing more than two dots of GFP fluorescence (20/50, 40%, Figure III.4 H and K). While some of the extra dots of γ-tubulin staining may represent staining of the cytoplasmic MTOCs, the cytoplasmic MTOCs appear only briefly at the end of mitosis (Hagan and Hyams, 1988)

and are therefore not well represented in asynchronous culture. A significant number of cells containing more than two GFP:Pcp1p foci also demonstrated severe defects in DNA segregation as indicated by DAPI staining (25/55, 46%). These defects include hypercondensation of chromosomes (Figure III.4F and Figure III.7D), misplacement of DNA (Figure III.4L), and fragmentation of the chromosomal mass into three or more DAPI-staining masses (Figure III.7 H, L, T).

Given the abnormalities in SPB number and DNA segregation patterns in MFP19, we evaluated the morphology of microtubules by immunofluorescence microscopy. As a control, we first analyzed strain MFP5, which expresses Pcp1p:GFP from the endogenous *pcp1*$^{+}$ promoter, and found that the GFP signal remains robust following combined aldehyde fixation (Figure III.6 A, E, I, M). In agreement with previous descriptions of mitosis in *S. pombe* (Hagan and Hyams, 1988), SPBs in MFP5 were located at the ends of the mitotic spindle and undergo separation concomitant with spindle elongation and chromosome segregation (Figure III.6 A-L). Following spindle disassembly, interphase cells demonstrate a cortical array of microtubules nucleated from the non-SPB cytoplasmic MTOCs that appear near the septum in late mitosis (Hagan and Hyams, 1988) (Figure III.6 M-P). In contrast to these control cells, many MFP19 cells containing more than two dots of GFP:Pcp1p also contained profound defects in microtubule architecture (20/31, 65%). Mitotic cells often demonstrated poorly formed

spindles that were associated with SPBs of varying intensity (Figure III.7A). We also observed cells with multiple short spindle fragments, each of which were associated with GFP foci and one or two DNA masses (Figure III.7 E-L). In these cells, the GFP foci localize to the ends of the short spindle structures (Figure III.7 G and K), and three DNA masses are present in each cell (Figure III.7 H and L). We also observed cells with mitotic spindle defects in later stages of mitosis. These cells often contained fractured, V-shaped spindles (9/20, 45%, Figure III.7 M-O). Many very large cells were observed with long spindle fragments (Figure III.7 Q-T). GFP foci were often associated with both the ends of the microtubule structures and along their axes. In these cells small gaps of tubulin staining along the length of the long microtubule structures (Figure III.7 Q-S, arrows) often corresponded with GFP. These cells often demonstrated three missegregated DNA masses (Figure III.6T), but the so-called "cut" (chromosomes untimely torn) phenotype (Yanagida, 1998) in which the septum abnormally severs DNA at the cell midzone was not observed.

Discussion

Spc110p is a coiled-coil calmodulin-binding protein that anchors the γ-tubulin complex to the spindle pole body (SPB) in the budding yeast *Saccharomyces cerevisiae* (Geiser et al., 1993; Knop and Schiebel, 1997; Nguyen et al., 1998). Localization of calmodulin to the SPB of the fission yeast *Schizosaccharomyces pombe* and the mitotic defects exhibited by a *S.*

pombe calmodulin mutant (Moser et al., 1997) prompted us to search for a Spc110p homologue in fission yeast. In this chapter we describe the cloning and characterization of the fission yeast protein Pcp1p (*pcp1*$^+$, pole target of calmodulin in *S. pombe*), the homologue of the budding yeast Spc110p.

We identified Pcp1p in the *S. pombe* genome database based on shared homology with the sequence of a calmodulin-binding protein fragment identified in the filamentous fungus *Aspergillus nidulans*. Pcp1p and Spc110p contain similar overall structures including a long, central coiled-coil domain flanked by noncoiled ends. All three fungal homologues contain a single, functional C-terminal calmodulin-binding site, and the homology between these calmodulin-binding sequences facilitated the identification of a related human centrosomal protein called kendrin (Flory et al., 2000) (see Chapter IV). Together, these proteins indicate the conservation from yeast to vertebrates of Spc110p-related molecules that bind calmodulin and localize to the SPB/centrosome. Moderate overexpression of Pcp1p results in an intriguing phenotype in which many cells accumulate SPB-like structures. A subset of these cells additionally exhibits mitotic spindle abnormalities and DNA missegregation. This striking overexpression phenotype indicates that Pcp1p may normally function to recruit other SPB components to the SPB, facilitate the SPB-nuclear envelope interaction, and participate in mitotic spindle formation. Furthermore, the Pcp1p overexpression phenotype is similar to that described for several human cancer lines that exhibit extra

centrosomes and defects in spindle morphology and DNA segregation (Lingle et al., 1998; Lingle and Salisbury, 1999; Pihan et al., 1998).

We show by immunoelectron microscopy that Pcp1p associates with the SPB prior to insertion of the SPB into the nuclear envelope. At the mitotic transition in *S. pombe* the SPB duplicates and undergoes a dramatic insertion event as it moves from the cytoplasmic periphery of the nuclear envelope into a "fenestra" in the nuclear envelope (Ding et al., 1997). Pcp1p incorporates into the fission yeast SPB prior to this insertion process, suggesting a mechanism distinct from that facilitating assembly of Spc110p into the budding yeast SPB. Spc110p, unlike Pcp1p, contains a nuclear localization sequence (NLS) and enters the nucleus prior to incorporation into the daughter SPB during the SPB duplication process (Adams and Kilmartin, 1999). Thus Pcp1p appears to be dependent on the SPB for entry on the nuclear envelope, while entry of Spc110p into the budding yeast nucleus is facilitated by the Spc110p NLS. This represents a fundamental difference in the way Pcp1p and Spc110p are assembled into the fission yeast SPB and budding yeast SPB, respectively.

Following mitotic insertion into the nuclear envelope, Pcp1p is maintained as an integral SPB component during microtubule nucleation and mitotic spindle assembly. The assembly mechanism of Pcp1p suggests a model in which Pcp1p affects mitotic spindle formation. Most γ-tubulin in the interphase fission yeast cell is found inside the nucleus just below the future

site of the fenestra which will allow insertion of the SPB (Ding et al., 1997). Nucleation is initiated just as the SPB inserts into the nuclear envelope (Ding et al., 1997), bringing Pcp1p into the nucleus and into the proximity of the γ-tubulin. Given that budding yeast Spc110p recruits the γ-tubulin complex to the inner plaque of the budding yeast SPB (Knop and Schiebel, 1997), microtubule nucleation in *S. pombe* may be initiated when Pcp1p is brought into contact with the nuclear pool of γ-tubulin by SPB insertion. It should prove interesting to examine whether Pcp1p directly interacts with the recently described fission yeast γ-tubulin complex (Vardy and Toda, 2000).

The phenotype of strain MFP19 that moderately overexpresses GFP:Pcp1p contains supernumerary SPB-like structures, a subset of which recruit the SPB proteins Sad1p and γ-tubulin. The ability of excess Pcp1p to recruit such disparate SPB components as Sad1p, a transmembrane-domain protein presumed to bind the nuclear envelope and/or motor proteins (Hagan and Yanagida, 1995) and γ-tubulin (Horio et al., 1991), an integral component of the fission yeast microtubule-nucleating machinery (Vardy and Toda, 2000), suggests that Pcp1p may be able to direct the formation of structures that are organized similarly to wild-type SPBs. Examination of microtubules in strain MFP19 reveals that these abnormal SPB-like structures disrupt mitotic spindle formation. A majority of MFP19 cells with defects in chromosome segregation contain aberrant spindle structures. We observed V-shaped spindles similar to those reported for *cut11*^{ts} alleles (West et al., 1998),

suggesting the spindle apparatus has lost its anchoring point at the SPB. This observation suggests that Pcp1p may mediate interaction between the SPB and the nuclear envelope.

We observe the formation of multiple spindle-like structures within single cells. Each of these "spindles," which are flanked on their ends by abnormal SPB-like structures containing GFP:Pcp1p, is associated with chromosomal DNA. This suggests that the abnormal SPB-like structures organized by excess Pcp1p contain intrinsic nucleation capability and can direct the formation of multiple spindles that are capable of capturing DNA. Alternatively, these microtubule structures may represent fragments of defective spindles, broken in the process of segregating DNA, that have been captured by Pcp1p:GFP-containing structures. Finally, we also observe abnormally large cells presumably subject to cell cycle arrest due to abortive mitosis. These cells contain large microtubule arrays with Pcp1p:GFP-containing structures both at the ends and along the longitudinal axes of these structures. The presence of GFP foci at the ends and along the length of these arrays suggests these arrays may be composed of multiple spindles and/or spindle fragments aggregated by a microtubule-bundling activity, for example that proposed for the *S. pombe* motor Cut7p (Hagan and Yanagida, 1992).

The phenotype of Pcp1p overexpression bears striking resemblance to that of a variety of human cancer cell lines and tissues that contain centrosomes of abnormal number and morphology (Lingle et al., 1998; Lingle

and Salisbury, 1999; Pihan et al., 1998). Immunostaining studies using antibodies directed against multiple centrosome markers, including the human Pcp1p orthologue kendrin (Flory et al., 2000)(also see Chapter IV), demonstrate that cancer cells contain extra centrosome-like structures in addition to abnormal spindle structures and missegregated DNA. We show here that moderate overexpression of Pcp1p in fission yeast cells similarly produces extra centrosome-like structures, abnormal spindle structures and missegregated DNA. This is in contrast to overexpression of budding yeast Spc110p, which results in the formation of large polymers of a calmodulin/Spc110p complex that associates with microtubules and results in lethality during the subsequent mitosis (Kilmartin and Goh, 1996). Given that Pcp1p overexpression is sufficient to induce a cancer-like phenotype in fission yeast cells, our observation that the kendrin mRNA transcript is specifically overexpressed in a subset of human cancer lines (Flory et al., 2000) implicates a role for the human Pcp1p orthologue kendrin in promoting carcinogenesis.

Materials and Methods

Database Searching and Sequence Analysis

The *S. pombe* genome was searched using the Sanger Center BLAST server with default settings (http://www.sanger.ac.uk/Projects/S_pombe/blast_server.shtml). Coiled-coil secondary structure was predicted using PAIRCOIL (Berger et al., 1995) (http://nightingale.lcs.mit.edu/cgi-bin/score). Sequence alignments were

performed using multiple algorithms bundled in the Biology Workbench (http://workbench.sdsc.edu).

Media

Escherichia coli media was LB (Miller, 1972) supplemented with 100 µg/ml ampicillin when needed. *S. pombe* rich media were YE (Gutz et al., 1972) and minimal medium (EMM) (Bio 101, Vista, CA) supplemented with 100 µg/ml adenine, leucine, histidine, and/or uracil. G418 (Gibco BRL) was added to YE agar at 100 µg/ml when required. For mating and meiotic induction of *S. pombe*, strains of opposite mating type were mixed and grown on YPD. YPD is YP (Sherman et al., 1986), supplemented with 2% glucose, 50 µg/ml adenine, and 25 µg/ml uracil.

Strains

S. pombe

The genotype of wild-type strain 99 is *h⁻, ade6-M210, leu1-32, ura4-D18, his3-D1* (Burke and Gould, 1994). A hemizygous strain carrying a single precise deletion of the *pcp1*$^{+}$ ORF was created by integrating the PCR product amplified from plasmid cassette KS-(Bahler et al., 1998) using oligonucleotides MF42 (5'AGTTTCTATATAATTTTATGCACTTGCGCTAGTTGGTGGATAATT TTAATAAATACATGCATCCGCAGTTACGTTCGCCAGGGTTTTCCCA GTCACGAC3') and MF43 (5'TTAAAATAATTATAGTAGTAGAATTAATTGAATGTTGTTAAAAA

AAAAGAGAGTAAAAAACGTAAGTATCCCAGAAGCGGATAACAATT TCACACAGGA3') into a Ura$^-$ diploid strain (*h$^+$/h$^-$, ade6-M210/ade6-M216, leu1-32/leu1-32, ura4-D18/ura4-D18, his3-D1/his3-D1*). Transformants with a Ura$^+$ phenotype were identified and cultured on YPD medium for 48 hours at 25°C to promote sporulation. Random spore analysis was then performed and the resulting colonies were screened for Ura$^+$ prototrophy.

To fuse *GFP* (green fluorescent protein) in-frame to the 3'end of the *pcp1$^+$* open-reading frame (ORF), a PCR product was first generated by amplification of plasmid cassette pFA6a-GFP(S65T)-kanMX6 (Bahler et al., 1998) using oligonucleotides MF16 (5'AAGAATGAGTGGCTAAAACAAGCTCAATTGAAACAATCATTGC AAAGAGCTGCCGCAAAGGCAAAGACCGCAAACTACCGGATCCCCG GGTTAATTAA3') and MF17 (5'AAATTAAAATAATTATAGTAGTAGAATTAATTGAATGTTGTTAA AAAAAAAGAGAGTAAAAAACGTAAGTATCCCAGAGAATTCGAGCT CGTTTAAAC3'). The resulting PCR product was integrated at the *pcp1$^+$* locus in strain MP5-1C (Moser et al., 1997) according to recommended methods (Bahler et al., 1998), creating strain MFP5 (*h$^-$, ade6-M216, leu1-32, ura4-D18, pcp1$^+$:GFP*). A 13XMyc tag was similarly added to the 3' end of the *pcp1$^+$* open-reading frame in strain 99 using plasmid cassette pFA6a-13Myc-kanMX6 (Bahler et al., 1998) and oligonucleotides MF16 and MF17 (see above), creating strain MFP10 (*h$^-$, ade6-M210, leu1-32, ura4-D18, his3-*

D1, pcp1⁺:13XMyc). Integrated fusions of *GFP* to the 5'end of the *pcp1⁺* ORF under control of wild-type (Maundrell, 1990) and attenuated *nmt1* promoter sequences (Basi et al., 1993) were created using plasmid cassettes pFA6a-kanMX6-P3nmt1-GFP and pFA6a-kanMX6-P81nmt1-GFP (Bahler et al., 1998) respectively. Oligonucleotides MF39 (5'ATCAGATTGGCTGATCACAGAATTCGCGTTTTCATCTTTAAATTT GGGAGATTGCGTATTAAAATCTCGTTCAGACATGATTTAACAAAGC GACTATA3') and MF40 (5'ATCAGATTGGCTGATCACAGAATTCGCGTTTTCATCTTTAAATTT GGGAGATTGCGTATTAAAATCTCGTTCAGACATTTTGTATAGTTCA TCCATGC3' were used for both PCR amplifications. The two resulting strains were named MFP19 (*h⁻, ade6-M210, leu1-32, ura4-D18, his3-D1, nmt1(highest strength)-GFP:pcp1⁺*) and MFP6 (*h⁻, ade6-M210, leu1-32, ura4-D18, his3-D1, nmt1(lowest strength)-GFP:pcp1⁺*)

All PCR reactions for tagging and deletion methods in *S. pombe* were performed using Expand polymerase (Roche Molecular Biochemicals) with Buffer 3, and all oligonucleotides (Integrated DNA Technologies, Coralville, IA) used for these methods were purified by the vendor using polyacrylamide gel electrophoresis. All integrations were verified by PCR analysis of the chromosomal *pcp1⁺* locus. The deletion allele was additionally confirmed by Southern blotting analysis.

Plasmids

S. pombe

A *S. pombe* genomic DNA fragment containing the entire *pcp1*$^+$ ORF was amplified from *S. pombe* chromosomal DNA using oligonucleotides MF23 (5'CTCATTGGTGTAACCGGAGC3') and MF24 (5'GCCTCCGATTGAGAGAATGC3') (Integrated DNA Technologies, Coralville, IA) and then digested with XbaI and EcoRV. The resulting XbaI-EcoRV fragment, which contains the entire *pcp1*$^+$ ORF, was then inserted into the unique XbaI and EcoRV sites of pBluescript KS$^+$ (Stratagene), creating plasmid pMF13. The *pcp1*$^+$ ORF sequence in pMF13 precisely matched corresponding sequence in the *S. pombe* database.

For protein A-calmodulin overlay assays, plasmid pMF27 encoding a fusion of glutathione-S-transferase (GST) to the Pcp1p C-terminal region was created. First, BamHI sites flanking the region of pMF13 encoding Pcp1p amino acids 960-1208 were engineered using oligo-mediated mutagenesis (Kunkel et al., 1987) with pMF13 as template and oligonucleotides MF45 (5'TACTAATCTGGGATCCTTACGTTTTTTAC3') and MF47 (5'GCTATAATAAGCAAGGATCCAAGTTGCAGG3') (Integrated DNA Technologies), creating plasmid pMF18. The resulting BamHI fragment in pMF18 was inserted into the unique BamHI site of pGEX-2T (Amerhsam Pharmacia), creating plasmid pMF27 containing an in-frame fusion of GST (glutathione-S-transferase) to Pcp1p residues 960-1208. Plasmid pMF59,

encoding a fusion of GST to a Pcp1p C-terminal truncation (residues 960-1141) lacking the predicted calmodulin-binding site, was created by site-directed mutagenesis of plasmid pMF27 using QuikChange (Stratagene) and oligonucleotides MF100 (5'CAGGATACGAAACATGCAATTAAATAAATTTACGTATGCTGCAG 3') and MF101 (5'CTGCAGCATACGTAAATTTATTTAATTGCATGTTTCGTATCCTG3') (Integrated DNA Technologies). QuikChange was used according to the manufacturer's recommendations except that the annealing temperature for PCR was raised to 64°C in all cases. Plasmid pMF11 encoding an in-frame fusion of the staphylococcal protein A IgG-binding domain to *S. pombe cam1*$^+$ was constructed by replacing an NcoI/PstI fragment encoding vertebrate calmodulin in pMF8 (a derivative of pRIT-2T (Amersham Pharmacia)) with an NcoI/PstI fragment containing *S. pombe cam1*$^+$ from plasmid pEC/pCAM (Moser et al., 1995).

A. nidulans

The hexahistidine tagged C-terminal fragment of *A. nidulans* 110p used in protein A calmodulin overlay assays was generated by first subcloning a 2.7 kB EcoRI/KpnI fragment containing the 3' end of *A. nidulans* 110p from pBluescript phagmid 2.5 identified in the initial expression screen, into pGEM-4Z (Promega). From the resulting plasmid a 2.7 kB SalI/EcoRI fragment was cloned into the EcoRI/SalI site of pET30b (Invitrogen) thereby

generating pA110C. The ΔCaM b.s. truncation was generated by subcloning a 2.3 kB EcoRI/FspI fragment of pBluescript 2.5 into the EcoRI/SmaI sites of pGEM-3Z (Promega). ΔCaM b.s. was subsequently generated by cloning the EcoRI/SacI fragment into the EcoRI/SacI sites of pET30b (Invitrogen).

Calmodulin overlay blot

S. pombe

Protein A-calmodulin overlay blotting was done as previously described (Stirling et al., 1992) with the following modifications. A protein A-Cam1p fusion protein and protein A alone were expressed in *E. coli* strain POP2136 (American Type Tissue Collection) using plasmid pMF11 and pRIT-2T (Pharmacia), respectively. Expression of protein A and the protein A-calmodulin fusion protein were induced in mid-log phase cultures by shifting the growth temperature from 30°C to 42°C for 2 hours. Cells were lysed in a French Pressure Cell (American Instrument Co., Silver Spring, MD), and one-step purification was performed on IgG-Sepharose (Pharmacia) according to the manufacturer's recommendations. Fusions of GST to Pcp1p fragments (amino acids 960-1208 and 960-1141) and GST alone were expressed in *E. coli* strain GM-1 (Coulondre and Miller, 1977) using plasmids pMF27, pMF59, and pGEX-2T (Amersham Pharmacia), respectively. Expression of GST and GST fusions were induced at mid log phase by culturing cells for 3 hours in the presence of 0.2 mM isopropyl ß-D-

thiogalactopyranoside. Bacterial lysates were prepared in 0.01 M sodium phosphate, pH 7.2, 1% ß-mercaptoethanol, 1% SDS, and 6M urea.

A. nidulans

A. nidulans CaM-Protein A overlays were performed as described (Joseph and Means, 2000; Stirling et al., 1992). Both hexahistidine-tagged fusion proteins were expressed in Bl21 bacteria by growing the culture to an A_{600nm} and inducing protein expression with the addition of 1 mM isopropyl ß-D-thiogalactopyranoside for 2 hr. The bacteria were then pelleted by centrifugation and lysed by resuspension in 8 M urea, 100 mM NaH_2PO_4 and 10 mM Tris-HCl, pH 6.8. The lysate was clarified by centrifugation and the proteins isolated using nickel nitriloacetic acid-agarose resin following the protocol recommended by Qiagen.

Fluorescence microscopy

Live *S. pombe* cells expressing GFP fusions were prepared for inspection by fluorescence microscopy as previously described (Moser et al., 1997). For immunofluorescence microscopy, *S. pombe* cells were grown to mid log phase in YE liquid medium at 30°C and then fixed, washed, digested, and stained according either to a procedure using formaldehyde alone as fixative (Sohrmann et al., 1996) or to the combined formaldehyde/glutaraldehyde method (Hagan and Hyams, 1988) with the following modifications. Phosphate-buffered saline (PBS) (Harlow and Lane, 1988), PBS supplemented with 1% bovine serum albumin and 0.05% sodium

azide (PBS/BSA), and 1.1M sorbitol in 0.1 M sodium phosphate buffer, pH 6.5 (SP) were substituted for PEM, PEMS and PEMBAL buffers, respectively. Cells fixed in formaldehyde alone were digested in 0.5 ml SP containing 0.5 mg/ml Zymolyase-100T (ICN) for approximately 1 hour at 30°. Cells fixed by the combined aldehyde method were digested in 1 ml SP containing 0.3 mg/ml Zymolyase-100T (ICN) and 1 mg/ml mutanase (Novo Nordisk BioChem) for approximately 1 hour at 30°C. Cells were incubated for 12-36 hours at room temperature on a rotating wheel in primary antibodies.

The antibodies were affinity-purified rabbit anti-Sad1p antibodies (1:25) (Hagan and Yanagida, 1995), mouse ascites anti-γ-tubulin antibody GTU-88 (1:100) (Sigma), affinity-purified rabbit anti-c-Myc antibodies (1:30) (Santa Cruz Biotechnology), or purified rat anti-tubulin monoclonal antibody YOL1/34 (1:50) (Harlan Sera-Lab) in 100-200 µl PBS/BSA. Following three washes in PBS/BSA, cells were resuspended in 200 µl PBS/BSA containing secondary antibody conjugates: rhodamine-isothiocyanate-labeled goat anti-rabbit IgG (1:800) (Boehringer Mannheim), Alexa 568 goat anti-mouse IgG (1:50) (Molecular Probes), anti-rabbit Oregon Green 488 goat anti-rat IgG (1:800) (Molecular Probes), or Alexa Fluor 568 goat anti-rat IgG (1:50) (Molecular Probes). Following incubations in secondary antibody for at least 4 hours at room temperature on a rotating wheel, cells were washed three times in PBS/BSA. DNA was stained with 100 ng/ml di-amidino phenyl

indole (DAPI) (Sigma Chemical Co.), and cells were then mounted onto 1.5 mm polylysine-coated glass Gold Seal coverslips (VWR) in Citifluor Glycerol (Ted Pella). Depolymerization of microtubules was induced by incubating cells on ice for 25 min prior to fixation (Hagan and Yanagida, 1995).

For standard immunofluorescence microscopy, cells were imaged using a Zeiss Axioplan microscope with x100 objectives and an Optivar set at 1.25. Images were captured using Imagepoint or Quantix cooled CCD video cameras (Photometrics). For deconvolution fluorescence microscopy, cells prepared as described above were imaged using a Zeiss Axiovert microscope with a 63x objective. The images were captured using a Quantix-LC cooled CCD video camera (Photometrics) and analyzed using DeltaVision software (Applied Precision). Fig. 1N, 6 A-P, and 7 A-T are deconvolved quick projections of 10-30 digital sections.

Immunoelectron microscopy

For immunoelectron microscopy, cells were grown in liquid culture to early-to-mid log phase and processed as described (Ding et al., 1997). Immunoelectron microscopy was done as previously described (Ding et al., 1997) with antibodies against GFP (Seedorf et al., 1999).

Figure III.1. Analysis of calmodulin-binding domain activity. The predicted calmodulin-binding sites in the C-terminal regions of Pcp1p and the *A. nidulans* Spc110p homologue physically bind calmodulin as shown by calmodulin overlay blotting and truncation analysis. A (left), Coomassie blue-stained acrylamide gel of protein extracts from *E. coli* cells expressing either fusions of GST to indicated residues of Pcp1p or GST alone. (right), Calmodulin overlay blotting showing specific binding of protein A-tagged *S. pombe* calmodulin to the GST-Pcp1p (960-1208) fusion protein. Arrows indicate the position of the full-length GST-Pcp1p fusion protein (960-1208) that binds calmodulin. A fusion between GST and Pcp1p residues 960-1141, which do not include the predicted calmodulin-binding site, does not bind calmodulin. B (left), Coomassie blue-stained polyacrylamide gel of purified hexahistidine-tagged C-terminal *A. nidulans* Spc110p homologue fragment. B (right), Calmodulin overlay blotting showing specific binding of protein A-conjugated *A. nidulans* calmodulin to the C-terminal fragment of the *A. nidulans* protein. Arrows indicate the position of the full-length protein that bind calmodulin. A purified hexahistidine-tagged C-terminal truncation of the *A. nidulans* Spc110p homologue that lacks the predicted calmodulin-binding site does not bind calmodulin.

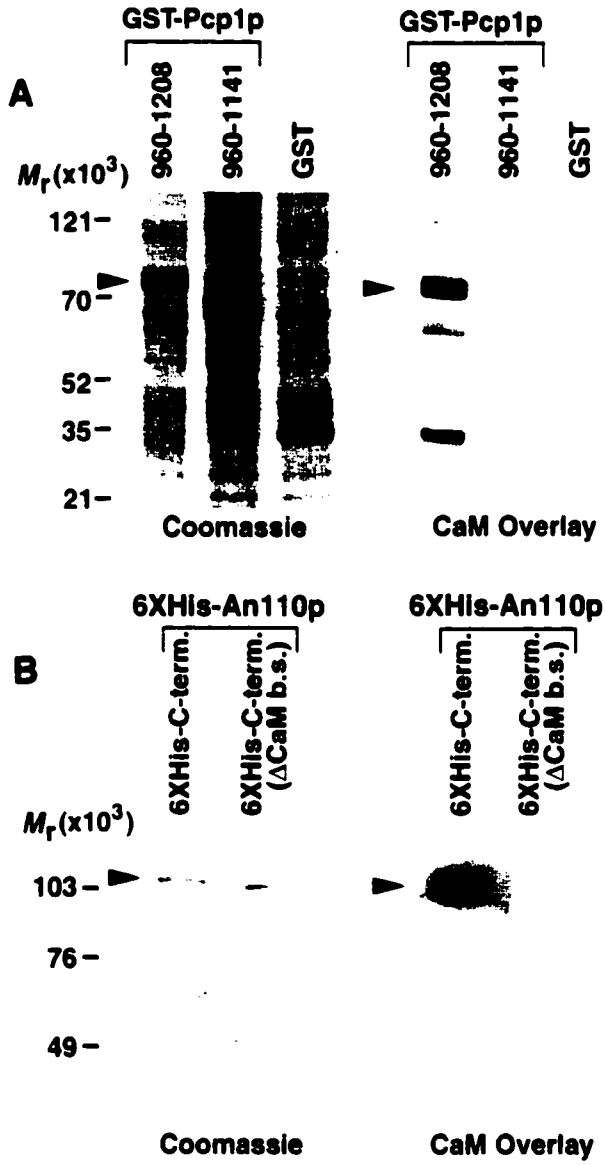
A
GST-Pcp1p
960-1208
960-1141
GST
M_r(x10^3)
121
70
52
35
21
Coomassie
GST-Pcp1p
960-1208
960-1141
GST
CaM Overlay
B
6XHis-An110p
6XHis-C-term.
6XHis-C-term. (ΔCaM b.s.)
M_r(x10^3)
103
76
49
Coomassie
6XHis-An110p
6XHis-C-term.
6XHis-C-term. (ΔCaM b.s.)
CaM Overlay

Figure III.2. Localization of Pcp1p:GFP to the SPB of *S. pombe*. A-H, An equal volume of a culture of strain MFP5 (*pcp1*$^{+}$*:GFP*) grown to logarithmic phase in supplemented liquid YE medium at 30° was mixed with supplemented EMM medium containing 1% low-melting-temperature agarose on microscope slide and visualized by fluorescence microscopy. Phase images showing cell outline in B, D, F, and H correspond to panels A, C, E, and G, respectively. I-N, Pcp1p colocalizes with Sad1p, a known *S. pombe* SPB component, but not the two cytoplasmic MTOCs that appear at the end of mitosis. MFP5 cultured as above was prepared for immunofluorescence according to the formaldehyde procedure described in Materials and Methods. The fluorescent signals in panels M and N were imaged using deconvolution fluorescence microscopy as described in Materials and Methods. O-T, Pcp1p localization to the ends of the mitotic spindle is not dependent on microtubules. MFP10 cultured as above was prepared for immunofluorescence according to the formaldehyde procedure described in Materials and Methods except that for panels R-S, cells were incubated on ice for 30 min prior to fixation to depolymerize microtubules. Unless otherwise noted, cells were imaged by standard fluorescence microscopy as described in Materials and Methods. All bars, 5 μm.

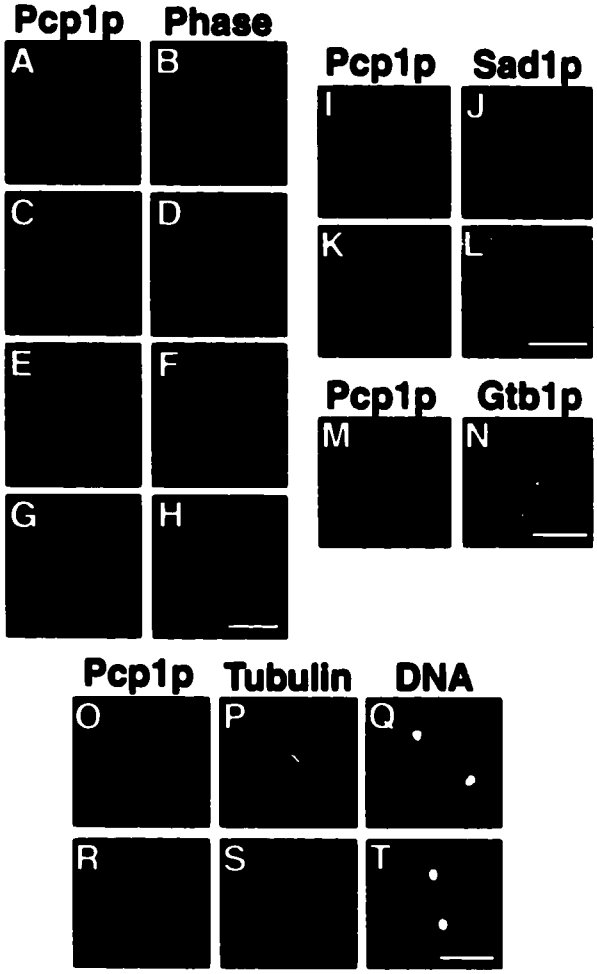
Pcp1p
Phase
A
B
C
D
E
F
G
H
Pcp1p
Sad1p
I
J
K
L
Pcp1p
Gtb1p
M
N
Pcp1p
Tubulin
DNA
O
P
Q
R
S
T

Figure III.3. Pcp1p:GFP localizes to the interphase and mitotic SPBs by immunoelectron microscopy. Strain MFP5 (*pcp1*$^{+}$*:GFP*) was grown to logarithmic phase at 32° and prepared for immunoelectron microscopy with primary antibodies against GFP and with gold-labeled secondary antibodies as described in Materials and Methods. A, Cross-section through an interphase nucleus showing gold particles on the spindle pole body (spb) in the cytoplasm near the nuclear envelope (ne). B, Duplicated side-by-side spindle pole bodies (spbs) both contain gold particles prior to insertion into the nuclear envelope. C and D, Cross-sections through mitotic nuclei showing gold particles on the spindle pole body (spb) that is associated with spindle microtubules (mts).

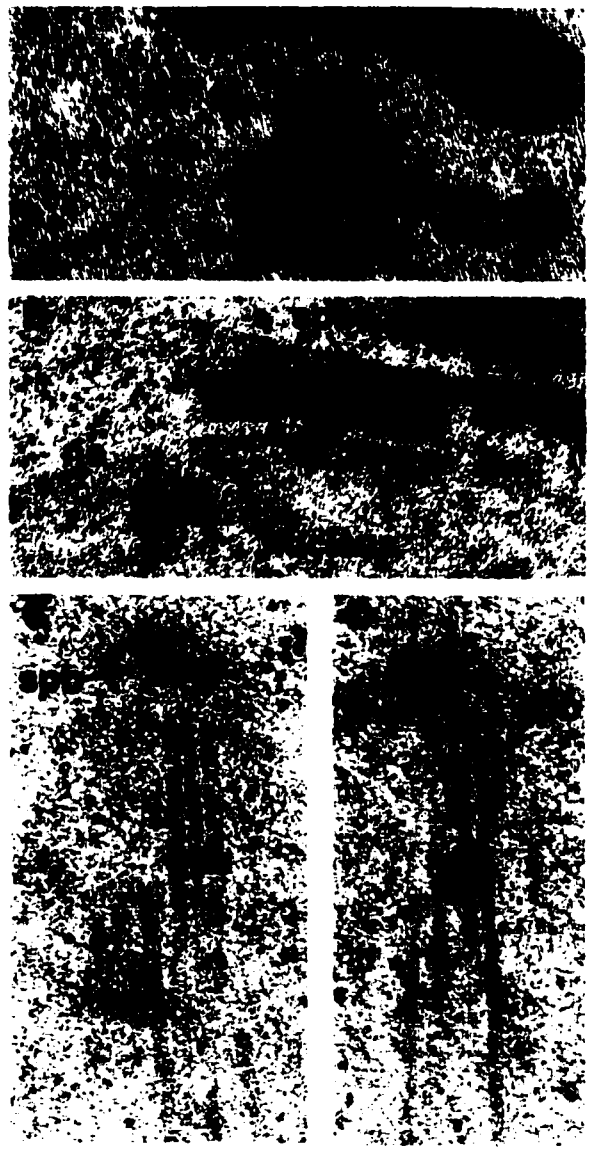

Figure III.4. Overexpression of GFP:Pcp1p results in formation of multiple structures containing Sad1p and γ-tubulin. Strain MFP19 (*nmt1-GFP: pcp1*$^{+}$) was grown to logarithmic phase in supplemented liquid YE medium at 30° and prepared for immunofluorescence microscopy according to the formaldehyde procedure described in Materials and Methods. All cells in this figure were imaged using deconvolution fluorescence microscopy as described in Materials and Methods. A-F, Colocalization of a subset of multiple GFP:Pcp1p foci with the SPB component Sad1p. G-L, Colocalization of a subset of multiple GFP:Pcp1p foci with γ-tubulin. F and L, Hypercondensed and missegregated chromosomes, respectively. Bar, 5 μm.

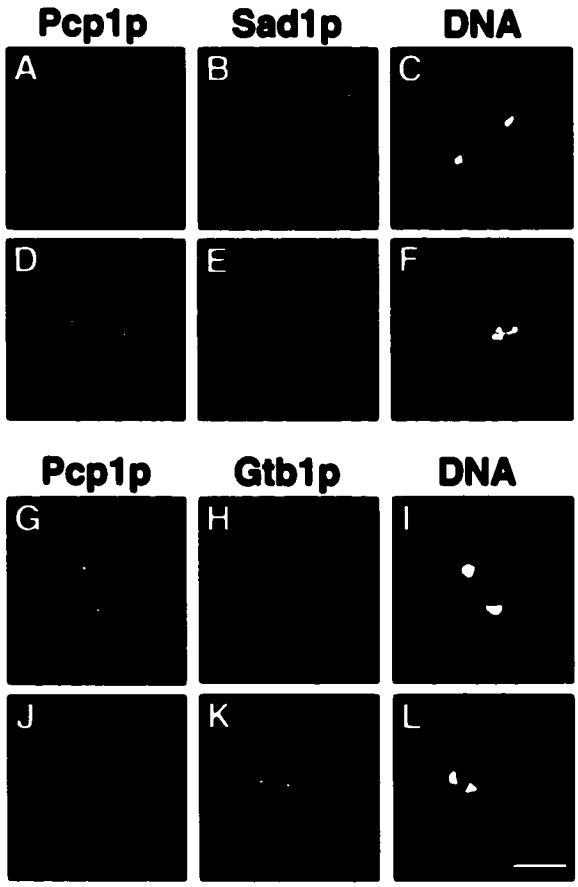
Pcp1p
Sad1p
DNA
A
B
C
D
E
F
Pcp1p
Gtb1p
DNA
G
H
I
J
K
L

Figure III.5. GFP:Pcp1p overexpression results in multiple abnormal cytoplasmic and nuclear structures by immunoelectron microscopy. Strain MFP19 (*nmt1-GFP: pcp1*$^{+}$) was grown to logarithmic phase at 32° and prepared for immunoelectron microscopy with primary antibodies against GFP and with gold-labeled secondary antibodies. A and B, Cross-section through an interphase nucleus showing gold particles on the spindle pole body (spb) and extra structures (es) in the cytoplasm near the nuclear envelope (ne). C, Abnormal structure showing gold labeling in cytoplasm near cell wall (white area in upper right corner). D, Abnormal structure showing gold labeling in nucleus (es) and spindle pole body and associated extra structure (spb and es) showing gold labeling near nuclear envelope (ne).

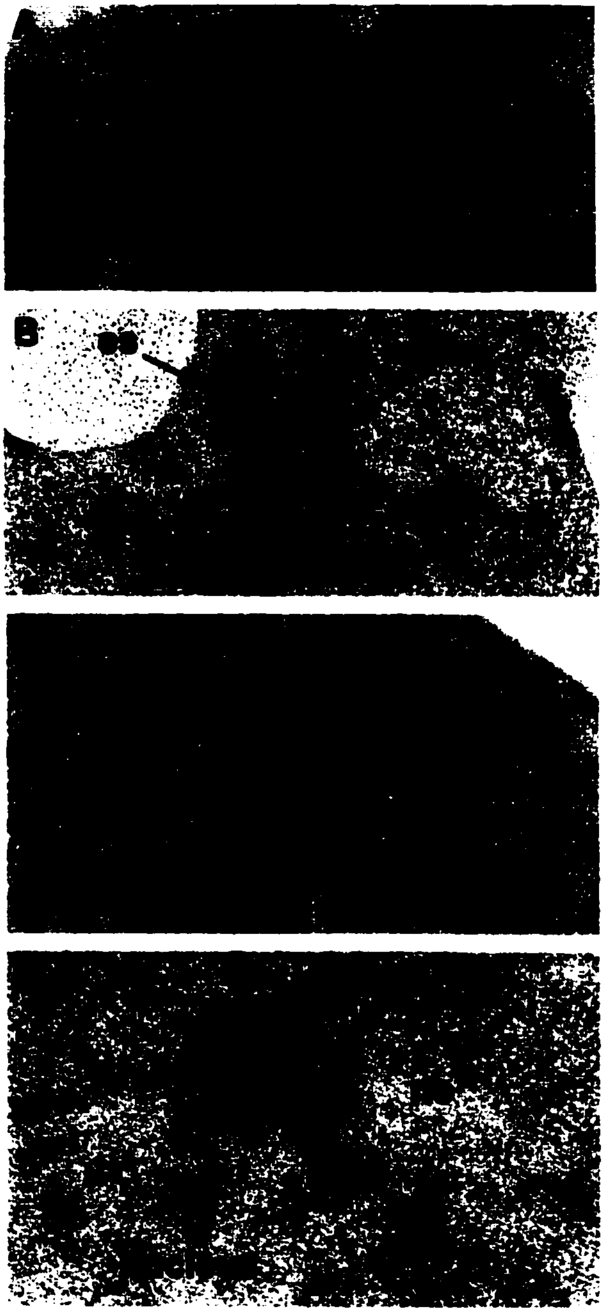
B

Figure III.6. Pcp1p:GFP, tubulin, and DNA morphologies in cells expressing wild-type levels of Pcp1p:GFP. Strain MFP5 (*pcp1⁺:GFP*) was grown to logarithmic phase in supplemented liquid YE medium at 30° and prepared for immunofluorescence microscopy according to the combined aldehyde procedure described in Materials and Methods. Fluorescent signals were imaged using deconvolution microscopy as described in Materials and Methods. A, Short spindle. E, Medium spindle. I, Full-length spindle; M, Cytoplasmic microtubules in an interphase cell. Bar, 5 μm.

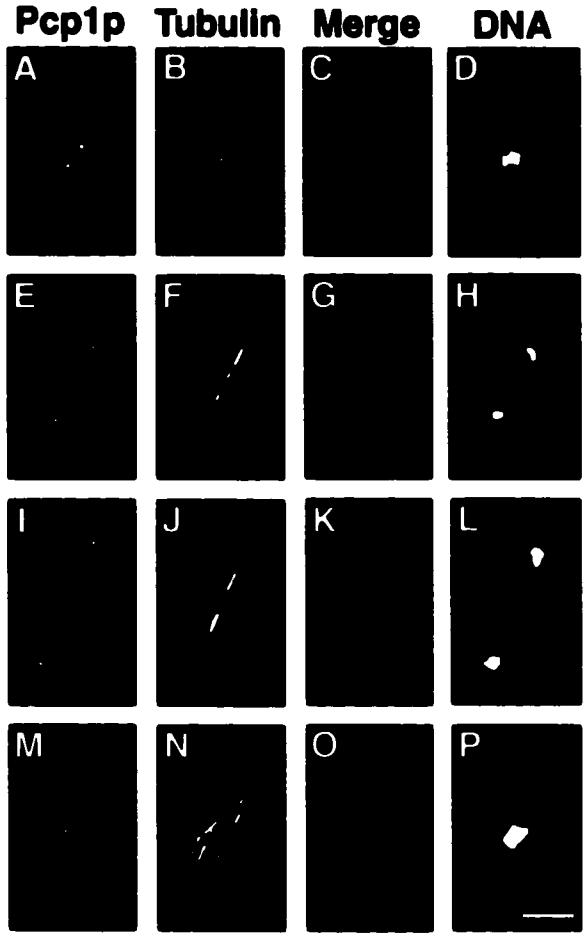
Pcp1p
Tubulin
Merge
DNA
A
B
C
D
E
F
G
H
I
J
K
L
M
N
O
P

Figure III.7. GFP:Pcp1p, tubulin, and DNA morphologies in cells overexpressing GFP:Pcp1p. A fresh isolate of strain MFP19 (*nmt1-GFP:pcp1*$^{+}$) from a –80° glycerol stock was grown to logarithmic phase in supplemented liquid YE medium at 30° and prepared for immunofluorescence microscopy according to the combined aldehyde procedure described in Materials and Methods. Fluorescent signals were imaged using deconvolution microscopy as described in Materials and Methods. A-D, GFP:Pcp1p foci of unequal intensity associated with a poorly-formed spindle and hypercondensed chromosomes. E-H and I-L, Two clusters of GFP:Pcp1p foci each associated with tubulin and chromosomal material. M-N, Three GFP:Pcp1p foci flanking an abnormal splayed, V-shaped spindle. Q-T, Multiple GFP foci in a large cell demonstrating a long, abnormally V-shaped spindle associated with three chromosomal masses. Bar, 5 μm.

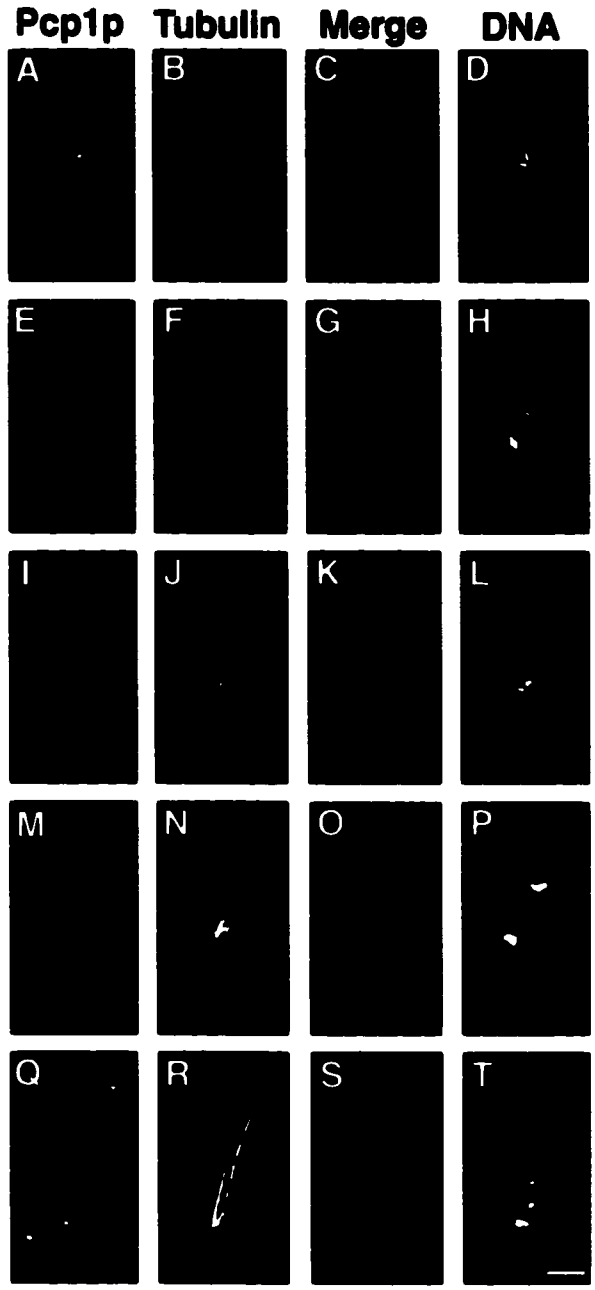
Pcp1p
Tubulin
Merge
DNA
A
B
C
D
E
F
G
H
I
J
K
L
M
N
O
P
Q
R
S
T

CHAPTER IV

A HUMAN CENTROSOMAL CALMODULIN-BINDING PROTEIN THAT SHARES HOMOLOGY WITH PERICENTRIN

Introduction

Similar to the spindle pole body (SPB) in fungi, the higher eukaryotic centrosome facilitates assembly of a mitotic spindle to faithfully segregate replicated chromosomes. The vertebrate centrosome consists of two centrioles surrounded by a fibrous layer (Kellogg et al., 1994), while the yeast SPB contains multiple laminated disk-shaped layers (Byers and Goetsch, 1975). Despite these striking morphological differences, the centrosome and SPB share many homologous molecular subunits, including calmodulin and components of the γ-tubulin complex (Knop et al., 1999; Zimmerman et al., 1999).

Given the conservation of calmodulin-binding Spc110p-related proteins in such divergent fungi as budding yeast (*Saccharomyces cerevisiae*), fission yeast (*Schizosaccharomyces pombe*), and a filamentous fungus (*Aspergillus nidulans*) as described in Chapter III, we predicted that vertebrate centrosomes might also contain a Spc110p-related calmodulin-binding protein. Furthermore, the conservation of both calmodulin (Li et al., 1999; Willingham et al., 1983; Zavortink et al., 1983) and Spc110p epitopes (Tassin et al., 1997) in mammalian centrosomes suggested the existence of a calmodulin-binding Spc110p orthologue. In higher eukaryotic cells,

nucleation of the spindle microtubules requires attachment of the centrosome to γ-tubulin (Moritz et al., 1998; Schnackenberg et al., 1998). Just as budding yeast Spc110p attaches the γ-tubulin complex to the core of the SPB (Knop and Schiebel, 1997; Nguyen et al., 1998), a calmodulin-binding Spc110p orthologue could serve to anchor the γ-tubulin complex the to vertebrate centrosomal core during microtubule nucleation.

Recruitment of the γ-tubulin complex to the centrosome is likely facilitated by pericentrin (Doxsey et al., 1994), a centrosomal protein that interacts with both γ-tubulin (Dictenberg et al., 1998) and the motor protein dynein (Purohit et al., 1999). The centrosomal proteins that subsequently anchor the γ-tubulin complex to the centrosome have not previously been identified. However, as shown in this chapter, we used knowledge of calmodulin-binding site sequences to identify a calmodulin-binding centrosomal protein in human cells whose molecular properties and subcellular distribution indicate a functional relatedness to yeast Spc110p. Like Spc110p in budding yeast, this protein may anchor the γ-tubulin complex to the centrosomal core in human cells. In mitotic carcinoma cells that contain many centrosomes (Lingle et al., 1998; Lingle and Salisbury, 1999; Pihan et al., 1998), this human Spc110p-related protein is localized exclusively to spindle poles. The work presented in this chapter was done in collaboration with M. Moser and R. Monnat, who identified and cultured human diploid fibroblasts and carcinoma lines and whose insight helped shape

the direction of our experiments. This work has been published and appears in Appendix B.

Results and Discussion

In order to identify vertebrate proteins similar to yeast Spc110p, we aligned the calmodulin-binding site of budding yeast Spc110p with the calmodulin-binding sites of two Spc110p homologues identified in the filamentous fungus *Aspergillus nidulans* and the fission yeast *Schizosaccharomyces pombe* (Appendix B, Figure 1a). These calmodulin site sequences share homology with one another (Appendix B, Figure 1a) but are distinct from the IQ-type calmodulin-binding site in myosins (consensus (I/V/L)Qxxx(R/K)Gxxx(RK), (Rhoads and Friedberg, 1997)). EST database searches using these calmodulin-binding site sequences identified two mouse EST clones and a related human EST clone. We used the human EST clone to probe a cDNA library and identified a large cDNA predicted to encode a protein named kendrin.

Kendrin contains two long central regions predicted to form coiled-coils (amino acid residues 256-1874 and 2559-3075) flanked by noncoiled regions (Appendix B, Figure 1b). The noncoiled N-terminal domain and the first coiled-coil region of kendrin (amino acid residues 1-2250) share striking homology with mouse pericentrin, a centrosome component that binds γ-tubulin (Dictenberg et al., 1998) (global alignment score = 5954, 61%

identity, Appendix B, Figure 1c). The C-terminal 1071 amino acids of kendrin containing the calmodulin-binding site show no significant homology to pericentrin (global alignment score = -757). Northern blotting revealed that full-length kendrin is encoded by a 10 kB transcript. A related 7.5 kB transcript encoding the portion of kendrin homologous to pericentrin was also detected (Appendix B, Figure 1d).

Although early reports labeled human kendrin as human pericentrin (Chen et al., 1996; Lapenta et al., 1998), three lines of evidence indicated that kendrin and pericentrin are different proteins encoded by different genes. First, both mouse and human kendrin ESTs (please see Appendix B for all relevant accession numbers) contain sequences that are not present in the mouse pericentrin cDNA (Doxsey et al., 1994). Conversely, mouse and human pericentrin EST's (defined as those corresponding to a unique 3' untranslated region in mouse pericentrin) contain sequences that are not present in kendrin cDNA. Second, human pericentrin is not encoded at the human kendrin locus. Kendrin has been mapped to chromosome 21 (21q22.3), and genomic sequence from this region includes 247 kB immediately downstream of the kendrin. This region appears to contain two additional genes (S100 and an unidentified ORF); however, the sequence for the human pericentrin EST's is not present. A final line of evidence comes from a comparison of the predicted kendrin and pericentrin proteins. If kendrin were simply a version of pericentrin with a long extension, we would

predict that the shared N-terminal 2250 amino acids would closely resemble or be identical to one another. In contrast, kendrin shows a mosaic of regions sharing high homology with mouse pericentrin (>80% identity), interspersed with multiple segments that share little or no sequence similarity (e.g. 186 residue segment with<22% conservative replacements; Appendix B, Figure 1c). Thus, mouse and human appear to contain two different genes, at different chromosomal loci, one encoding pericentrin and the other encoding kendrin.

The unique C-terminal region of kendrin directly binds calmodulin as shown by protein A-calmodulin overlay blotting (Appendix B, Figure 2a). Alanine mutagenesis of five residues in the predicted calmodulin-binding site (Appendix B, Figure 1a) dramatically decreased calmodulin binding (Appendix B, Figure 2b), confirming that calmodulin-binding activity maps to the residues predicted by sequence analysis. The five mutated residues were chosen on the basis of their conservation (Appendix B, Figure 1a) and their importance predicted from previously characterized families of calmodulin-binding sites catalogued by Dr. M. Ikura and coworkers (http://calcium.oci.utoronto.ca/ctdb/). Thus, calmodulin binding to kendrin is disrupted by mutations in five conserved residues of the predicted calmodulin-binding site.

To better understand the *in vivo* function of kendrin, we examined the subcellular localization of kendrin throughout the cell cycle in primary human

diploid fibroblasts and in human cancer cell lines that demonstrate abnormal centrosomal structures (Pihan et al., 1998). In diploid fibroblasts, antibodies raised against a unique fragment of the kendrin C-terminus (amino acids 2628-2969, Appendix B, Figure 1a) recognized centrosomes, but not microtubules, in both mitotic (Appendix B, Figure 3 a-d) and interphase (Appendix B, Figure 3 e-h) cells costained for γ- or α-tubulin. In control experiments, depletion of anti-kendrin antibodies eliminated staining of centrosomes (Appendix B, Figure 3 i versus 3 j), while selective removal of anti-GST antibodies did not diminish centrosomal staining (not shown). Also in diploid fibroblasts, immunofluorescence microscopy in combination with optical sectioning and deconvolution localized kendrin in close proximity to the distal portion of the centrioles stained by anti-centrin antibodies (Appendix B, Figure 3k).

In interphase HS578T breast carcinoma cells, kendrin colocalized with γ-tubulin to multiple aberrant centrosomal structures (226/237 foci or 95%, Appendix B, Figure 3 l and m). Colocalization of kendrin and γ-tubulin to more than two structures was observed in 90% of cells (52/58 cells, Appendix B, Figure 3 l and m). In striking contrast, a majority of mitotic HS578T breast cancer cells demonstrated a restriction of kendrin staining to two dots at the mitotic spindle poles (52/67 cells or 78%, Appendix B, Figure 3o). Costaining for kendrin and α-tubulin revealed that mitotic HS578T cells containing two dots of kendrin staining formed normal bipolar mitotic

spindles (52/52 cells). Although γ-tubulin localized to all structures in mitotic cells that contain kendrin (151/151 foci), the converse was not true: a majority of mitotic cells exhibited additional structures containing γ-tubulin but not kendrin (43/67 cells or 64%, Appendix B, Figure 3p). A smaller fraction of mitotic cells had one, three or greater than three structures containing kendrin (15/59 cells or 25%), and all of these cells formed aberrant, multipolar spindles (15/15 cells, Appendix B, Figure 3 r-t). In mitotic breast cancer cells costained for kendrin and α-tubulin, every focus of kendrin staining was associated with microtubules (59/59 cells, 127/127 foci). Finally in mitotic breast cancer cells, every focus of kendrin contained pericentrin (131/131 foci, Appendix B, Figure 3 u-w), even in cells containing abnormal numbers of kendrin foci. Thus, our localization data indicate that kendrin and pericentrin, but not γ-tubulin, are restricted to centrosomes at mitotic spindle ends in mitotic breast cancer cells. We have observed similar localization patterns for kendrin in mitotic colon cancer cells (not shown), indicating that kendrin localization is consistent in different types of human cancer cells.

In summary, several lines of evidence indicate that kendrin is a human orthologue of budding yeast Spc110p. Spc110p and kendrin share similar predicted protein structures and localize to analogous structures, the SPB (Geiser et al., 1993) and centrosome, respectively. The N-terminal region of Spc110p binds the γ-tubulin complex (Knop and Schiebel, 1997; Nguyen et

al., 1998) and the N-terminal region of kendrin is highly homologous to mouse pericentrin, which binds γ-tubulin as shown by coimmunoprecipitation, copurification, colocalization and fluorescence resonance energy transfer experiments (Dictenberg et al., 1998). The C-terminal region of Spc110p binds core SPB components (Adams and Kilmartin, 1999; Elliott et al., 1999), and kendrin localizes near centrioles at the vertebrate centrosomal core. Finally, the C-terminal regions of Spc110p (Geiser et al., 1993) and kendrin each contain a distinct calmodulin-binding site that targets Spc110p to the SPB (Kilmartin and Goh, 1996; Stirling et al., 1996; Sundberg et al., 1996) and that may target kendrin to spindle poles.

The distinct subcellular localization pattern of kendrin in interphase and mitotic cancer cells is consistent with kendrin playing an essential role in regulating the formation of spindle microtubules. Kendrin is tightly restricted during mitosis to the poles of the mitotic spindle in cancer cells containing extra centrosomal material, and all mitotic cancer cells containing tri- and tetrapolar spindles contained three or four kendrin foci, respectively, at the abnormal spindle poles. Kendrin may regulate spindle formation by recruiting pericentrin and γ-tubulin to nascent spindle poles.

Recently, a similar role has been suggested for the *Drosophila melanogaster* abnormal spindle protein (Asp). Asp, a centrosomal protein containing potential calmodulin-binding sites (Saunders et al., 1997), appears to regulate the mitotic spindle apparatus by tethering γ-tubulin complexes

together (do Carmo Avides and Glover, 1999). Despite the similarities between Asp and kendrin, the functions of these two proteins are likely distinct. Kendrin and Asp share no homology with one another, while kendrin is clearly related to pericentrin, which interacts with γ-tubulin (Dictenberg et al., 1998). The predicted structure of kendrin, like that of Spc110p, contains long central coiled-coil domains flanked by noncoiled ends, while the secondary structure of Asp is predicted to be primarily α-helical with short stretches of coiled-coil near its C-terminus (Saunders et al., 1997). Additionally, Asp is predicted to contain an actin-binding domain (Saunders et al., 1997), a feature found in neither kendrin nor Spc110p. The calmodulin-binding site of kendrin is similar to that of *S. cerevisiae* Spc110p and of the Spc110p homologues we identified in *A. nidulans* and *S. pombe*, while the IQ-type calmodulin-binding site of Asp is more similar to those found in myosins. Finally, Asp localizes to both the centrosome and the spindle and was initially purified as a microtubule-associated protein (Saunders et al., 1997), while kendrin is restricted to the centrosome, as is Spc110p. These differences indicate that the activities of kendrin may be more similar to those of Spc110p than to those of Asp. Further analysis of the functional relationships among kendrin, pericentrin, γ-tubulin, and Asp will shed light on the mechanisms controlling the complex process of mitotic spindle formation and should aid in the understanding of centrosomal abnormalities that accompany cancerous growth.

Materials and Methods

Materials and Methods for Chapter IV can be found in Appendix B.

CHAPTER V

ANALYSIS OF THE RELATIONSHIP BETWEEN MOUSE PERICENTRIN AND HUMAN KENDRIN

Introduction

Pericentrin is a critical component of the centrosome, the organelle that organizes the mitotic spindle microtubules that segregate chromosomes during cell division (Kellogg et al., 1994). Pericentrin recruits factors, including γ-tubulin (Dictenberg et al., 1998), required for microtubule nucleation. Although pericentrin was originally cloned from mouse, the cross-reactivity of mouse pericentrin antibodies with centrosomes from many vertebrates suggests that pericentrin is a highly conserved protein. Two transcripts of 9.5 and 7.0 kB were described for mouse pericentrin, and the published mouse pericentrin cDNA corresponds to the 7.0 kB transcript (Doxsey et al., 1994). A mouse cDNA corresponding to the 9.5 kB transcript has not yet been isolated.

As described in Chapter IV, a human isoform of pericentrin was recently identified that maps to human chromosome 21q22.3 (Chen et al., 1996; Lapenta et al., 1998). This protein, named kendrin (Li and Joshi, 1999), shares strong overall homology with mouse pericentrin in the N-terminal 2000 residues (Flory et al., 2000). However, kendrin also contains a unique C-terminal calmodulin-binding region that renders it much larger than mouse pericentrin (370 kD versus 220 kD). Northern blot analysis revealed two

transcripts with homology to kendrin, 10 and 7.5 kB. A 10 kB cDNA encodes the full-length 370 kD kendrin protein including the calmodulin-binding region. Northern blot analysis indicated that the 7.5 kB transcript shares homology with the 5' end of the 10 Kb cDNA, but not with the 3' end that encodes the calmodulin-binding region (Flory et al., 2000).

I provide evidence in this chapter that mouse pericentrin and human kendrin are homologues. These proteins are encoded by homologous genes in mice and humans, respectively. Mouse pericentrin represents a smaller pericentrin isoform encoded by the 7.0 kB transcript in mice, whereas human kendrin represents a longer, calmodulin-binding pericentrin isoform encoded by the 10 kB transcript in humans. In addition, we provide evidence for a short pericentrin isoform in humans and a large isoform in mice, suggesting that both pericentrin isoforms exist in mice and humans. For nomenclature, we will use *PCNT(HSA)* for the gene encoding the *Homo sapiens* pericentrin homologue and *Pcnt(MMU)* for the *Mus musculus* gene encoding the pericentrin homologue, differentiating between the long and short isoforms with –L and –S suffixes, respectively. Thus, kendrin is now referred to as pericentrin-L and the form of pericentrin perviously characterized in mouse is pericentrin-S.

Results and Discussion

The human and mouse genomic regions containing the *PCNT(HSA)* and *Pcnt(MMU)* genes, respectively, share extensive synteny, indicating these

genes are homologues. *PCNT(HSA)* maps to human chromosome 21 (21q.22.3) (Chen et al., 1996; Lapenta et al., 1998), a completely sequenced human chromosome (Hattori et al., 2000). The human chromosome 21.q22.3 region containing *PCNT(HSA)* shares synteny with a large segment of mouse chromosome 10 spanning 1.1 cM (positions 41.0-42.1) as shown by MegaBLAST analysis (http://www.ncbi.nlm.nih.gov/Homology/human21.html#PCNT). These syntenic genomic regions contain 24 homologous genes arranged in the same order (Fig. 1). This region of mouse chromosome 10 contains the *Pcnt (MMU)* gene in the exact location predicted by the position of *PCNT(HSA)* in the corresponding syntenic human chromosome 21 region. *PCNT(HSA)* and *Pcnt(MMU)* are directly flanked on both sides by homologous genes (5', *MCM3AP/GANP*; 3', *S100B/S100b*; Fig. 1), and are thus contained within the interval of synteny.

Multiple lines of evidence indicate that both *Pcnt(MMU)* and *PCNT(HSA)* encode a short pericentrin isoform. Northern blots of RNA from human and mouse tissues demonstrate mice and humans contain two transcripts homologous to pericentrin, a 7-7.5 kB transcript and a 9.5-10 kB transcript (Doxsey et al., 1994; Flory et al., 2000). Antibodies to pericentrin-S that recognize a protein of 220 kDa on Western blots react with both human and mouse centrosomes, providing evidence for pericentrin-S encoded by the ~7.5 kB transcript in both mice and humans (Doxsey et al., 1994). The

sequence of the 7.5 kB transcript in humans remains to be determined. Surprisingly, the *PCNT(HSA)* exon matching the 3' end of the ORF in the published mouse pericentrin-S cDNA does not contain the stop codon (nucleotide 6054 in mouse pericentrin-S cDNA) expected for the short form of pericentrin in humans. Furthermore, the mouse pericentrin-S 3' UTR region encompassing cDNA nucleotides 6421-6945 does not match any portion of human chromosome 21, which as noted above contains *PCNT(HSA)*. In agreement, EST BE457800, which matches the putative mouse pericentrin 3' UTR, does *not* share homology with any portion of human chromosome 21. The mouse pericentrin 3' UTR region encompassing cDNA nucleotides 6421-6945 actually shares much stronger homology with human chromosome 17. These data suggest that pericentrin cDNA 3' UTR regions including nucleotides 6421-6945 may have been mistakenly fused with the mouse pericentrin-S cDNA during construction of the cDNA library from which the composite pericentrin-S cDNA clone was assembled.

Given these sequence discrepancies, we further analyzed sequences encoding mouse pericentrin through isolation and analysis of additional corresponding mouse EST and genomic clones. Mouse EST AI747881 was identified that shares homology with the 3' ORF of the published mouse pericentrin-S cDNA. We obtained EST AI747881 (Research Genetics), which was constructed using reverse transcription primed from the 3' polyadenylated mRNA tail. We completely sequenced both strands of the

insert cDNA, and this sequence suggests that the mouse pericentrin-S cDNA does not terminate at nucleotide 6054 as previously reported (Doxsey et al., 1994). Our sequence analysis of EST AI747881 is verified by corresponding mouse genomic sequence from small shotgun clones in the public sequence database.

Finally, multiple lines of evidence support the presence of pericentrin-L with the calmodulin-binding site in both mice and humans. Pericentrin-L, first identified as kendrin in humans, is represented in the sequence databases as a complete cDNA that matches the cDNA predicted from the genomic sequence, 2 different partial cDNAs, and 71 ESTS that encode portions of the C-terminus pericentrin-L calmodulin-binding domain. Moreover, antibody to the unique C-terminal region not found in the short form, recognizes human centrosomes (Flory et al., 2000). In mouse, the genomic sequence for 3' end of the long form of pericentrin has not yet been deposited in the public mouse genomic database, but 12 mouse ESTs that encode a protein with homology to the C-terminal region of pericentrin-L in humans provide ample evidence for the presence of pericentrin-L in mice. As yet unidentified mRNA processing mechanisms may regulate the expression of pericentrin-L and -S from one gene in mice and human cells.

Together these analyses provide evidence for a large, calmodulin-binding pericentrin isoform and a smaller pericentrin isoform in both humans and mice. Data presented in this chapter also indicate relatedness between

pericentrin and the *Saccharomyces cerevisiae* centrosome protein Spc110p. Budding yeast Spc110p contains a C-terminal calmodulin-binding domain (Geiser et al., 1993) like that found in pericentrin-L (Flory et al., 2000). Pericentrin-L, *S. cerevisiae* Spc110p, and two other recently-identified fungal centrosome proteins related to Spc110p define a unique family of centrosomal calmodulin targets (Flory et al., 2000). This family may in general affect mitotic spindle formation by attaching γ-tubulin to the centrosome in a calmodulin-dependent manner, as does Spc110p in *S. cerevisiae* (Knop and Schiebel, 1997; Nguyen et al., 1998). Finally, the 10 kB transcript encoding pericentrin-L is specifically overexpressed in carcinoma cell lines (Flory et al., 2000), many of which contain centrosomes of abnormal size and number (Lingle et al., 1998; Pihan et al., 1998). Further examination of pericentrin function using antibodies specific for the human pericentrin-L (Flory et al., 2000) should complement and refine previous studies of pericentrin in normal and cancerous vertebrate cells that have been done using anti-pericentrin antibodies that likely recognize both pericentrin isoforms.

Figure V.1. Synteny map showing related regions of human chromosome 21 (21q22.3) and mouse chromosome 10. Human pericentrin (*PCNT(HSA)*) and mouse pericentrin (*Pcnt(MMU)*) are flanked on both sides by homologous genes (*MCM3AP/GANP* and *S100B/S100b*) and are thus contained within the genomic regions sharing synteny.

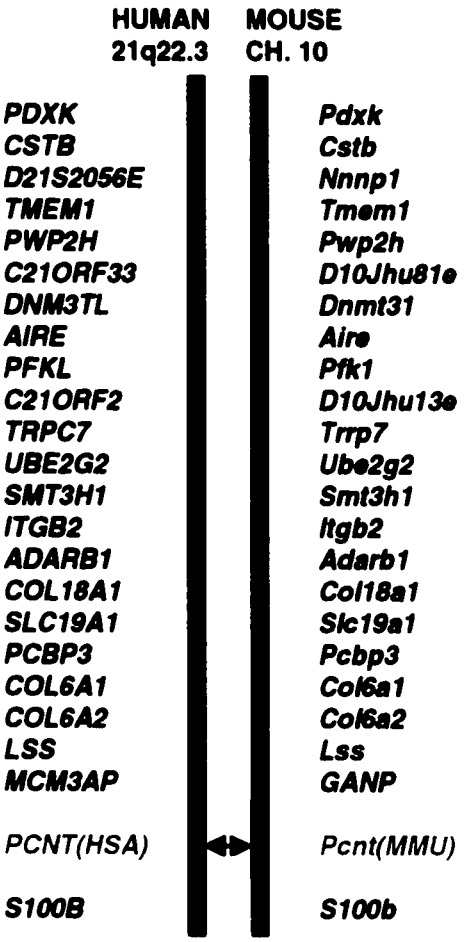
HUMAN
21q22.3
MOUSE
CH. 10
PDXK
CSTB
D21S2056E
TMEM1
PWP2H
C21ORF33
DNM3TL
AIRE
PFKL
C21ORF2
TRPC7
UBE2G2
SMT3H1
ITGB2
ADARB1
COL18A1
SLC19A1
PCBP3
COL6A1
COL6A2
LSS
MCM3AP
PCNT(HSA)
S100B
Pdxk
Cstb
Nnnp1
Tmem1
Pwp2h
D10Jhu81e
Dnmt31
Aire
Pfk1
D10Jhu13e
Trrp7
Ube2g2
Smt3h1
Itgb2
Adarb1
Col18a1
Slc19a1
Pcbp3
Col6a1
Col6a2
Lss
GANP
Pcnt(MMU)
S100b

CHAPTER VI

FUTURE DIRECTIONS

Investigation of the functional mechanisms underlying the abilities of the fungal SPB and higher eukaryotic centrosome to promote mitotic spindle assembly has reached an exciting stage. Recent advances in analytical techniques, such as mass spectrometry, in combination with the accelerating pace of genome sequencing, has revealed many of the molecular subunits of these structures. Cloning the complete set of SPB and centrosomal proteins will permit biochemical assays to be conducted on purified, recombinant proteins to dissect the relative functions of centrosomal subunits. Eventually, it may be possible to reconstitute specific centrosomal activities *in vitro*. Furthermore, the growing field of bioinformatics allows sophisticated analyses of cloned sequences to identify homologies, and common functional roles, between SPB and centrosome proteins. My contribution to understanding these homologies has been the cloning and characterization of proteins related to the budding yeast protein Spc110p from the centrosomes of the fission yeast *Schizosaccharomyces pombe* and humans. Below, I offer suggestions for further investigation of these proteins.

Analysis of interaction between Pcp1p and the fission yeast γ-tubulin complex

In *S. cerevisiae*, Spc110p physically anchors the γ-tubulin (Tub4p) complex to the budding yeast SPB (Knop and Schiebel, 1997; Nguyen et al., 1998), which is permanently embedded in the nuclear envelope throughout the

cell cycle (Byers and Goetsch, 1975). By contrast, most γ-tubulin in fission yeast resides in the nucleus just under the site of SPB insertion (Ding et al., 1997). This nuclear pool of γ-tubulin, which is complexed to Alp4p (Spc97p) and Alp6p (Spc98p) (Vardy and Toda, 2000), is brought into contact with the SPB, and associated Pcp1p, only after insertion of the SPB into the nuclear envelope fenestra (Ding et al., 1997). The insertion process may activate the nucleation capacity of the SPB by linking Pcp1p with the fission yeast γ-tubulin complex. This model could be tested using a combination of two-hybrid analysis and a fluorescence resonance energy transfer (FRET) experiment. A positive directed two-hybrid interaction between the Pcp1p N-terminus and Alp6 would indicate physical interaction analogous to that between budding yeast Spc110p N-terminus and Spc98p (Nguyen et al., 1998).

Furthermore, the insertion model for SPB activation presented above predicts that Pcp1p containing an N-terminal yellow fluorescent protein (YFP) tag would demonstrate a FRET interaction with cyan fluorescent protein (CFP)-tagged Alp6p in mitotic fission yeast cells containing inserted SPBs. This could be assessed using PCR-mediated gene tagging (Bahler et al., 1998) to create cells containing integrated YFP- and CFP-tagged alleles of Pcp1p and Alp6p, respectively. FRET interactions could then be measured in asynchronous or synchronized *S. pombe* cultures using deconvolution

microscopy according to developed protocols (D. Hailey, University of Washington, unpublished data).

Analysis of interaction between human pericentrin-L and –S isoforms

Both mouse and human pericentrin are expressed as two proteins of different size. Deconvolution immunofluorescence microscopy analysis of pericentrin-L (kendrin in human cells) indicates that the C-terminus of this protein lies between the distal ends of centrosomal centrioles (Flory et al., 2000). Pericentrin-S, which has been studied extensively by others in rodent cells, exists in a cytoplasmic complex with γ-tubulin (Dictenberg et al., 1998) and is transported, perhaps by a dynein-dependent mechanism (Purohit et al., 1999), to the centrosome. Upon reaching the centrosome the coiled-coil domain of pericentrin-S may oligomerize with the homologous coiled-coil domain of pericentrin-L. This model could be tested *in vitro* using purified recombinant pericentrin-S and pericentrin-L. Epitope-tagged pericentrin-S has already been expressed in the reticulocyte system (Dictenberg et al., 1998). Epitope-tagged human pericentrin-L (kendrin), now cloned (M. Flory and T. Davis, unpublished data), could be expressed in and purified from insect cells using the baculovirus system. Standard immunoprecipitation analyses (Dictenberg et al., 1998), taking advantage of pericentrin-L-specific antibodies (Flory et al., 2000) and epitope-tag-specific antibodies, could be

used to assess binding. Self interactions between the pericentrin-L and -S isoforms could also be tested.

Analysis of interaction between pericentrin-L and the human γ-tubulin complex

Recombinant epitope-tagged pericentrin-L (human kendrin) purified from baculovirus-infected insect cells could also be used to test for interactions with components of the human γ-tubulin complex (Murphy et al., 1998). Tim Stearns and colleagues at Stanford University have successfully expressed components of the human γ-tubulin complex in tissue culture cells, and have assessed their interaction with pericentrin-S (T. Stearns and S. Doxsey, personal communication). It would be interesting to use immunoprecipitation techniques to examine whether the binding sites identified in the pericentrin-S are also active in pericentrin-L (kendrin). I predict that pericentrin-L (kendrin) will interact with the human homologue of budding yeast Spc98p.

Depletion of pericentrin-L from human tissue culture cells

Antibodies specific for pericentrin-L (human kendrin) (Flory et al., 2000) are now available for loss-of-function experiments in cultured human cells. Reagents have recently been developed that allow transfection of proteins, including antibodies, into mammalian cell lines antibodies

(Immunoportation Ltd., Essex, UK). This technique would allow specific loss-of-function targeting of pericentrin-L (kendrin) to assess the functions of the long isoform of pericentrin. The resulting phenotype could then be assessed using immunofluorescence microscopy, taking advantage of the large set of antibodies against centrosomal and mitotic spindle proteins currently available. This type of *in vivo* loss-of-function experiment would complement the *in vitro* protein interaction assays discussed above, and should help to distinguish between the functions of the long and short isoforms of pericentrin.

BIBLIOGRAPHY

Adams, I.R., and J.V. Kilmartin. 1999. Localization of core spindle pole body (SPB) components during SPB duplication in Saccharomyces cerevisiae. *J Cell Biol.* 145:809-823.

Bahler, J., J.Q. Wu, M.S. Longtine, N.G. Shah, A. McKenzie, 3rd, A.B. Steever, A. Wach, P. Philippsen, and J.R. Pringle. 1998. Heterologous modules for efficient and versatile PCR-based gene targeting in Schizosaccharomyces pombe. *Yeast.* 14:943-951.

Basi, G., E. Schmid, and K. Maundrell. 1993. TATA box mutations in the Schizosaccharomyces pombe nmt1 promoter affect transcription efficiency but not the transcription start point or thiamine repressibility. *Gene.* 123:131-136.

Berger, B., D.B. Wilson, E. Wolf, T. Tonchev, M. Milla, and P.S. Kim. 1995. Predicting coiled coils by use of pairwise residue correlations. *Proc. Natl. Acad. Sci. USA.* 92:8259-8263.

Brinkley, B.R., and T.M. Goepfert. 1998. Supernumerary centrosomes and cancer: Boveri's hypothesis resurrected. *Cell Motil Cytoskeleton.* 41:281-288.

Brockerhoff, S.E., C.G. Edmonds, and T.N. Davis. 1992. Structural analysis of wild-type and mutant yeast calmodulins by limited proteolysis and electrospray ionization mass spectrometry. *Protein Sci.* 1:504-516.

Brockerhoff, S.E., R.C. Stevens, and T.N. Davis. 1994. The unconventional myosin, Myo2p, is a calmodulin target at sites of cell growth in Saccharomyces cerevisiae. *J Cell Biol.* 124:315-323.

Bullitt, E., M.P. Rout, J.V. Kilmartin, and C.W. Akey. 1997. The yeast spindle pole body is assembled around a central crystal of Spc42p. *Cell.* 89:1077-1086.

Burke, J.D., and K.L. Gould. 1994. Molecular cloning and characterization of the Schizosaccharomyces pombe his3 gene for use as a selectable marker. *Mol Gen Genet.* 242:169-176.

Byers, B., and L. Goetsch. 1975. Behavior of spindles and spindle plaques in the cell cycle and conjugation of Saccharomyces cerevisiae. *J Bacteriol.* 124:511-523.

Chen, H., A. Gos, M.A. Morris, and S.E. Antonarakis. 1996. Localization of a human homolog of the mouse pericentrin gene (PCNT) to chromosome 21qter. *Genomics.* 35:620-624.

Chial, H.J., M.P. Rout, T.H. Giddings, and M. Winey. 1998. Saccharomyces cerevisiae Ndc1p is a shared component of nuclear pore complexes and spindle pole bodies. *J Cell Biol.* 143:1789-1800.

Coulondre, C., and J.H. Miller. 1977. Genetic studies of the lac repressor. III. Additional correlation of mutational sites with specific amino acid residues. *J Mol Biol.* 117:525-567.

Cunningham, K.W., and G.R. Fink. 1996. Calcineurin inhibits VCX1-dependent H+/Ca2+ exchange and induces Ca2+ ATPases in Saccharomyces cerevisiae. *Mol Cell Biol.* 16:2226-2237.

Cyert, M.S., R. Kunisawa, D. Kaim, and J. Thorner. 1991. Yeast has homologs (CNA1 and CNA2 gene products) of mammalian calcineurin, a calmodulin-regulated phosphoprotein phosphatase [published erratum appears in Proc Natl Acad Sci U S A 1992 May 1;89(9):4220]. *Proc Natl Acad Sci U S A.* 88:7376-7380.

Cyert, M.S., and J. Thorner. 1992. Regulatory subunit (CNB1 gene product) of yeast Ca2+/calmodulin- dependent phosphoprotein phosphatases is required for adaptation to pheromone. *Mol Cell Biol.* 12:3460-3469.

Davis, T.N. 1992. A temperature-sensitive calmodulin mutant loses viability during mitosis. *J Cell Biol.* 118:607-617.

Davis, T.N., M.S. Urdea, F.R. Masiarz, and J. Thorner. 1986. Isolation of the yeast calmodulin gene: calmodulin is an essential protein. *Cell.* 47:423-431.

Dictenberg, J.B., W. Zimmerman, C.A. Sparks, A. Young, C. Vidair, Y. Zheng, W. Carrington, F.S. Fay, and S.J. Doxsey. 1998. Pericentrin and gamma-tubulin form a protein complex and are organized into a novel lattice at the centrosome. *J Cell Biol.* 141:163-174.

Ding, R., K.L. McDonald, and J.R. McIntosh. 1993. Three-dimensional reconstruction and analysis of mitotic spindles from the yeast, Schizosaccharomyces pombe. *J Cell Biol.* 120:141-151.

Ding, R., R.R. West, D.M. Morphew, B.R. Oakley, and J.R. McIntosh. 1997. The spindle pole body of Schizosaccharomyces pombe enters and leaves the nuclear envelope as the cell cycle proceeds. *Mol Biol Cell.* 8:1461-1479.

do Carmo Avides, M., and D.M. Glover. 1999. Abnormal spindle protein, Asp, and the integrity of mitotic centrosomal microtubule organizing centers. *Science.* 283:1733-1735.

Doxsey, S.J., P. Stein, L. Evans, P.D. Calarco, and M. Kirschner. 1994. Pericentrin, a highly conserved centrosome protein involved in microtubule organization [see comments]. *Cell.* 76:639-650.

Elliott, S., M. Knop, G. Schlenstedt, and E. Schiebel. 1999. Spc29p is a component of the Spc110p subcomplex and is essential for spindle pole body duplication. *Proc Natl Acad Sci U S A.* 96:6205-6210.

Erickson, H.P. 2000. Gamma-tubulin nucleation: template or protofilament? [news; comment]. *Nat Cell Biol.* 2:E93-96.

Flory, M.R., M.J. Moser, R.J. Monnat, Jr., and T.N. Davis. 2000. Identification of a human centrosomal calmodulin-binding protein that shares homology with pericentrin. *Proc Natl Acad Sci U S A.* 97:5919-5923.

Forsburg, S.L. 1993. Comparison of Schizosaccharomyces pombe expression systems. *Nucleic Acids Res.* 21:2955-2956.

Geiser, J.R., H.A. Sundberg, B.H. Chang, E.G. Muller, and T.N. Davis. 1993. The essential mitotic target of calmodulin is the 110-kilodalton component of the spindle pole body in Saccharomyces cerevisiae. *Mol Cell Biol.* 13:7913-7924.

Geiser, J.R., D. van Tuinen, S.E. Brockerhoff, M.M. Neff, and T.N. Davis. 1991. Can calmodulin function without binding calcium? *Cell.* 65:949-959.

Gutz, H., H. Heslot, U. Leupold, and N. Loprieno. 1972. *Schizosaccharomycs pombe. In* Handbook of Genetics. R.C. King, editor, Plenum, New York.

Hagan, I., and M. Yanagida. 1992. Kinesin-related cut7 protein associates with mitotic and meiotic spindles in fission yeast. *Nature.* 356:74-76.

Hagan, I., and M. Yanagida. 1995. The product of the spindle formation gene sad1+ associates with the fission yeast spindle pole body and is essential for viability. *J Cell Biol.* 129:1033-1047.

Hagan, I.M., and J.S. Hyams. 1988. The use of cell division cycle mutants to investigate the control of microtubule distribution in the fission yeast Schizosaccharomyces pombe. *J Cell Sci.* 89:343-357.

Hattori, M., A. Fujiyama, T.D. Taylor, H. Watanabe, T. Yada, H.S. Park, A. Toyoda, K. Ishii, Y. Totoki, D.K. Choi, E. Soeda, M. Ohki, T. Takagi,

Y. Sakaki, S. Taudien, K. Blechschmidt, A. Polley, U. Menzel, J. Delabar, K. Kumpf, R. Lehmann, D. Patterson, K. Reichwald, A. Rump, M. Schillhabel, and A. Schudy. 2000. The DNA sequence of human chromosome 21. The chromosome 21 mapping and sequencing consortium [see comments]. *Nature*. 405:311-319.

Hiraoka, Y., T. Toda, and M. Yanagida. 1984. The NDA3 gene of fission yeast encodes beta-tubulin: a cold-sensitive nda3 mutation reversibly blocks spindle formation and chromosome movement in mitosis. *Cell*. 39:349-358.

Horio, T., S. Uzawa, M.K. Jung, B.R. Oakley, K. Tanaka, and M. Yanagida. 1991. The fission yeast gamma-tubulin is essential for mitosis and is localized at microtubule organizing centers. *J Cell Sci*. 99:693-700.

Joseph, J.D., and A.R. Means. 2000. Identification and characterization of two Ca2+/CaM-dependent protein kinases required for normal nuclear division in aspergillus nidulans [In Process Citation]. *J Biol Chem*. 275:38230-38238.

Kahana, J.A., B.J. Schnapp, and P.A. Silver. 1995. Kinetics of spindle pole body separation in budding yeast. *Proc Natl Acad Sci U S A*. 92:9707-9711.

Keating, T.J., and G.G. Borisy. 2000. Immunostructural evidence for the template mechanism of microtubule nucleation [see comments]. *Nat Cell Biol*. 2:352-357.

Kellogg, D.R., M. Moritz, and B.M. Alberts. 1994. The centrosome and cellular organization. *Annu Rev Biochem.* 63:639-674.

Khodjakov, A., and C.L. Rieder. 1999. The sudden recruitment of gamma-tubulin to the centrosome at the onset of mitosis and its dynamic exchange throughout the cell cycle, do not require microtubules. *J Cell Biol.* 146:585-596.

Kilmartin, J.V., S.L. Dyos, D. Kershaw, and J.T. Finch. 1993. A spacer protein in the Saccharomyces cerevisiae spindle poly body whose transcript is cell cycle-regulated. *J Cell Biol.* 123:1175-1184.

Kilmartin, J.V., and P.Y. Goh. 1996. Spc110p: assembly properties and role in the connection of nuclear microtubules to the yeast spindle pole body. *Embo J.* 15:4592-4602.

Knop, M., G. Pereira, S. Geissler, K. Grein, and E. Schiebel. 1997. The spindle pole body component Spc97p interacts with the gamma-tubulin of Saccharomyces cerevisiae and functions in microtubule organization and spindle pole body duplication. *Embo J.* 16:1550-1564.

Knop, M., G. Pereira, and E. Schiebel. 1999. Microtubule organization by the budding yeast spindle pole body. *Biol Cell.* 91:291-304.

Knop, M., and E. Schiebel. 1997. Spc98p and Spc97p of the yeast gamma-tubulin complex mediate binding to the spindle pole body via their interaction with Spc110p. *Embo J.* 16:6985-6995.

Knop, M., and E. Schiebel. 1998. Receptors determine the cellular localization of a gamma-tubulin complex and thereby the site of microtubule formation. *Embo J.* 17:3952-3967.

Kunkel, T.A., J.D. Roberts, and R.A. Zakour. 1987. Rapid and efficient site-specific mutagenesis without phenotypic selection. *Methods Enzymol.* 154:367-382.

Lapenta, V., V. Sossi, P. Gosset, C. Vayssettes, T. Vitali, N. Rabatel, F. Tassone, J.L. Blouin, H.S. Scott, S.E. Antonarakis, N. Creau, and C. Brahe. 1998. Construction of a 2.5-Mb integrated physical and gene map of distal 21q22.3. *Genomics.* 49:1-13.

Li, C.J., R. Heim, P. Lu, Y. Pu, R.Y. Tsien, and D.C. Chang. 1999. Dynamic redistribution of calmodulin in HeLa cells during cell division as revealed by a GFP-calmodulin fusion protein technique. *J Cell Sci.* 112:1567-1577.

Li, Q., and H.C. Joshi. 1999. accession U52962. .

Lillie, S.H., and S.S. Brown. 1994. Immunofluorescence localization of the unconventional myosin, Myo2p, and the putative kinesin-related protein, Smy1p, to the same regions of polarized growth in Saccharomyces cerevisiae. *J Cell Biol.* 125:825-842.

Lingle, W.L., W.H. Lutz, J.N. Ingle, N.J. Maihle, and J.L. Salisbury. 1998. Centrosome hypertrophy in human breast tumors: implications for

genomic stability and cell polarity. *Proc Natl Acad Sci U S A.* 95:2950-2955.

Lingle, W.L., and J.L. Salisbury. 1999. Altered centrosome structure is associated with abnormal mitoses in human breast tumors. *Am J Pathol.* 155:1941-1951.

Lu, K.P., S.A. Osmani, A.H. Osmani, and A.R. Means. 1993. Essential roles for calcium and calmodulin in G2/M progression in Aspergillus nidulans. *J Cell Biol.* 121:621-630.

Marks, J., I.M. Hagan, and J.S. Hyams. 1986. Growth polarity and cytokinesis in fission yeast: the role of the cytoskeleton. *J Cell Sci Suppl.* 5:229-241.

Martin, O.C., R.N. Gunawardane, A. Iwamatsu, and Y. Zheng. 1998. Xgrip109: a gamma tubulin-associated protein with an essential role in gamma tubulin ring complex (gammaTuRC) assembly and centrosome function. *J Cell Biol.* 141:675-687.

Maundrell, K. 1990. nmt1 of fission yeast. A highly transcribed gene completely repressed by thiamine. *J Biol Chem.* 265:10857-10864.

McCully, E.K., and C.F. Robinow. 1971. Mitosis in the fission yeast Schizosaccharomyces pombe: a comparative study with light and electron microscopy. *J Cell Sci.* 9:475-507.

Means, A.R. 1994. Calcium, calmodulin and cell cycle regulation. *FEBS Lett.* 347:1-4.

Miller, J.H. 1972. Experiments in Molecular Genetics. Cold Spring Harbor Laboratory, Cold Spring Harbor, New York.

Mitchison, J.M., and P. Nurse. 1985. Growth in cell length in the fission yeast Schizosaccharomyces pombe. *J Cell Sci.* 75:357-376.

Moritz, M., M.B. Braunfeld, V. Guenebaut, J. Heuser, and D.A. Agard. 2000. Structure of the gamma-tubulin ring complex: a template for microtubule nucleation [see comments]. *Nat Cell Biol.* 2:365-370.

Moritz, M., M.B. Braunfeld, J.W. Sedat, B. Alberts, and D.A. Agard. 1995. Microtubule nucleation by gamma-tubulin-containing rings in the centrosome. *Nature.* 378:638-640.

Moritz, M., Y. Zheng, B.M. Alberts, and K. Oegema. 1998. Recruitment of the gamma-tubulin ring complex to Drosophila salt- stripped centrosome scaffolds. *J Cell Biol.* 142:775-786.

Moser, M.J., M.R. Flory, and T.N. Davis. 1997. Calmodulin localizes to the spindle pole body of Schizosaccharomyces pombe and performs an essential function in chromosome segregation. *J Cell Sci.* 110:1805-1812.

Moser, M.J., S.Y. Lee, R.E. Klevit, and T.N. Davis. 1995. Ca2+ binding to calmodulin and its role in Schizosaccharomyces pombe as revealed by mutagenesis and NMR spectroscopy. *J Biol Chem.* 270:20643-20652.

Murphy, S.M., L. Urbani, and T. Stearns. 1998. The mammalian gamma-tubulin complex contains homologues of the yeast spindle pole body components spc97p and spc98p. *J Cell Biol.* 141:663-674.

Nabeshima, K., H. Kurooka, M. Takeuchi, K. Kinoshita, Y. Nakaseko, and M. Yanagida. 1995. p93dis1, which is required for sister chromatid separation, is a novel microtubule and spindle pole body-associating protein phosphorylated at the Cdc2 target sites. *Genes Dev.* 9:1572-1585.

Nguyen, T., D.B.N. Vinh, D.K. Crawford, and T.N. Davis. 1998. A genetic analysis of interactions with Spc110p reveals distinct functions of Spc97p and Spc98p, components of the yeast gamma-tubulin complex. *Mol Biol Cell.* 9:2201-2216.

Oegema, K., C. Wiese, O.C. Martin, R.A. Milligan, A. Iwamatsu, T.J. Mitchison, and Y. Zheng. 1999. Characterization of two related Drosophila gamma-tubulin complexes that differ in their ability to nucleate microtubules. *J Cell Biol.* 144:721-733.

Ohya, Y., and D. Botstein. 1994. Diverse essential functions revealed by complementing yeast calmodulin mutants. *Science.* 263:963-966.

Ohya, Y., H. Kawasaki, K. Suzuki, J. Londesborough, and Y. Anraku. 1991. Two yeast genes encoding calmodulin-dependent protein kinases. Isolation, sequencing and bacterial expressions of CMK1 and CMK2. *J Biol Chem.* 266:12784-12794.

Osborne, M.A., G. Schlenstedt, T. Jinks, and P.A. Silver. 1994. Nuf2, a spindle pole body-associated protein required for nuclear division in yeast. *J Cell Biol.* 125:853-866.

Pausch, M.H., D. Kaim, R. Kunisawa, A. Admon, and J. Thorner. 1991. Multiple Ca2+/calmodulin-dependent protein kinase genes in a unicellular eukaryote. *Embo J.* 10:1511-1522.

Pihan, G.A., A. Purohit, J. Wallace, H. Knecht, B. Woda, P. Quesenberry, and S.J. Doxsey. 1998. Centrosome defects and genetic instability in malignant tumors. *Cancer Res.* 58:3974-3985.

Pozos, T.C., I. Sekler, and M.S. Cyert. 1996. The product of HUM1, a novel yeast gene, is required for vacuolar Ca2+/H+ exchange and is related to mammalian Na+/Ca2+ exchangers. *Mol Cell Biol.* 16:3730-3741.

Purohit, A., S.H. Tynan, R. Vallee, and S.J. Doxsey. 1999. Direct interaction of pericentrin with cytoplasmic dynein light intermediate chain contributes to mitotic spindle organization. *J Cell Biol.* 147:481-492.

Rasmussen, C., C. Garen, S. Brining, R.L. Kincaid, R.L. Means, and A.R. Means. 1994. The calmodulin-dependent protein phosphatase catalytic subunit (calcineurin A) is an essential gene in Aspergillus nidulans. *Embo J.* 13:3917-3924.

Rasmussen, C.D., K.P. Lu, R.L. Means, and A.R. Means. 1992. Calmodulin and cell cycle control. *J Physiol Paris.* 86:83-88.

Rasmussen, C.D., R.L. Means, K.P. Lu, G.S. May, and A.R. Means. 1990. Characterization and expression of the unique calmodulin gene of Aspergillus nidulans. *J Biol Chem.* 265:13767-13775.

Rhoads, A.R., and F. Friedberg. 1997. Sequence motifs for calmodulin recognition. *Faseb J.* 11:331-340.

Saunders, R.D., M.C. Avides, T. Howard, C. Gonzalez, and D.M. Glover. 1997. The Drosophila gene abnormal spindle encodes a novel microtubule- associated protein that associates with the polar regions of the mitotic spindle. *J Cell Biol.* 137:881-890.

Schnackenberg, B.J., A. Khodjakov, C.L. Rieder, and R.E. Palazzo. 1998. The disassembly and reassembly of functional centrosomes in vitro. *Proc Natl Acad Sci U S A.* 95:9295-9300.

Seedorf, M., M. Damelin, J. Kahana, T. Taura, and P.A. Silver. 1999. Interactions between a nuclear transporter and a subset of nuclear pore complex proteins depend on Ran GTPase. *Mol Cell Biol.* 19:1547-1557.

Sherman, F., G.R. Fink, and J.B. Hicks. 1986. Methods in Yeast Genetics. Cold Spring Harbor Laboratory, Cold Spring Harbor, New York.

Sohrmann, M., C. Fankhauser, C. Brodbeck, and V. Simanis. 1996. The dmf1/mid1 gene is essential for correct positioning of the division septum in fission yeast. *Genes Dev.* 10:2707-2719.

Spang, A., S. Geissler, K. Grein, and E. Schiebel. 1996. gamma-Tubulin-like Tub4p of Saccharomyces cerevisiae is associated with the spindle pole body substructures that organize microtubules and is required for mitotic spindle formation. *J Cell Biol.* 134:429-441.

Stirling, D.A., A. Petrie, D.J. Pulford, D.T. Paterson, and M.J. Stark. 1992. Protein A-calmodulin fusions: a novel approach for investigating calmodulin function in yeast. *Mol Microbiol.* 6:703-713.

Stirling, D.A., T.F. Rayner, A.R. Prescott, and M.J. Stark. 1996. Mutations which block the binding of calmodulin to Spc110p cause multiple mitotic defects. *J Cell Sci.* 109:1297-1310.

Stirling, D.A., and M.J. Stark. 1996. The phosphorylation state of the 110 kDa component of the yeast spindle pole body shows cell cycle dependent regulation. *Biochem Biophys Res Commun.* 222:236-242.

Stirling, D.A., K.A. Welch, and M.J. Stark. 1994. Interaction with calmodulin is required for the function of Spc110p, an essential component of the yeast spindle pole body. *Embo J.* 13:4329-4342.

Sun, G.H., A. Hirata, Y. Ohya, and Y. Anraku. 1992. Mutations in yeast calmodulin cause defects in spindle pole body functions and nuclear integrity. *J Cell Biol.* 119:1625-1639.

Sundberg, H.A., L. Goetsch, B. Byers, and T.N. Davis. 1996. Role of calmodulin and Spc110p interaction in the proper assembly of spindle pole body compenents. *J Cell Biol.* 133:111-124.

Takeda, T., and M. Yamamoto. 1987. Analysis and in vivo disruption of the gene coding for calmodulin in Schizosaccharomyces pombe. *Proc Natl Acad Sci U S A.* 84:3580-3584.

Tanaka, K., and T. Kanbe. 1986. Mitosis in the fission yeast Schizosaccharomyces pombe as revealed by freeze-substitution electron microscopy. *J Cell Sci.* 80:253-268.

Tassin, A.M., C. Celati, M. Moudjou, and M. Bornens. 1998. Characterization of the human homologue of the yeast spc98p and its association with gamma-tubulin. *J Cell Biol.* 141:689-701.

Tassin, A.M., C. Celati, M. Paintrand, and M. Bornens. 1997. Identification of an Spc110p-related protein in vertebrates. *J Cell Sci.* 110:2533-2545.

Vardy, L., and T. Toda. 2000. The fission yeast gamma-tubulin complex is required in G(1) phase and is a component of the spindle assembly checkpoint. *Embo J.* 19:6098-6111.

Waddle, J.A., T.S. Karpova, R.H. Waterston, and J.A. Cooper. 1996. Movement of cortical actin patches in yeast. *J Cell Biol.* 132:861-870.

West, R.R., E.V. Vaisberg, R. Ding, P. Nurse, and J.R. McIntosh. 1998. cut11(+): A gene required for cell cycle-dependent spindle pole body anchoring in the nuclear envelope and bipolar spindle formation in Schizosaccharomyces pombe. *Mol Biol Cell.* 9:2839-2855.

Wiese, C., and Y. Zheng. 2000. A new function for the gamma-tubulin ring complex as a microtubule minus-end cap [see comments]. *Nat Cell Biol.* 2:358-364.

Wigge, P.A., O.N. Jensen, S. Holmes, S. Soues, M. Mann, and J.V. Kilmartin. 1998. Analysis of the Saccharomyces spindle pole by matrix-assisted laser desorption/ionization (MALDI) mass spectrometry. *J Cell Biol.* 141:967-977.

Willingham, M.C., J. Wehland, C.B. Klee, N.D. Richert, A.V. Rutherford, and I.H. Pastan. 1983. Ultrastructural immunocytochemical localization of calmodulin in cultured cells. *J Histochem Cytochem.* 31:445-461.

Winey, M., and B. Byers. 1993. Assembly and functions of the spindle pole body in budding yeast. *Trends Genet.* 9:300-304.

Winey, M., C.L. Mamay, E.T. O'Toole, D.N. Mastronarde, T.H. Giddings, Jr., K.L. McDonald, and J.R. McIntosh. 1995. Three-dimensional ultrastructural analysis of the Saccharomyces cerevisiae mitotic spindle. *J Cell Biol.* 129:1601-1615.

Yanagida, M. 1998. Fission yeast cut mutations revisited: control of anaphase. *Trends Cell Biol.* 8:144-149.

Yoshida, T., T. Toda, and M. Yanagida. 1994. A calcineurin-like gene ppb1+ in fission yeast: mutant defects in cytokinesis, cell polarity, mating and spindle pole body positioning. *J Cell Sci.* 107:1725-1735.

Zavortink, M., M.J. Welsh, and J.R. McIntosh. 1983. The distribution of calmodulin in living mitotic cells. *Exp Cell Res.* 149:375-385.

Zheng, Y., M.L. Wong, B. Alberts, and T. Mitchison. 1995. Nucleation of microtubule assembly by a gamma-tubulin-containing ring complex. *Nature*. 378:578-583.

Zimmerman, W., C.A. Sparks, and S.J. Doxsey. 1999. Amorphous no longer: the centrosome comes into focus. *Curr Opin Cell Biol.* 11:122-128.

Appendix A: Calmodulin localizes to the spindle pole body of *Schizosaccharomyces pombe* and performs an essential function in chromosome segregation

Journal of Cell Science 110, 1805-1812 (1997)
Printed in Great Britain © The Company of Biologists Limited 1997
JCS8134

Calmodulin localizes to the spindle pole body of *Schizosaccharomyces pombe* and performs an essential function in chromosome segregation

Michael J. Moser[1,*,†], Mark R. Flory[2,*] and Trisha N. Davis[1,‡]

[1]Department of Biochemistry, Box 357350, University of Washington, Seattle, WA 98195, USA
[2]Molecular and Cellular Biology Program, University of Washington, Seattle, WA 98195, USA

*The first two authors contributed equally to this work
†Present address: Department of Pathology, Box 357470, University of Washington, Seattle, WA 98195, USA
‡Author for correspondence (e-mail: tdavis@u.washington.edu)

SUMMARY

The essential calmodulin genes in both *Saccharomyces cerevisiae* and *Schizosaccharomyces pombe* were precisely replaced with genes encoding fusions between calmodulin and the green fluorescent protein (GFP). In living budding yeast the GFP-calmodulin fusion protein (GFP-Cmd1p) localized simultaneously to sites of cell growth and to the spindle pole body (SPB), the yeast analog of the centrosome. Having demonstrated proper localization of GFP-calmodulin in budding yeast, we examined the localization of a fusion between GFP and calmodulin (GFP-Cam1p) in fission yeast, where calmodulin had not been localized by any method. We find GFP-Cam1p also localizes both to sites of polarized cell growth and to the fission yeast SPB. The localization of calmodulin to the SPB by GFP fusion was confirmed by indirect immunofluorescence. Antiserum to *S. pombe* calmodulin labeled the ends of the mitotic spindle stained with anti-tubulin antiserum. This pattern was identical to that seen using antiserum to Sad1p, a known SPB component. We then characterized the defects in a temperature-sensitive *S. pombe* calmodulin mutant. Mutant *cam1-E14* cells synchronized in S phase completed DNA synthesis, but lost viability during transit of mitosis. Severe defects in chromosome segregation, including hypercondensation, fragmentation, and unequal allocation of chromosomal material were observed. Immunofluorescence analysis of tubulin revealed a population of cells containing either broken or mislocalized mitotic spindles, which were never observed in wild-type cells. Taken together with the subcellular localization of calmodulin, the observed spindle and chromosome segregation defects suggest that calmodulin performs an essential role during mitosis at the fission yeast SPB.

Key words: Calmodulin, Mitosis, Centrosome, GFP, Yeast

INTRODUCTION

Calmodulin is a small eukaryotic protein that reversibly binds Ca^{2+}. Study of calmodulin in genetically tractable organisms has yielded many insights into calmodulin function. Calmodulin is essential for proliferation in fungi, including the yeasts *Saccharomyces cerevisiae* (Davis et al., 1986), and *Schizosaccharomyces pombe* (Takeda and Yamamoto, 1987), as well as the filamentous fungi *Aspergillus nidulans* (Rasmussen et al., 1990). The function of calmodulin has been extensively studied in *S. cerevisiae* with appreciable work also performed in *A. nidulans*. Although both species are fungi, the relative importance of the Ca^{2+}-dependent functions for calmodulin differ markedly.

In *S. cerevisiae*, the Ca^{2+}-binding function of calmodulin is dispensable for cell growth and division. Mutant calmodulins in which the Ca^{2+}-binding sites are inactivated support growth (Geiser et al., 1991). Furthermore, neither the Ca^{2+}-calmodulin-dependent protein kinase nor the Ca^{2+}-calmodulin-dependent phosphatase calcineurin are required for growth (Cyert et al., 1991; Cyert and Thorner, 1992; Moser et al., 1996; Ohya et al., 1991; Pausch et al., 1991). However, Ca^{2+}-calmodulin and the Ca^{2+}-calmodulin dependent enzymes are required for survival in mating pheromone and for maintaining ion homeostasis (Cunningham and Fink, 1996; Moser et al., 1996; Pozos et al., 1996). Thus, the conservation of the Ca^{2+}-binding sites in calmodulin throughout evolution is readily explained.

Diverse techniques have identified two essential Ca^{2+}-independent functions for calmodulin during the *S. cerevisiae* cell cycle. First, calmodulin is required to bind Spc110p, a coiled-coil protein that connects the inner and central layers of the spindle pole body (SPB), the yeast mitotic microtubule organizing center (Geiser et al., 1993; Kilmartin et al., 1993; Stirling et al., 1994). Calmodulin localizes to the SPB and this localization is dependent on the calmodulin-binding site in Spc110p (Spang et al., 1996). This interaction is essential for proper assembly of spindle pole components because mutations in the C-terminal calmodulin-binding site of Spc110p result in the formation of large electron-dense structures that appear to nucleate microtubules (Sundberg et al., 1996). The presence of calmodulin at the SPB is also required for proper function of the spindle during mitosis (Davis, 1992; Kilmartin and Goh, 1996; Stirling et al., 1996; Sun et al., 1992a; Sundberg et al., 1996).

Calmodulin is also important for polarized growth in

S. cerevisiae (Davis, 1992; Ohya and Botstein, 1994). The polarized growth function of budding yeast calmodulin is mediated by interaction with an unconventional type V myosin, Myo2p (Brockerhoff et al., 1994). Calmodulin binds in a Ca^{2+}-independent manner in vitro to a region of Myo2p containing IQ sites (Brockerhoff et al., 1994). This binding is believed to be responsible for the co-localization of calmodulin and Myo2p throughout the cell cycle (Brockerhoff et al., 1992, 1994; Lillie and Brown, 1994; Sun et al., 1992b).

In striking contrast to *S. cerevisiae*, *A. nidulans* requires Ca^{2+}-calmodulin for cell cycle progression. *A. nidulans* calmodulins mutated in the Ca^{2+}-binding sites do not support growth and division. Calmodulin appears to function at two points in the *A. nidulans* cell cycle (Rasmussen et al., 1992). Deletion of the gene encoding the calcineurin A subunit causes *A. nidulans* to arrest early in the cell cycle, suggesting an essential role for Ca^{2+}-calmodulin at the G_1 to S phase transition (Rasmussen et al., 1994). Later in the cell cycle, depletion of calmodulin blocks the ability of *A. nidulans* to progress from a *nimT* block between G_2 and M (Lu et al., 1993). The unique gene encoding *A. nidulans* Ca^{2+}-calmodulin-dependent protein kinase is also essential (Means, 1994). Thus, *A. nidulans* requires Ca^{2+}-calmodulin during cell cycle progression to activate both calcineurin and Ca^{2+}-calmodulin-dependent protein kinase. If calmodulin functions at the SPB or at sites of polarized growth and whether these putative functions are Ca^{2+}-dependent in *A. nidulans* is not known.

S. pombe requires at least one intact Ca^{2+}-binding site for growth (Moser et al., 1995). Thus, like *A. nidulans*, *S. pombe* appears to require Ca^{2+}-calmodulin for some aspect of cellular proliferation. The importance of Ca^{2+}-binding to calmodulin in fission yeast might suggest that Ca^{2+}-dependent calmodulin targets that are essential in *A. nidulans* might also be essential in *S. pombe*. However, the only Ca^{2+}-dependent calmodulin binding protein found so far in *S. pombe*, calcineurin, is not essential for growth although over-expression of calcineurin does affect SPB and nuclear positioning (Yoshida et al., 1994). Essential Ca^{2+}-calmodulin dependent enzymes may yet be found in *S. pombe*. Alternatively, the essential Ca^{2+}-independent SPB and polarized growth functions of calmodulin found in *S. cerevisiae* might also exist in *S. pombe*, but they may be Ca^{2+}-dependent. As a starting point in assessing the essential roles of calmodulin in *S. pombe*, the subcellular localization of calmodulin was determined and compared to that in *S. cerevisiae*. We also characterized the defects conferred by temperature-sensitive mutations in *S. pombe* calmodulin. These cytological and genetic methods suggest that calmodulin functions in *S. pombe* strongly resemble those previously identified in *S. cerevisiae*, thus suggesting universal functions for calmodulin.

MATERIALS AND METHODS

Media

S. cerevisiae rich medium was YPD and minimal medium was SD (Sherman et al., 1986) supplemented as described (Geiser et al., 1991). Uracil auxotrophs were isolated on SD complete medium containing 1 mg/ml 5-fluoro-orotic acid (5-FOA) (Toronto Research).

S. pombe rich media were YE (Gutz et al., 1972) and minimal medium (EMM2) (Mitchison, 1970) supplemented with 100 μg/ml adenine, leucine and uracil. Either 5-FOA or G418 (Gibco BRL) were added to YE agar at mg/ml and 100 μg/ml, respectively.

Plasmids

S. pombe

Plasmid pZA59 containing GFP engineered with a C-terminal Gly-Ala spacer and N- and C-terminal *Bsp*HI restriction sites that can be inserted upstream of a gene containing an *Nco*I site at the initiating ATG was constructed by PCR amplification using plasmid TU#65 (Chalfie et al., 1994) as a template with primers 5'GGTCATGAG-TAAAGGAGAAGAAC3' and 5'CGTACCTACTTGATATGTT TCCGCGGCCGCGACCACGACCACGACCGCGGTAGTACTT TATCC3'. The PCR product was cloned using the pGEM T-Vector (Promega). Plasmid pZA66 encoding S65T-GFP (Heim et al., 1995) lacking an internal *Nco*I site was constructed by oligo-mediated mutagenesis (Kunkel et al., 1987) with pZA59 as a template using primer: 5'GGAAAACTACCTGTTCCTTGGCCAACACTTGTCAC-TACTTTCACTTATGGTGTTCAATGC3'. Plasmid pZA61 (*ars1, LEU2, GFP::cam1*$^+$), plasmid pZA72 (*ars1, LEU2, S65T-GFP::cam1*$^+$) and plasmid pZA73 (*ars1, LEU2, S65T-GFP::cam1-E14*) containing N-terminal fusions of GFP to *S. pombe cam1* were constructed by ligating the 747 bp *Bsp*HI fragments from either plasmid pZA59 or pZA66 into the unique *Nco*I site at the initiating ATG of *cam1*$^+$ in plasmids pIRT2/CAM1ΔINT (*ars1, LEU2, cam1*$^+$*Δintron*) (Moser et al., 1995) and pZA70 (*ars1, LEU2, S65T-GFP::cam1-E14Δintron*).

S. cerevisiae

The 747 bp *Bsp*HI fragment from pZA66 containing S65T-GFP was ligated in frame to the *CMD1* gene at the initiating ATG at the unique *Nco*I sites in plasmid pJG7 (Geiser et al., 1991), and plasmids pHS9 and pHS24 (Geiser et al., 1993); resulting in plasmid pMM135 (*CEN, URA3* and *S65T-GFP::CMD1*), plasmid pMM137 (*S65T-GFP::cmd1-6*), and plasmid pMM138 (*S65T-GFP::cmd1-1*), respectively.

Strains

S. pombe

The genotype of wild-type strain MP5-1C is *h*$^-$, *ade6-M216, cam1*$^+$, *leu1-32, ura4-D18*; that of MP33-6B is *h*$^-$, *ade6-M210, cam1*$^+$, *leu1-32, ura4-D18*. Calmodulin mutant strains MP64 (*h*$^-$, *ade1-D25, ade6-M210, cam-E14, leu1-32, ura4-D18*), MP76 (*h*$^-$, *ade1-D25, ade6-M210, GFP::cam1*$^+$, *leu1-32, ura4-D18*) and MFP7 (*h*$^-$, *ade1-D25, ade6-M210, S65T-GFP::cam1*$^+$, *leu1-32, ura4-D18*) were constructed as follows. Strain MP24-6C (*h*$^-$, *ade1-D25, ade6-M210, cam1Δ::ura4*$^+$, *leu1-32, ura4-D18*) containing plasmid pADE1/VCAM encoding G418 resistance, *ade1*$^+$, and vertebrate calmodulin (Moser et al., 1995) was transformed with plasmid pZA10 (*cam-E14*) (Moser et al., 1995), plasmid pZA61 (*GFP::cam1*$^+$), or plasmid pZA72 (*LEU2, S65T-GFP::cam1*$^+$) and leucine prototrophs were selected. Leu$^+$ transformants that had lost the pADE1/VCAM plasmid were identified as those unable to produce red colony pigment and sensitive to G418. Strains dependent solely on *LEU2* plasmid encoded mutant calmodulin were first grown on YE medium and then colonies resistant to 5-FOA were selected. Resistant colonies had undergone recombination between the plasmid encoded *cam1* sequences and the chromosomal *cam1Δ::ura4*$^+$ locus. Strains resistant to 5-FOA were screened for uracil and leucine auxotrophy to isolate integrant strains that had undergone replacement and then lost the plasmids. Proper integration was confirmed by Southern blot analysis. The identity of the *cam1-E14* mutations introduced into strain MP64 were further checked by PCR and DNA sequence analysis. In an attempt to localize Cam1-E14p within cells, a fusion of S65T-GFP to *cam1-E14* carried on plasmid pZA73 was introduced into MP24-6C. We were unable to isolate FOA resistant strains that were leucine auxotrophs. Southern blot analysis showed that the FOA resistant, leucine prototroph strains we did isolate contained multiple copies of the *GFP::cam1-E14* plasmid integrated at the *cam1* locus. The GFP-calmodulin in these cells was overexpressed at levels 15 times higher than the wild-type GFP fusion, as measured by FACS (data not shown).

As a consequence, GFP-Cam1-E14p fusion localized uniformly throughout the cell at both permissive and non-permissive temperature, as did plasmid encoded fusion protein. Fusion of GFP to the temperature-sensitive calmodulin encoded by *cam1-E14* is a lethal mutation that can only be rescued by overexpression.

S. cerevisiae

Strain MMY28 (*MAT***a**; *ade2-1oc*; *ade3Δ-100*; *can1-100*; *S65T-GFP::CMD1*, *his3-11,15*, *leu2,3-112*; *lys2Δ::HIS3*; *trp1-1*; *ura3-1*) was constructed as follows. Strain TDY55-5D (*MAT***a**; *ade2-1oc*; *ade3Δ-100*; *can1-100*; *cmd1Δ::TRP1*; *his3-11,15*; *leu2,3-112*; *lys2Δ::HIS3*; *trp1-1*; *ura3-1*) (Geiser et al., 1991) containing a *cmd1-1*, *URA3* plasmid pTD79 (Davis, 1992) was transformed with a gel purified 2.3 kb *Sal*I/*Bam*HI fragment from plasmid pMM135. After selecting for growth at 37°C, colonies resistant to 5-FOA were selected. Strains resistant to 5-FOA were screened for uracil and tryptophan auxotrophy, and considered to be integrants of *S65T-GFP::CMD1*. Proper integration in MMY28 was confirmed by Southern blot, PCR, and DNA sequence analysis. Plasmids pMM135, pMM137, and pMM138 were introduced into strain TDY55-5D containing plasmid pTD56 (*2μ*, *ADE3*, *LYS2*, *CMD1*) (Geiser et al., 1991). Only pMM135 and pMM137 encoding GFP-Cmd1p and GFP-Cmd1-6p could replace the Cmd1p from plasmid pTD56, forming white sectoring colonies from which Lys$^-$, Ura$^+$ strains incapable of red pigment formation could be isolated. Plasmid pMM138 does not allow white sector formation, indicating that the GFP-Cmd1-1p fusion cannot replace the *CMD1* encoded wild-type protein. Thus, fusion of GFP to a temperature-sensitive budding yeast calmodulin is also a lethal mutation.

Microscopy

Unless noted otherwise, cells were viewed using a Zeiss Axioplan microscope with a ×100 1.4 NA objective and an optovar set at 1.25. Filter set for GFP was the XF14 (425DF45, 475DCLPO2, 535DF55) (Omega Optical). Images were captured using an Imagepoint cooled CCD video camera (Photometrics) fitted to the microscope in conjunction with IP Lab software (Signal Analytics). Images were prepared for publication with Photoshop 4.0 (Adobe Systems, Inc.).

Preparation of cells for indirect immunofluorescence

Cells were grown in YE liquid medium at 30°C and then fixed, washed, digested, and stained using the combined aldehyde method (Hagan and Hyams, 1988) with the following modifications. Phosphate-buffered saline (PBS) (Harlow and Lane, 1988), PBS supplemented with 1% bovine serum albumin and 0.05% sodium azide (PBS/BSA), and 1.1 M sorbitol in 0.1 M sodium phosphate buffer, pH 6.5 (SP) were substituted for PEM, PEMS and PEMBAL buffers, respectively. Digestions were performed in 100 μl SP containing 0.5 mg/ml Zymolyase-100T (ICN) and 10 mg/ml mutanase (Novo Nordisk BioChem) for 30 minutes at 30°C. Cells were simultaneously incubated overnight at room temperature on a rotating platform in primary antisera: purified rat anti-tubulin monoclonal antibody YOL1/34 (1:50) (Kilmartin et al., 1982) and rabbit anti-Cam1p polyclonal antiserum (1:50) (Moser et al., 1995), or affinity-purified rabbit anti-Sad1p antibodies (1:25) (Hagan and Yanagida, 1995) in 100 μl PBS/BSA. Following three washes in PBS/BSA, cells were resuspended in 100 μl PBS/BSA containing secondary antibody conjugates: fluorescein isothiocyanate-labeled rabbit anti-rat IgG (1:50) (Boehringer/Mannheim), Oregon Green 488-labeled goat anti-rat IgG (1:50) (Molecular Probes), and rhodamine isothiocyanate-labeled goat anti-rabbit IgG (1:50) (Boehringer/Mannheim). Following incubations in secondary antibody for at least 4 hours at room temperature on a rotating platform, cells were washed three times in PBS/BSA. DNA was stained with 100 ng/ml di-amidino phenyl indole (DAPI) (Sigma Chemical Co.), and cells were then mounted onto polylysine-coated 10-well slides (Cel-Line Associates, Inc.) in Citifluor Glycerol (Ted Pella).

Characterization of the temperature-sensitive *S. pombe* calmodulin mutant

Strains MP5-1C and MP64 were cultured in YE liquid medium at a permissive temperature of 30°C to a logarithmic phase of growth. Hydroxyurea was added to the cultures at a final concentration of 11 mM. After 4 hours the drug was removed by filtration, the cells were washed and transferred to fresh medium at the nonpermissive temperature of 37°C. At 20 minute intervals, samples were removed and titered for viability in triplicate or fixed as described above.

RESULTS

Localization of calmodulin using calmodulin fusions to green fluorescent protein (GFP)

S. cerevisiae

Indirect immunofluorescence previously showed that calmodulin localizes to two different regions in the budding yeast cell. First calmodulin localizes to sites of cell growth and overlaps the location of actin patches in buds (Brockerhoff and Davis, 1992; Sun et al., 1992b). Secondly, calmodulin localizes to the spindle pole body (Geiser et al., 1993; Stirling et al., 1994). The presence of calmodulin at both these sites has been confirmed by immunoelectron microscopy (Spang et al., 1996; Sundberg et al., 1996) (H. Sundberg and T. N. Davis, unpublished results). Using the previous techniques, calmodulin was not seen at both subcellular locations at the same time, because fixation procedures that preserved the sites of cell growth did not allow visualization at the SPB and vice versa. Therefore, we extended our experiments in *S. cerevisiae* to living cells by visualizing the location of a fusion between S65T-GFP and the N terminus of budding yeast calmodulin. A gene encoding the GFP-Cmd1p fusion protein expressed under control of the *CMD1* promoter and terminator was integrated in place of the wild-type *CMD1* gene. The fluorescent GFP-Cmd1p in living cells shows a pattern consistent with a location at both the SPB and at areas of polarized growth. Unbudded cells and cells with small buds each contain one dot of fluorescence as expected for either a single SPB or for two SPBs in the side-by-side configuration. These cells also have a bright patch of fluorescence at the nascent bud site or the small bud (Fig. 1A). Cells with a medium bud contain two small fluorescent dots near the neck region of the cell as expected for a protein at the poles of the short spindle (Fig. 1B). In addition patches of fluorescence appear in the bud similar to the pattern seen for the actin capping protein, Cap2p (Waddle et al., 1996). In a large budded cell, both mother and daughter contain a dot of GFP-Cmd1p presumably corresponding to their single SPB (Fig. 1C). In addition a bright ring appears at the neck (Fig. 1C). Importantly, the Ca^{2+}-binding mutant GFP-Cmd1-6p fusion had a pattern of localization identical to that of the wild-type fusion protein (Fig. 1D-F). This is the first demonstration that a mutant calmodulin defective in binding Ca^{2+} localizes to the SPB in addition to sites of cell growth.

S. pombe

The localization of calmodulin in *S. pombe* cells was determined using fusions of *S. pombe* calmodulin to GFP. A gene encoding a fusion of wild-type GFP to the N terminus of wild-type *S. pombe* calmodulin expressed under the control of the *cam1*$^+$ promoter and terminator was integrated in place of the *cam1*$^+$ gene. Because we were examining living cells, the behavior of the GFP-Cam1p in single cells could be observed over a period of time. GFP-calmodulin displayed two distinct patterns of localization. First, small fluorescent dots behaved exactly as previously demonstrated for both the budding and fission yeast SPBs

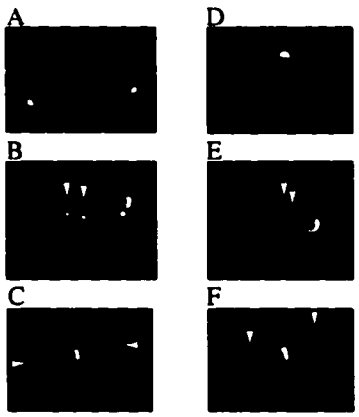

Fig. 1. Localization of GFP-Cmd1p to the SPB of *S. cerevisiae*. An equal volume of a culture of strain MMY28 (*GFP::CMD1*) (A-C) or strain TDY55-5D containing plasmid pMM137 (*GFP::cmd1-6*) (D-F) grown in YPD medium at 21°C was mixed with supplemented SD (SDC) medium containing 1% low-melting-temperature agarose on a microscope slide and visualized as described in Materials and Methods. GFP-calmodulin localization to the SPB (arrowheads). Bar, 5 μm.

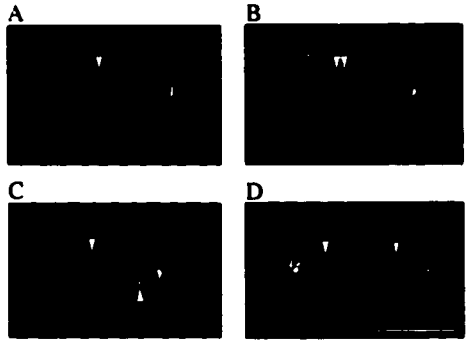

Fig. 2. Localization of GFP-Cam1p to the SPB of *S. pombe*. An equal volume of a culture of strain MP76 grown in YE medium at 21°C was mixed with EMM2 medium containing 1% low-melting-temperature agarose on a microscope slide. Cells were visualized with a MRC600 laser scanning confocal microscope (Bio-Rad) on 10% power with a ×60 objective. GFP-calmodulin localization to the SPB (arrowheads). A and B are images of the same cell taken 1 minute apart. Note that the focal plane optimal for visualization of the SPB results in poor visualization of the cortical cytoskeleton. A QuickTime movie of the GFP-Cam1p behavior at the SPB can be viewed at http://www.cityscape.co.uk/users/ag64/. Bars, 5 μm.

(Byers, 1981; Hagan and Hyams, 1988; McCully and Robinow, 1971) (Fig. 2A-D). In cells early in the cell cycle as judged by their small size, a single spot of fluorescence was observed at the edge of the nucleus (Fig. 2A). The dot of fluorescence elongated and eventually divided (Fig. 2B). Later the separation between the dots increased (Fig. 2C) with one spot of the pair eventually being distributed to each new daughter cell following mitosis and cytokinesis (Fig. 2D). Notably, calmodulin was not seen at the additional MTOCs that nucleate microtubules near the septum in *S. pombe* cells following mitosis.

We observed a second pattern of fluorescence indicating that GFP-Cam1p localized at regions of the fission yeast cell undergoing polarized growth (Fig. 3A-D). In cells undergoing septation and cytokinesis, bright fluorescence was found on both sides of the growing septum dividing the cell (Fig. 3A). In a newly divided cell immediately following cytokinesis, fluorescence was seen to move from the septum to the opposite or 'old' end of the cell (Fig. 3B,C). The old end corresponds to the former end of the mother cell and is in opposition to the end directly created by septation. *S. pombe* cells are known to only grow from the old end just after division (Mitchison and Nurse, 1985). Later the fluorescence redistributed to both ends of the lengthening cell (Fig. 3D). This bipolar localization coincides with an event in the *S. pombe* cell cycle known as NETO, or new end take off, the time when both ends of the cell begin to grow (Mitchison and Nurse, 1985). A strain containing an integrated fusion of S65T-GFP to *cam1** (MFP7) was found to have a fluorescence pattern that was identical to that observed with the fusion to wild-type GFP except that the fluorescence was much easier to detect (data not shown).

Indirect immunofluorescence of *S. pombe* calmodulin

Indirect immunofluorescence using antiserum to fission yeast calmodulin gave a pattern very similar to that seen with GFP-Cam1p. The growing ends and the septum as well as what appeared to be the SPB all were stained by the antiserum. The presence of fission yeast calmodulin at the SPB was confirmed by comparing the localization of calmodulin to that of Sad1p. Sad1p is a recognized component of the *S. pombe* SPB and remains permanently associated with the SPB throughout the cell cycle (Hagan and Hyams, 1988). Attempts were made to localize Sad1p in cells containing GFP-calmodulin fusions, but the combined aldehyde fixation procedures necessary for tubulin immunofluorescence were found to eliminate GFP fluorescence. Instead we found that the localization of calmod-

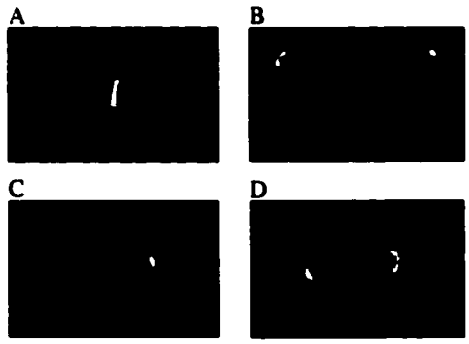

Fig. 3. Localization of GFP-Cam1p to sites of polarized growth in *S. pombe*. Cells were visualized as described for Fig. 2. Images C and D are of the same cell taken 9 minutes apart. Note that the focal plane optimal for visualization of the cortical cytoskeleton results in poor visualization of the SPB. Bars, 5 μm.

ulin, tubulin and DNA matched that of Sad1p, tubulin and DNA in cells processed in parallel (Fig. 4). Tubulin staining, representing the elongating spindle, was observed between the two dots of calmodulin staining. Sad1p dots were found to be similarly localized to the ends of the spindle. The localization of Sad1p, in relation to tubulin and DNA, is identical to that previously described (Hagan and Yanagida, 1995).

Phenotypic analysis of a temperature-sensitive *S. pombe* calmodulin mutant

When the Ca^{2+}-binding-site mutant *cam1-E14* allele is carried on a plasmid it does not confer temperature-sensitivity (Moser et al., 1995). However, when *cam1-E14* is integrated as a single copy in place of the wild-type *cam1*$^+$ gene, fission yeast cannot form colonies at temperatures above 32°C. Calmodulin mutant and wild-type fission yeast were arrested in S phase with hydroxyurea at a temperature permissive for growth and then released from arrest and shifted to the restrictive temperature. The wild-type culture completed S phase and proceeded normally through mitosis and then cytokinesis. The septation index peaked 80 minutes after the shift to 37°C and the number of viable cells began to increase 100 minutes after the shift (Fig. 5). In contrast, 80 minutes after the shift to 37°C cells in the mutant culture began to lose viability (Fig. 5). Cytokinesis in the mutant culture was delayed and asynchronous although most of the cells did eventually form a septum.

The calmodulin localization and cell-cycle timing studies suggested that mitotic defects might underlie the loss of viability in the calmodulin mutant strain. Therefore, an analysis of DNA and spindle morphology was performed on synchronized cultures of both the wild-type and calmodulin mutant following incubation at non-permissive temperature. DNA-specific staining with DAPI in control cells revealed the chromatin as a brightly staining crescent with a faintly stained nucleolus completing the sphere of the nucleus. As the cells progressed through mitosis, the nucleus divided and the chromatin segregated to either end of the dividing cell. Two discrete nuclei formed, followed by septation.

Analysis of microtubule distribution by indirect immunofluorescence revealed the disappearance of cytoplasmic microtubules concomitant with formation of a mitotic spindle in cells undergoing mitotic transit. As previously described (Hagan and Hyams, 1988), early short spindles aligned nearly perpendicular to the length of the cell and spanned the centrally-located chromosomal DNA mass (Fig. 6A). Later, spindle alignment became more parallel with the long axis of the elongating cell. The spindle midpoint corresponded with the midpoint of the cell. As well, chromatin segregating along medium to full-length spindles was always found near the two endpoints of the spindle (Fig. 6B). At full spindle extension, the newly segregated chromosomal masses were observed at the two ends of the cell (Fig. 6C). Following mitosis, spindle microtubules disappeared and post-anaphase arrays of cytoplasmic microtubules became apparent (Fig. 6D). Cytokinesis resulted in two daughter cells each containing an equal mass of segregated chromosomal DNA.

The *cam1-E14* mutant cells exhibited several abnormal phenotypes. When the culture first began to lose viability (80 minutes), the chromosomal DNA appeared strikingly condensed in 20% of the cells (n=200). Metaphase plates with three pairs of discrete chromosomes could often be observed (Fig. 7A). The DNA also frequently appeared to be broken or fragmented by improper distribution along the spindle (Fig. 7B). For comparison, only 2.5% of the wild-type cells contained abnormal DNA at that time point. Anti-tubulin immunofluorescence staining of mutant spindles was more

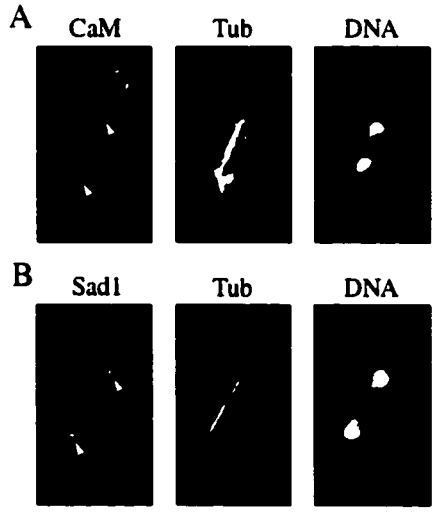

Fig. 4. Localization of calmodulin/tubulin and Sad1p/tubulin at the *S. pombe* SPB. A culture of *S. pombe* strain MP5-1C (*cam1*$^+$) grown at 30°C to logarithmic phase in YE supplemented with adenine, leucine and uracil was prepared for immunofluorescence as described in Materials and Methods. Cam1p or Sad1p localization to the SPB (arrowheads). Bar, 5 μm.

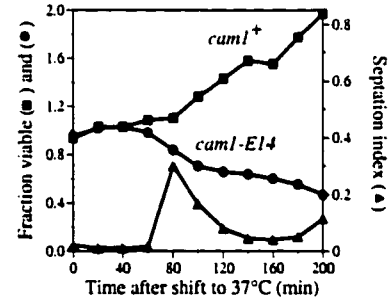

Fig. 5. Viability of wild-type and calmodulin mutant cells following shift to nonpermissive temperature. Cultures of strain MP33-6B (*cam1*$^+$) (■) and strain MP64 (*cam1-E14*) (●) were arrested by treatment with hydroxyurea at 30°C, washed and released at 37°C as described in Materials and Methods. At the times shown, samples were removed and either titered or fixed in 3.7% formaldehyde. The degree of synchrony attained was comparable to that attained previously (Enoch et al., 1992). The septation index (▲) is the fraction of cells with a septum. Only the wild-type septation index is shown for clarity.

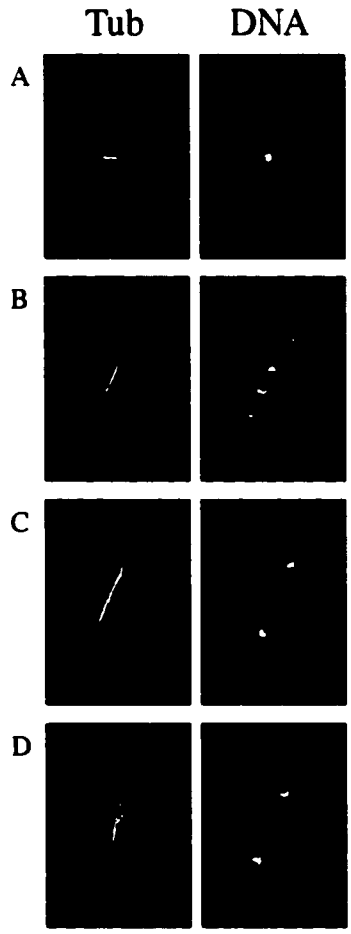

Fig. 6. Tubulin and DNA morphology in synchronized wild-type cells. Cultures of strain MP5-1C (*cam1*$^+$) synchronized with hydroxyurea were incubated at 37°C , fixed, and prepared for immunofluorescence as described in Materials and Methods. (A) Short spindle; (B) medium spindle; (C) full-length spindle; (D) cytoplasmic microtubules. Bar, 5 μm.

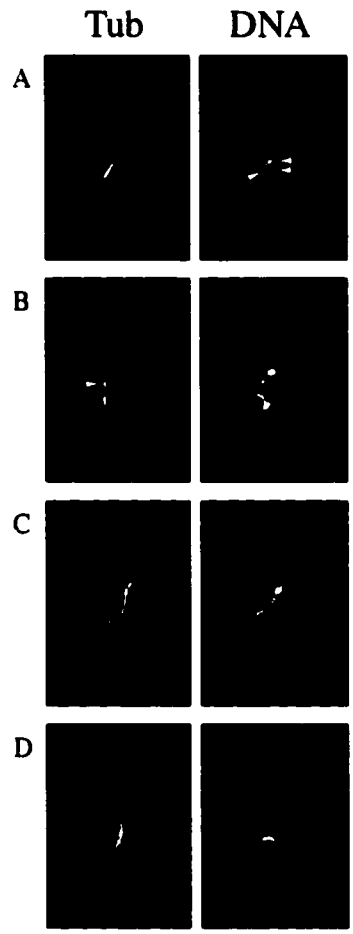

Fig. 7. Tubulin and DNA morphology in synchronized calmodulin mutant cells. Cultures of strain MP64 (*cam1-E14*) synchronized with hydroxyurea were incubated at 37°C , fixed, and prepared for immunofluorescence as described in Materials and Methods. (A) Hyper-condensed chromosomes (arrowheads); (B) fragmented chromatin and spindle with abnormal spur (arrowhead); (C) broken spindle; (D) mislocalized chromatin and cytoplasmic microtubules. Bar, 5 μm.

diffuse and less uniform than wild type (Fig. 7B). Perhaps the most striking class of cells was those that appeared to have broken mitotic spindles (Fig. 7C).

At later times, mutant cells appeared with chromosomes that were missegregated. Some cells divided with two nuclei on one side of the septum while other cells divided with only one DAPI-staining mass that often appeared abnormally large. Cytoplasmic microtubules of normal morphology were found assembled in association with the mislocalized chromatin (Fig. 7D). At 240 minutes after the shift, 27% of the mutant cells contained mislocalized DNA and 11% contained no apparent nuclear DNA.

DISCUSSION

We demonstrate that calmodulin localizes to the SPB in *S. pombe*. Antiserum to calmodulin appears at the end of the spindle in a pattern identical to Sad1p, a molecular marker whose localization has been previously defined with respect to

SPB position (Hagan and Yanagida, 1995). A GFP-Cam1p fusion protein allowed examination of the SPB in living cells and demonstrated that in living cells the SPB went through the stages previously observed in fixed isolates (Hagan and Hyams, 1988; McCully and Robinow, 1971; Tanaka and Kanbe, 1986). Unlike a GFP fusion to Dis1p (Nabeshima et al., 1995), GFP-Cam1p is the first molecular marker for SPBs that can be seen in living *S. pombe* cells throughout the cell cycle. This integrated marker should allow monitoring of SPB behavior in mutant fission yeast cells.

Localization of calmodulin using both a green fluorescent protein fusion and indirect immunofluorescence also indicates an association between *S. pombe* calmodulin and areas of polarized growth. GFP-Cam1p was observed in the region of the septum as it formed, then at only one end of newly formed cells. Later, fluorescence was seen at both ends of the growing cell. These behaviors are similar to those of known components of the polarized fission yeast actin cytoskeleton (Marks et al., 1986).

The SPB localization and the polarized localization of GFP-Cam1p can easily be differentiated using two criteria. First, the SPB fluorescence is best seen in a focal plane that bisects the center of the cell while the polarized localization is more clearly seen when the focus is in a plane that is level with the surface of the cell. The second criterion can only be applied to live cells. The spot of SPB fluorescence remains relatively constant in location for several minutes. During this time interval, the fluorescence associated with cortical cytoskeleton can be seen to undergo extensive remodeling, as has been previously reported in *S. cerevisiae* (Waddle et al., 1996).

Subcellular localization of calmodulin to the SPB and the cortical cytoskeleton suggests roles for *S. pombe* calmodulin in mitosis and in polarized cell growth, respectively. Analysis of the restrictive-temperature phenotype of a temperature-sensitive calmodulin mutant further substantiates a mitotic function for *S. pombe* calmodulin and indicates a role for calmodulin in facilitating chromosome segregation. At the restrictive temperature, *S. pombe* cells containing a temperature-sensitive Ca^{2+}-binding-site calmodulin mutant begin to lose viability after DNA replication, at a time when wild-type cells are completing mitosis and initiating cytokinesis. Examination of the DNA of the mutant cell reveals abnormal chromatin and spindle morphologies that are consistent with a failure in chromosome segregation. First, at the time when the cells begin to lose viability, the chromatin appears to condense and fragment. The chromatin may appear as distinct chromosomes like that found in cold-sensitive fission yeast *nda3* mutants when incubated at the non-permissive temperature (Hiraoka et al., 1984). The *nda3*$^+$ gene encodes β-tubulin, an essential component of the mitotic spindle apparatus. Consistent with a presumed defect in spindle assembly, mutant cells were found that appear to contain broken spindles. However, while the tubulin defect in the *nda3* mutant is detected by a spindle checkpoint causing a reversible mitotic arrest at the restrictive temperature, the defect in the *cam1-E14* mutant cells does not cause arrest. The *cam1-E14* calmodulin mutant continues to divide, resulting in cells with DNA mislocalized on only one side of the septum and a significant number of cells containing no nuclear DNA. This observation suggests several, as yet untested hypotheses. Calmodulin may have a role in a mitotic checkpoint function. Alternatively, the calmodulin defect may simply not be detected by the checkpoint mechanism. Furthermore, the fact that the mutant cells can form a septum suggests that any defect the *cam1-E14* mutant may have in polarized growth is not severe enough to manifest itself before the lethal effects of mitotic failure.

In *S. cerevisiae*, GFP-calmodulin fusions are easily seen at the SPB and at sites of cell growth in living cells. This is the first demonstration of the presence of calmodulin at both structures at the same time. Previous methods employing fixation showed calmodulin at only one place or the other (Brockerhoff et al., 1992; Geiser et al., 1993; Stirling et al., 1994; Sun et al., 1992b; Sundberg et al., 1996). Furthermore, although the *cmd1-6* Ca^{2+}-binding calmodulin mutant is viable (Geiser et al., 1991), immunofluorescence methods have not been able to detect the Cmd1-6p protein product at the SPB. The GFP-Cmd1-6p fusion provides the first cytological evidence that the interaction between calmodulin and the budding yeast SPB is Ca^{2+}-independent. GFP-calmodulin serves as an excellent integrated marker for the SPB allowing the observation of SPB behavior in living cells. Our results are similar to those observed previously examining the location of Nuf2p-GFP, a protein that associates with the microtubules near the SPB (Kahana et al., 1995; Osborne et al., 1994).

Calmodulin appears to perform a similar mitotic function in both fission and budding yeasts. The subcellular localization pattern of calmodulin in both *S. cerevisiae* and *S. pombe* is quite similar. Calmodulin can be found at the SPB and at sites of cell growth associated with the polarized cortical cytoskeleton. The mitotic phenotypes of temperature-sensitive calmodulin mutants from both species are also related. Like the *cam1-E14* mutant, the *S. cerevisiae cmd1-1* mutant loses viability at non-permissive temperature during mitosis and accumulates cells with broken spindles and fragmented DNA (Davis, 1992). Calmodulin in *S. cerevisiae* is known to function in mitosis by direct interaction with the SPB component Spc110p. Therefore, we propose that calmodulin also performs an essential mitotic function via an interaction at the *S. pombe* SPB. Yet, unlike in *S. cerevisiae* (Geiser et al., 1991), in *S. pombe* at least one wild-type Ca^{2+}-binding-site in calmodulin is required to maintain viability (Moser et al., 1995). Thus, the essential interaction between *S. pombe* calmodulin and the SPB may be a Ca^{2+}-dependent process. However, any determination of the Ca^{2+}-dependence of the interaction between calmodulin and centrosome components from *S. pombe* as well as from other species awaits their isolation and characterization.

We thank I. Hagan for affinity-purified antibodies against Sad1p, P. Y. Lum for assistance with laser scanning confocal microscopy, and NovoNordisk for kindly providing mutanase. This work was supported by National Institutes of Health grants T32 GM-08437 (to M.J.M.), T32 GM-07270-22 (to M.R.F.), and GM40506 (to T.N.D.).

REFERENCES

Brockerhoff, S. E. and Davis, T. N. (1992). Calmodulin concentrates at regions of cell growth in *Saccharomyces cerevisiae*. *J. Cell Biol.* **118**, 619-629.

Brockerhoff, S. E., Edmonds, C. G. and Davis, T. N. (1992). Structural analysis of wild-type and mutant yeast calmodulins by limited proteolysis and electrospray ionization mass spectrometry. *Protein Sci.* **1**, 504-516.

Brockerhoff, S. E., Stevens, R. C. and Davis, T. N. (1994). The unconventional myosin, Myo2p, is a calmodulin target at sites of cell growth in *Saccharomyces cerevisiae*. *J. Cell Biol.* **124**, 315-323.

Byers, B. (1981). Cytology of the yeast life cycle. In *The Molecular Biology of the Yeast* Saccharomyces – *Life Cycle and Inheritance* (ed. J. N. Strathern, E. W. Jones and J. R. Broach), pp. 59-96. Cold Spring Harbor Laboratory Press, Cold Spring Harbor, NY.

Chalfie, M., Tu, Y., Euskirchen, G., Ward, W. W. and Prasher, D. C. (1994).

Green fluorescent protein as a marker for gene expression. *Science* **263**, 802-805.

Cunningham, K. W. and Fink, G. R. (1996). Calcineurin inhibits *VCX1*-dependent H^+/Ca^{2+} exchange and induces Ca^{2+}-ATPases in *Saccharomyces cerevisiae*. *Mol. Cell Biol.* **16**, 2226-2237.

Cyert, M. S., Kunisawa, R., Kaim, D. and Thorner, J. (1991). Yeast has homologs (*CNA1* and *CNA2* gene products) of mammalian calcineurin, a calmodulin-regulated phosphoprotein phosphatase [published erratum appears in *Proc. Nat. Acad. Sci. USA* (1992) **89**, 4220]. *Proc. Nat. Acad. Sci. USA* **88**, 7376-7380.

Cyert, M. S. and Thorner, J. (1992). Regulatory subunit (*CNB1* gene product) of yeast Ca^{2+}/calmodulin-dependent phosphoprotein phosphatases is required for adaptation to pheromone. *Mol. Cell Biol.* **12**, 3460-3469.

Davis, T. N., Urdea, M. S., Masiarz, F. R. and Thorner, J. (1986). Isolation of the yeast calmodulin gene: calmodulin is an essential protein. *Cell* **47**, 423-431.

Davis, T. N. (1992). A temperature-sensitive calmodulin mutant loses viability during mitosis. *J. Cell Biol.* **118**, 607-617.

Enoch, T., Carr, A. M. and Nurse, P. (1992). Fission yeast genes involved in coupling mitosis to completion of DNA replication. *Genes Dev.* **6**, 2035-2046.

Geiser, J. R., van Tuinen, D., Brockerhoff, S. E., Neff, M. M. and Davis, T. N. (1991). Can calmodulin function without binding calcium? *Cell* **65**, 949-959.

Geiser, J. R., Sundberg, H. A., Chang, B. H., Muller, E. G. and Davis, T. N. (1993). The essential mitotic target of calmodulin is the 110-kilodalton component of the spindle pole body in *Saccharomyces cerevisiae*. *Mol. Cell Biol.* **13**, 7913-7924.

Gutz, H., Heslot, H., Leupold, U. and Loprieno, N. (1972). *Schizosaccharomyces pombe*. In *Handbook of Genetics*, vol. 1 (ed. R. C. King), pp. 395. Plenum, New York.

Hagan, I. M. and Hyams, J. S. (1988). The use of cell division cycle mutants to investigate the control of microtubule distribution in the fission yeast *Schizosaccharomyces pombe*. *J. Cell Sci.* **89**, 343-357.

Hagan, I. and Yanagida, M. (1995). The product of the spindle formation gene *sad1*$^+$ associates with the fission yeast spindle pole body and is essential for viability. *J. Cell Biol.* **129**, 1033-1047.

Harlow, E. and Lane, D. (1988). *Antibodies: A Laboratory Manual*. Cold Spring Harbor Laboratory Press, Cold Spring Harbor, NY.

Heim, R., Cubitt, A. B. and Tsien, R. Y. (1995). Improved green fluorescence. *Nature* **373**, 663-664.

Hiraoka, Y., Toda, T. and Yanagida, M. (1984). The *nda3* gene of fission yeast encodes beta-tubulin: a cold-sensitive *nda3* mutation reversibly blocks spindle formation and chromosome movement in mitosis. *Cell* **39**, 349-358.

Kahana, J. A., Schnapp, B. J. and Silver, P. A. (1995). Kinetics of spindle pole body separation in budding yeast. *Proc. Nat. Acad. Sci. USA* **92**, 9707-9711.

Kilmartin, J. V., Wright, B. and Milstein, C. (1982). Rat monoclonal antitubulin antibodies derived by using a new nonsecreting rat cell line. *J. Cell Biol.* **93**, 576-582.

Kilmartin, J. V., Dyos, S. L., Kershaw, D. and Finch, J. T. (1993). A spacer protein in the *Saccharomyces cerevisiae* spindle pole body whose transcript is cell cycle-regulated. *J. Cell Biol.* **123**, 1175-1184.

Kilmartin, J. V. and Goh, P. Y. (1996). Spc110p: assembly properties and role in the connection of nuclear microtubules to the yeast spindle pole body. *EMBO J.* **15**, 4592-4602.

Kunkel, T. A., Roberts, J. D. and Zakour, R. A. (1987). Rapid and efficient site-specific mutagenesis without phenotypic selection. *Meth. Enzymol.* **154**, 367-382.

Lillie, S. H. and Brown, S. S. (1994). Immunofluorescence localization of the unconventional myosin, Myo2p, and the putative kinesin-related protein, Smy1p, to the same regions of polarized growth in *Saccharomyces cerevisiae*. *J. Cell Biol.* **125**, 825-842.

Lu, K. P., Osmani, S. A., Osmani, A. H. and Means, A. R. (1993). Essential roles for calcium and calmodulin in G2/M progression in *Aspergillus nidulans*. *J. Cell Biol.* **121**, 621-630.

Marks, J., Hagan, I. M. and Hyams, J. S. (1986). Growth polarity and cytokinesis in fission yeast: the role of the cytoskeleton. *J. Cell Sci. Suppl. 5*, 229-241.

McCully, E. K. and Robinow, C. F. (1971). Mitosis in the fission yeast *Schizosaccharomyces pombe*: a comparative study with light and electron microscopy. *J. Cell Sci.* **9**, 475-507.

Means, A. R. (1994). Calcium, calmodulin and cell cycle regulation. *FEBS Lett.* **347**, 1-4.

Mitchison, J. M. (1970). Physiological and cytological methods for Schizosaccharomyces pombe. *Meth. Cell Physiol.* **4**, 131-165.

Mitchison, J. M. and Nurse, P. (1985). Growth in cell length in the fission yeast *Schizosaccharomyces pombe*. *J. Cell Sci.* **75**, 357-376.

Moser, M. J., Lee, S. M., Klevit, R. E. and Davis, T. N. (1995). Ca^{2+} binding to calmodulin and its role in *Schizosaccharomyces pombe* as revealed by mutagenesis and NMR spectroscopy. *J. Biol. Chem.* **270**, 20643-20652.

Moser, M. J., Geiser, J. R. and Davis, T. N. (1996). Ca^{2+}-calmodulin promotes survival of pheromone-induced growth arrest by activation of calcineurin and Ca^{2+}-calmodulin-dependent protein kinase. *Mol. Cell Biol.* **16**, 4824-4831.

Nabeshima, K., Kurooka, H., Takeuchi, M., Kinoshita, K., Nakaseko, Y. and Yanagida, M. (1995). p93dis1, which is required for sister chromatid separation, is a novel microtubule and spindle pole body-associating protein phosphorylated at the Cdc2 target sites. *Genes Dev.* **9**, 1572-85.

Ohya, Y., Kawasaki, H., Suzuki, K., Londesborough, J. and Anraku, Y. (1991). Two yeast genes encoding calmodulin-dependent protein kinases. Isolation, sequencing and bacterial expressions of *CMK1* and *CMK2*. *J. Biol. Chem.* **266**, 12784-12794.

Ohya, Y. and Botstein, D. (1994). Diverse essential functions revealed by complementing yeast calmodulin mutants. *Science* **263**, 963-966.

Osborne, M. A., Schlenstedt, G., Jinks, T. and Silver, P. A. (1994). Nuf2, a spindle pole body-associated protein required for nuclear division in yeast. *J. Cell Biol.* **125**, 853-866.

Pausch, M. H., Kaim, D., Kunisawa, R., Admon, A. and Thorner, J. (1991). Multiple Ca^{2+}/calmodulin-dependent protein kinase genes in a unicellular eukaryote. *EMBO J.* **10**, 1511-1522.

Pozos, T. C., Sekler, I. and Cyert, M. S. (1996). The product of *HUM1*, a novel yeast gene, is required for vacuolar Ca^{2+}/H^+ exchange and is related to mammalian Na^+/Ca^{2+} exchangers. *Mol. Cell Biol.* **16**, 3730-3741.

Rasmussen, C. D., Means, R. L., Lu, K. P., May, G. S. and Means, A. R. (1990). Characterization and expression of the unique calmodulin gene of *Aspergillus nidulans*. *J. Biol. Chem.* **265**, 13767-13775.

Rasmussen, C. D., Lu, K. P., Means, R. L. and Means, A. R. (1992). Calmodulin and cell cycle control. *J. Physiol.* **86**, 83-88.

Rasmussen, C., Garen, C., Brining, S., Kincaid, R. L., Means, R. L. and Means, A. R. (1994). The calmodulin-dependent protein phosphatase catalytic subunit (calcineurin A) is an essential gene in *Aspergillus nidulans*. *EMBO J.* **13**, 3917-3924.

Sherman, F., Fink, G. R. and Hicks, J. B. (1986). *Methods in Yeast Genetics*. Cold Spring Harbor Laboratory Press, Cold Spring Harbor, New York.

Spang, A., Grein, K. and Schiebel, E. (1996). The spacer protein Spc110p targets calmodulin to the central plaque of the yeast spindle pole body. *J. Cell Sci.* **109**, 2229-2237.

Stirling, D. A., Welch, K. A. and Stark, M. J. (1994). Interaction with calmodulin is required for the function of Spc110p, an essential component of the yeast spindle pole body. *EMBO J.* **13**, 4329-4342.

Stirling, D. A., Rayner, T. F., Prescott, A. R. and Stark, M. J. R. (1996). Mutations which block the binding of calmodulin to Spc110p cause multiple mitotic defects. *J. Cell Sci.* **109**, 1297-1310.

Sun, G. H., Hirata, A., Ohya, Y. and Anraku, Y. (1992a). Mutations in yeast calmodulin cause defects in spindle pole body functions and nuclear integrity. *J. Cell Biol.* **119**, 1625-1639.

Sun, G. H., Ohya, Y. and Anraku, Y. (1992b). Yeast calmodulin localizes to sites of cell growth. *Protoplasma* **166**, 1625-1639.

Sundberg, H. A., Goetsch, L., Byers, B. and Davis, T. N. (1996). Role of calmodulin and Spc110p interaction in the proper assembly of spindle pole body components. *J. Cell Biol.* **133**, 111-124.

Takeda, T. and Yamamoto, M. (1987). Analysis and *in vivo* disruption of the gene coding for calmodulin in *Schizosaccharomyces pombe*. *Proc. Nat. Acad. Sci. USA* **84**, 3580-3584.

Tanaka, K. and Kanbe, T. (1986). Mitosis in the fission yeast *Schizosaccharomyces pombe* as revealed by freeze-substitution electron microscopy. *J. Cell Sci.* **80**, 253-268.

Waddle, J. A., Karpova, T. S., Waterson, R. H. and Cooper, J. A. (1996). Movement of cortical actin patches in yeast. *J. Cell Biol.* **132**, 861-870.

Yoshida, T., Toda, T. and Yanagida, M. (1994). A calcineurin-like gene *ppb1*$^+$ in fission yeast: mutant defects in cytokinesis, cell polarity, mating and spindle pole body positioning. *J. Cell Sci.* **107**, 1725-1735.

(Received 6 November 1996 – Accepted 29 May 1997)

Appendix B: Identification of a human centrosomal calmodulin-binding protein that shares homology with pericentrin

Identification of a human centrosomal calmodulin-binding protein that shares homology with pericentrin

Mark R. Flory*, Michael J. Moser†, Raymond J. Monnat, Jr.†, and Trisha N. Davis*‡§

*Program in Molecular and Cellular Biology, †Department of Pathology, and ‡Department of Biochemistry, University of Washington, Seattle, WA 98195

Communicated by J. Richard McIntosh, University of Colorado, Boulder, CO, February 25, 2000 (received for review October 6, 1999)

Eukaryotic chromosome segregation depends on the mitotic spindle apparatus, a bipolar array of microtubules nucleated from centrosomes. Centrosomal microtubule nucleation requires attachment of γ-tubulin ring complexes to a salt-insoluble centrosomal core, but the factor(s) underlying this attachment remains unknown. In budding yeast, this attachment is provided by the coiled-coil protein Spc110p, which links the yeast γ-tubulin complex to the core of the yeast centrosome. Here, we show that the large coiled-coil protein kendrin is a human orthologue of Spc110p. We identified kendrin by its C-terminal calmodulin-binding site, which shares homology with the Spc110p calmodulin-binding site. Kendrin localizes specifically to centrosomes throughout the cell cycle. N-terminal regions of kendrin share significant sequence homology with pericentrin, a previously identified murine centrosome component known to interact with γ-tubulin. In mitotic human breast carcinoma cells containing abundant centrosome-like structures, kendrin is found only at centrosomes associated with spindle microtubules.

Eukaryotic cell division requires assembly of a mitotic spindle to faithfully segregate replicated chromosomes. A key step in spindle assembly is the nucleation of stable microtubules from the centrosome. One protein involved in nucleation is γ-tubulin, which forms a ring complex with approximately seven other proteins (1, 2). Immunoelectron microscopic tomography of purified centrosomes indicates that γ-tubulin ring complexes (γ-TURCs) localize to centrosomal pericentriolar material and associate with the minus ends of microtubules during *in vitro* nucleation from purified centrosomes (3). Fluorescence microscopy of stably integrated γ-tubulin-green fluorescent protein (GFP) fusions has demonstrated that γ-tubulin is rapidly recruited to the centrosome during mitosis (4), suggesting that recruitment and attachment of soluble γ-TURCs to the centrosome are essential precursors to microtubule nucleation. Recruitment of γ-TURCs to the centrosome is likely facilitated by pericentrin, a centrosomal protein that interacts with both γ-tubulin (5) and the motor protein dynein (6). The centrosomal proteins that subsequently anchor γ-TURCs to the centrosome have not yet been identified, but *in vitro* fractionation of purified centrosomes indicates that one or more salt-insoluble centrosomal proteins of the centrosomal core, or "centromatrix," are essential for nucleation. These centromatrix proteins may serve as anchors for γ-TURCs during nucleation (7, 8).

In budding yeast, the coiled-coil protein Spc110p anchors the yeast γ-tubulin complex to the yeast centrosome, or spindle pole body (SPB) (9). The N-terminal region of Spc110p binds directly to the yeast γ-tubulin complex (9, 10), whereas the Spc110p C-terminal region, when bound to calmodulin, binds to the core of the SPB (11–13). The 70-kDa coiled-coil central region of Spc110p acts as a spacer between the spindle microtubules and the core of the SPB (14). The conservation of both calmodulin (15–17) and Spc110p epitopes (18) in mammalian centrosomes suggested the existence of a calmodulin-binding Spc110p orthologue, but its identity has remained elusive. Moreover, the striking structural differences between the yeast spindle pole body and the centrosome cast doubt that the protein or proteins conferring anchoring activity in higher eukaryotic cells would bear any resemblance to Spc110p. However, using knowledge of calmodulin-binding site sequences, we have identified a calmodulin-binding centrosomal protein in human cells whose molecular properties and subcellular distribution indicate a functional relatedness to yeast Spc110p. Like Spc110p in budding yeast, this protein may anchor γ-TURCs to the centrosomal core in human cells.

Materials and Methods

Identification and Analysis of Kendrin cDNA. Murine and human expressed sequence tag (EST) clones with potential calmodulin-binding sites were identified by using Advanced BLAST (http://www.ncbi.nlm.nih.gov/blast/blast.cgi) using TBLASTN with "expect" set at 1000.[¶] A human breast carcinoma STRETCH cDNA library (CLONTECH) was screened with the ^{32}P-labeled human EST cDNA using Hybond-N filters (Amersham Pharmacia) according to the manufacturer's recommendations. We screened approximately 1×10^6 plaques and obtained 18 positive clones. PCR on plaque-purified positive clones using Expand polymerase (Roche Molecular Biochemicals) identified a clone with an insert of 5.8 kb for further analysis. A full-length human cDNA, named kendrin, was subsequently deposited in the database by Li and Joshi.[¶]

Coiled-coil secondary structure was predicted by using PAIRCOIL (19) (http://nightingale.lcs.mit.edu/cgi-bin/score) with default settings. All numbering of nucleotides and amino acids refers to kendrin cDNA and protein sequences, respectively. The kendrin database entry now includes the designation *PCNT*, for *Homo sapiens* pericentrin.[¶] However, as discussed below, evidence suggests that kendrin is not the human form of pericentrin. Therefore, we use the designation kendrin, rather than pericentrin, to refer to the human protein.

Northern Blotting. Multiple tissue and cancer line Northern blots (CLONTECH) were probed with ^{32}P-labeled DNA fragments according to the manufacturer's recommendations. Hybridization signals were detected on Hyperfilm-MP (Amersham

Abbreviations: SPB, spindle pole body; γ-TURC, γ-tubulin ring complex; GST, glutathione S-transferase; EST, expressed sequence tag.

§To whom reprint requests should be addressed. E-mail: tdavis@u.washington.edu.

¶Accession numbers: Murine EST clones homologous to the C-terminal calmodulin-binding domain of three Spc110p-related fungal proteins, AA600395 and AA000932; human EST clone, AA333809; kendrin cDNA, U52962; *PCNT*, NM_006031; representative human EST clone homologous to the 3′ untranslated region of murine pericentrin but not homologous to any sequenced regions of human chromosome 21 (as of 1/25/2000), AI970199; human chromosome 21 contigs containing the kendrin genomic locus, NT_002306 and NT_002102.

The publication costs of this article were defrayed in part by page charge payment. This article must therefore be hereby marked "advertisement" in accordance with 18 U.S.C. §1734 solely to indicate this fact.

Pharmacia) or by using a Storm PhosphorImager (Molecular Dynamics).

Protein A-Calmodulin Overlay Blotting. Protein A-calmodulin overlay blotting was done as previously described (20) with the following modifications. Protein A and a protein A-vertebrate calmodulin fusion were expressed in *Escherichia coli* by using plasmid pRIT-2T (Amersham Pharmacia). Fusions of glutathione *S*-transferase (GST) to kendrin fragments (amino acids 2628–2969 and 3158–3321) and GST alone were expressed in *E. coli* by using plasmid pGEX-2T (Amersham Pharmacia). A mutagenized GST-kendrin fusion (3158–3321) containing five alanine substitution mutations in the calmodulin-binding site (Fig. 1 *a*) was also expressed. Bacterial lysates were prepared in 0.01 M sodium phosphate, pH 7.2, 1% β-mercaptoethanol, 1% SDS, and 6 M urea. Protein A alone stains only the upper light background band seen in all lanes of the calmodulin overlay blots shown in Fig. 2 *a* and *b*.

Antibody Generation. GST-kendrin (amino acids 2628–2969) fusion protein was expressed in bacteria using plasmid pGEX-2T (Amersham Pharmacia), solubilized in 150 mM Tris, pH 8, 500 mM NaCl, 1% Triton X-100, and purified using glutathione Sepharose according to the manufacturer (Amersham Pharmacia). Antibodies against this fusion were prepared in hens, and the IgY fraction was purified from egg white (Aves Laboratories, Tigard, OR). The purified IgY fraction recognized a ≈370-kDa band on immunoblots of whole cell extracts prepared from cultured human cells (not shown).

Cell Culture. Primary human diploid fibroblasts and HS578T human breast carcinoma cells were grown on glass coverslips in high glucose (4.5 g/liter) DMEM supplemented with 10% FCS (HyClone) and, for HS578T cells, 10 μg/ml bovine insulin. HCC1937 human colon carcinoma cells were grown in RPMI 1640 medium supplemented with 5% FCS, 1 mM sodium pyruvate and buffered with 25 mM Hepes, 25 mM sodium bicarbonate. All culture media contained 100 units/ml penicillin G sulfate and 100 μg/ml streptomycin sulfate. Cultures were grown in a humidified, 5% CO_2, 37°C incubator.

Immunofluorescence Microscopy. Coverslips with attached cells were washed once in PBS and then fixed at −20° in 70% acetone/30% methanol for ≥20 min or methanol for 6 min, dried at room temperature for 30 min, and either used immediately or stored at −20°. All incubations were <1 h at room temperature. Coverslips were rehydrated in blocking solution (PBS supplemented with 3% BSA and 0.04% sodium azide). Primary antibodies were diluted in blocking solution as follows: chicken IgY anti-kendrin 1618 at 1:800, rabbit anti-γ-tubulin at 1:3000 (Sigma), mouse ascites anti-centrin 20H5 at 1:500 (21), rabbit anti-pericentrin M1-100-2 at 1:800 (generous gift from S. Doxsey, University of Massachusetts Medical Center, Worcester, MA) and rat anti-α-tubulin at 1:250 (Harlan, Haslett, MI). After five washes in blocking solution, bound antibody was detected with secondary antibody diluted in blocking solution: goat anti-chicken IgY Alexa 568 at 1:1000 (Molecular Probes) and either goat anti-rabbit FITC at 1:1000 (Molecular Probes), goat anti-mouse FITC at 1:50 (Roche Molecular Biochemicals), or goat anti-rat Oregon Green at 1:500 (Molecular Probes). After five washes in blocking solution, coverslips were briefly incubated in PBS containing 100 ng/ml 4′,6-diamidino-2-phenylindole (Sigma) and then mounted in Citifluor (Ted Pella, Redding, CA).

For control experiments, anti-kendrin IgY antibodies were incubated with nitrocellulose strips containing immobilized GST, and unbound antibodies were collected. Antibodies not binding to GST strips were subsequently incubated with strips containing the GST-kendrin (amino acids 2628–2969) fusion protein, and the resulting flow-through collected. Unbound antibodies collected after initial incubation with GST strips and flow-through after subsequent incubation with GST-kendrin

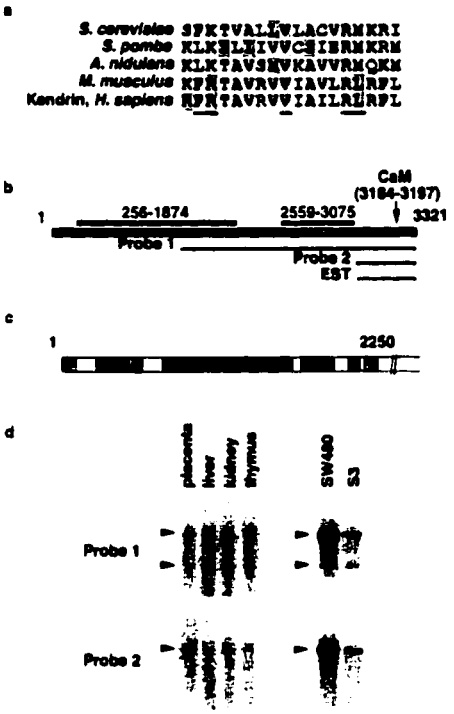

Fig. 1. Kendrin, a large coiled-coil protein, contains a C-terminal calmodulin-binding site and shares homology with murine pericentrin. (*a*) Alignment of the *Saccharomyces cerevisiae* Spc110p calmodulin-binding site with related protein sequences detected in the fission yeast *S. pombe* (M.F. and T.D., unpublished data), the filamentous fungus *A. nidulans* (J. Joseph and A. Means, unpublished data), and humans (kendrin). Green, unanimously conserved residues at one position; yellow, three or four conserved residues in one position; purple, additional similar residues. Kendrin calmodulin-binding site residues changed to alanine by mutagenesis are underlined. (*b*) Schematic drawing of the kendrin protein showing locations of coiled-coil regions (blue lines and numbers), calmodulin-binding site (CaM), and region used for antibody generation (hatched area). Gray lines, human kendrin EST and two Northern blotting probes encoding corresponding kendrin segments. (*c*) Analysis of the N-terminal 2250 amino acids that share high overall homology with murine pericentrin. Schematic drawn to scale indicates segments of kendrin that share >80% identity with pericentrin (red boxes), >80% identity or conservative replacement with pericentrin (purple boxes), <80% identity or conservative replacement with pericentrin (gray boxes), or that are not found in pericentrin (white boxes). The C-terminal region of kendrin beyond residue 2250 is not shown here as it is unique and is not found in pericentrin. (*d*) Full-length kendrin is encoded by a 10-kb transcript, which shares homology with a 7.5-kb transcript, as shown by Northern blotting. Probe 1 (5.8 kb cDNA library clone insert) and Probe 2 (cDNA including kendrin nucleotides 9008–9976), the relative positions of which are shown in *b*, were hybridized to both a multiple tissue Northern blot (CLONTECH) and a cancer line blot (CLONTECH). Arrows indicate transcripts at ≈10 kb and ≈7.5 kb (*Top*) or at 10 kb (*Bottom*). Human tissues are as indicated. Cancer cell lines are SW480, colorectal adenocarcinoma; S3, HeLa cell.

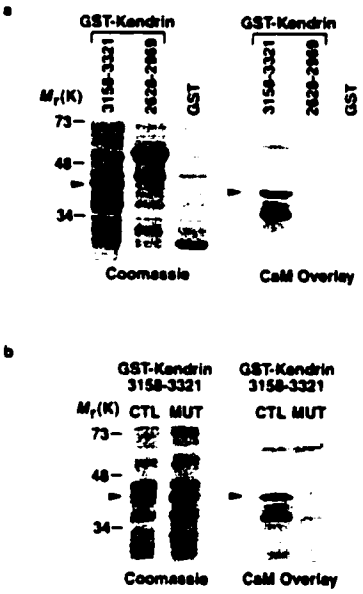

Fig. 2. The predicted calmodulin-binding site in the kendrin C-terminal region physically binds calmodulin as shown by calmodulin overlay blotting and mutation analysis. (*a*) (*Left*) Coomassie blue-stained acrylamide gel of protein extracts from *E. coli* cells expressing either fusions of GST to indicated residues of kendrin or GST alone. (*Right*) Calmodulin overlay blot showing specific binding of protein A-tagged calmodulin to the GST-kendrin (3158–3321) fusion protein. Arrows indicate the position of the full-length GST-kendrin fusion protein (3158–3321), which binds calmodulin. A fusion between GST and a coiled-coil region of kendrin does not bind calmodulin, nor does GST alone. (*b*) Same as in *a*, but comparing binding of calmodulin to GST-kendrin (3158–3321) fusion protein (CTL, control fragment) and a GST-kendrin (3158–3321) fusion protein (MUT, mutagenized fragment) containing five alanine substitutions in residues predicted to be crucial for calmodulin binding. Positions of alanine substitution mutations shown in Fig. 1*a*.

strips were used to stain human diploid fibroblasts in parallel at a final dilution of 1:800.

For standard immunofluorescence microscopy, cells were imaged by using a Zeiss Axioplan microscope with 40× and 100× objectives and an Optivar set at 1.25. Images were captured by using Imagepoint or Quantix cooled charge-coupled device (CCD) video cameras (Photometrics, Tucson, AZ). For deconvolution immunofluorescence microscopy (Fig. 2*k*), cells prepared as described above were imaged by using a Zeiss Axiovert microscope with a 63× objective. The images were captured by using a Quantix-LC cooled CCD video camera (Photometrics) and analyzed by using DELTAVISION software (Applied Precision, Issaquah, WA). Fig. 3*k* shows a projection of the seven sections containing kendrin and centrin (centriolar) staining.

Results and Discussion

To identify vertebrate proteins similar to yeast Spc110p, we aligned the calmodulin-binding site of budding yeast Spc110p with the calmodulin-binding sites of two Spc110p homologues identified in the filamentous fungus *Aspergillus nidulans* and the fission yeast *Schizosaccharomyces pombe* (Fig. 1*a*). These calmodulin site sequences share homology with one another (Fig. 1*a*) but are distinct from the IQ-type calmodulin-binding site in myosins [consensus (I/V/L)Qxxx(R/K)Gxxx(R/K), (22)]. EST database searches using these calmodulin-binding site sequences identified two murine EST clones and a related human EST clone. We used the human EST clone to probe a cDNA library and identified a large cDNA predicted to encode a protein named kendrin.

Kendrin contains two long central regions predicted to form coiled-coils (amino acid residues 256–1874 and 2559–3075) flanked by noncoiled regions (Fig. 1*b*). The noncoiled N-terminal domain and the first coiled-coil region of kendrin (amino acid residues 1–2250) share striking homology with murine pericentrin, a centrosome component that binds γ-tubulin (5) (global alignment score = 5954, 61% identity; Fig. 1*c*). The C-terminal 1071 amino acids of kendrin containing the calmodulin-binding site show no significant homology to pericentrin (global alignment score = −757). Northern blotting revealed that full-length kendrin is encoded by a 10-kb transcript. A related 7.5-kb transcript encoding the portion of kendrin homologous to pericentrin was also detected (Fig. 1*d*).

Although early reports labeled human kendrin as human pericentrin (23, 24), three lines of evidence indicate that kendrin and pericentrin are different proteins encoded by different genes. First, both mouse and human kendrin ESTs[9] contain sequences that are not present in the murine pericentrin cDNA (25). Conversely, mouse and human pericentrin ESTs (defined as those corresponding to a unique 3′ untranslated region in murine pericentrin)[9] contain sequences that are not present in kendrin cDNA. Second, human pericentrin is not encoded at the human kendrin locus. Kendrin has been mapped to chromosome 21 (21q22.3), and genomic sequence from this region includes 247 kb immediately downstream of the kendrin locus.[9] This region appears to contain two additional genes (S100 and an unidentified ORF); however, the sequence for the human pericentrin ESTs is not present. A final line of evidence comes from a comparison of the predicted kendrin and pericentrin proteins. If kendrin were simply a version of pericentrin with a long extension, we would predict that the shared N-terminal 2250 amino acids would closely resemble or be identical to one another. In contrast, kendrin shows a mosaic of regions sharing high homology with murine pericentrin (>80% identity), interspersed with multiple segments that share little or no sequence similarity (e.g., 186 residue segment with <22% conservative replacements; Fig. 1*c*). Thus, mouse and human appear to contain two different genes, at different chromosomal loci, one encoding pericentrin and the other encoding kendrin.

The unique C-terminal region of kendrin directly binds calmodulin, as shown by protein A-calmodulin overlay blotting (Fig. 2*a*). Alanine mutagenesis of five residues in the predicted calmodulin-binding site (Fig. 1*a*) dramatically decreased calmodulin binding (Fig. 2*b*), confirming that calmodulin-binding activity maps to the residues predicted by sequence analysis. The five mutated residues were chosen on the basis of their conservation (Fig. 1*a*) and their importance predicted from previously characterized families of calmodulin-binding sites catalogued by Dr. M. Ikura and coworkers (http://calcium.oci.utoronto.ca/ctdb/). Thus, calmodulin binding to kendrin is disrupted by mutations in five conserved residues of the predicted calmodulin-binding site.

To better understand the *in vivo* function of kendrin, we examined the subcellular localization of kendrin throughout the cell cycle in primary human diploid fibroblasts and in human cancer cell lines that demonstrate abnormal centrosomal structures (26). In diploid fibroblasts, antibodies raised against a unique fragment of the kendrin C terminus (amino acids 2628–2969; Fig. 1*b*) recognized centrosomes, but not microtubules, in both mitotic (Fig. 3 *a–d*) and interphase (Fig. 3 *e–h*) cells costained for γ- or α-tubulin. In control experiments, depletion of anti-kendrin antibodies eliminated staining of centrosomes

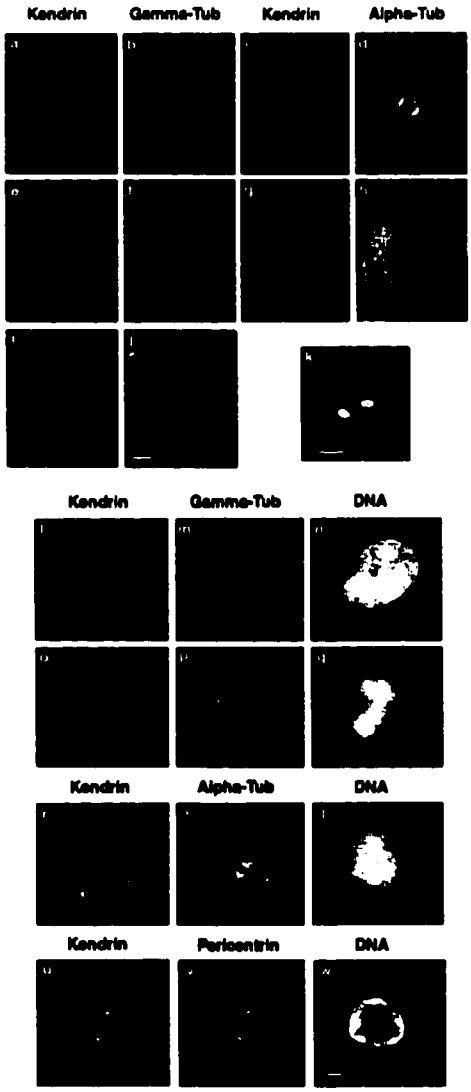

Fig. 3. Kendrin localizes to centrosomes throughout the cell cycle and is restricted to spindle poles in mitotic cancer cells. (*a* and *b*) Colocalization of kendrin and γ-tubulin at centrosomes in a human diploid fibroblast transiting mitosis. (*c* and *d*) Kendrin labels the poles of the spindle apparatus in a mitotic fibroblast. (*e* and *f*) Colocalization of kendrin and γ-tubulin at an interphase fibroblast centrosome. (*g* and *h*) Localization of kendrin at an interphase fibroblast centrosome near the rim of the nucleus, from which cytoplasmic microtubules are excluded. (*i*) Depletion of anti-kendrin antibodies eliminates staining of the centrosome, which has been labeled in the same cell by anti-γ-tubulin antibodies (*j*). (*k*) Kendrin (red) localizes in close proximity to paired centrioles (green), labeled with anti-centrin antibodies (21). (*l–n*) Colocalization of kendrin and γ-tubulin to multiple centrosomal structures in an interphase HS578T breast cancer cell with uncondensed DNA. (*o–q*) A mitotic HS578T cancer cell containing condensed chromatin in which kendrin is restricted to spindle poles, whereas γ-tubulin labels both spindle poles and extra centrosomal structures. (*r–t*) Kendrin at all poles of a tetrapolar spindle in a HS578T cancer cell attempting mitosis; the kendrin focus at the lower right in *r* was visible in a separate focal plane and was digitally merged with the focal plane containing the other three kendrin foci. (*u–w*) Colocalization of kendrin and pericentrin in a mitotic HS578T cancer cell containing condensed DNA. (Size bar in *j*, 10 μm, applies to *a–j*; size bar in *k*, 1 μm; size bar in *w*, 5 μm, applies to *l–w*.)

(Fig. 3 *i* vs. *j*), whereas selective removal of anti-GST antibodies did not diminish centrosomal staining (not shown). Also, in diploid fibroblasts, immunofluorescence microscopy in combination with optical sectioning and deconvolution localized kendrin in close proximity to the distal portion of the centrioles stained by anti-centrin antibodies (Fig. 3*k*).

In interphase HS578T breast carcinoma cells, kendrin colocalized with γ-tubulin to multiple aberrant centrosomal structures (226/237 foci or 95%; Fig. 3 *l* and *m*). Colocalization of kendrin and γ-tubulin to more than two structures was observed in 90% of cells (52/58 cells; Fig. 3 *l* and *m*). In striking contrast, a majority of mitotic HS578T breast cancer cells demonstrated a restriction of kendrin staining to two dots at the mitotic spindle poles (52/67 cells or 78%; Fig. 3*o*). Costaining for kendrin and α-tubulin revealed that mitotic HS578T cells containing two dots of kendrin staining formed normal bipolar mitotic spindles (52/52 cells). Although γ-tubulin localized to all structures in mitotic cells that contain kendrin (151/151 foci), the converse was not true: a majority of mitotic cells exhibited additional structures containing γ-tubulin but not kendrin (43/67 cells or 64%; Fig. 3*p*). A smaller fraction of mitotic cells had one, three, or greater than three structures containing kendrin (15/59 cells or 25%), and all of these cells formed aberrant, multipolar spindles (15/15 cells, Fig. 3 *r–t*). In mitotic breast cancer cells costained for kendrin and α-tubulin, every focus of kendrin staining was associated with microtubules (59/59 cells, 127/127 foci). Finally, in mitotic breast cancer cells, every focus of kendrin contained pericentrin (131/131 foci, Fig. 3 *u–w*), even in cells containing abnormal numbers of kendrin foci. Thus, our localization data indicate that kendrin and pericentrin, but not γ-tubulin, are restricted to centrosomes at mitotic spindle ends in mitotic breast cancer cells. We have observed similar localization patterns for kendrin in mitotic colon cancer cells (not shown), indicating that kendrin localization is consistent in different types of human cancer cells.

In summary, several lines of evidence indicate that kendrin is a human orthologue of budding yeast Spc110p. Spc110p and kendrin share similar predicted protein structures and localize to analogous structures, the SPB (27) and centrosome, respectively. The N-terminal region of Spc110p binds the γ-tubulin complex (9, 10), and the N-terminal region of kendrin is highly homologous to murine pericentrin, which binds γ-tubulin as shown by coimmunoprecipitation, copurification, colocalization, and fluorescence resonance energy transfer experiments (5). The C-terminal region of Spc110p binds core SPB components (28, 29), and kendrin localizes near centrioles at the vertebrate centrosomal core. Finally, the C-terminal regions of Spc110p (27) and kendrin each contain a distinct calmodulin-binding site that targets Spc110p to the SPB (11–13) and that may target kendrin to spindle poles.

The distinct subcellular localization pattern of kendrin in interphase and mitotic cancer cells is consistent with kendrin playing an essential role in regulating the formation of spindle microtubules. Kendrin is tightly restricted during mitosis to the poles of the mitotic spindle in cancer cells containing extra centrosomal material, and all mitotic cancer cells containing tri- and tetrapolar spindles contained three or four kendrin foci, respectively, at the abnormal spindle poles. Kendrin may regu-

late spindle formation by recruiting pericentrin and γ-tubulin to nascent spindle poles.

Recently, a similar role has been suggested for the *Drosophila melanogaster* abnormal spindle protein (Asp). Asp, a centrosomal protein containing potential calmodulin-binding sites (30), appears to regulate the mitotic spindle apparatus by tethering γ-TURCs together (31). Despite the similarities between Asp and kendrin, the functions of these two proteins are likely distinct. Kendrin and Asp share no homology with one another, whereas kendrin is clearly related to pericentrin, which interacts with γ-tubulin (5). The predicted structure of kendrin, like that of Spc110p, contains long central coiled-coil domains flanked by noncoiled ends, whereas the secondary structure of Asp is predicted to be primarily α-helical with short stretches of coiled-coil near its C terminus (30). Additionally, Asp is predicted to contain an actin-binding domain (30), a feature found in neither kendrin nor Spc110p. The calmodulin-binding site of kendrin is similar to that of *S. cerevisiae* Spc110p and of the Spc110p homologues we identified in *A. nidulans* and *S. pombe*, whereas the IQ-type calmodulin-binding site of Asp is more similar to those found in myosins. Finally, Asp localizes to both the centrosome and the spindle and was initially purified as a microtubule-associated protein (30), whereas kendrin is restricted to the centrosome, as is Spc110p. These differences indicate that the activities of kendrin may be more similar to those of Spc110p than to those of Asp. Further analysis of the functional relationships among kendrin, pericentrin, γ-tubulin, and Asp will shed light on the mechanisms controlling the complex process of mitotic spindle formation and should aid in the understanding of centrosomal abnormalities that accompany cancerous growth.

We thank James Joseph and Anthony Means for providing data before publication, Steve Doxsey for antibodies to pericentrin, and Shannon Payne for human breast carcinoma lines. We would also like to thank Susan Francis, Eric Muller, Breck Byers, and David Morris for helpful comments on the manuscript. This work was supported by National Institutes of Health Grant R01 GM40506 (to T.N.D.), Training Grant T32 GM-07270-22 (to M.R.F.), and Grants R01 CA48022 and P01 AG01751 (to R.J.M. and M.J.M.).

1. Zheng, Y., Wong, M. L., Alberts, B. & Mitchison, T. (1995) *Nature (London)* **378**, 578–583.
2. Oegema, K., Wiese, C., Martin, O. C., Milligan, R. A., Iwamatsu, A., Mitchison, T. J. & Zheng, Y. (1999) *J. Cell Biol.* **144**, 721–733.
3. Moritz, M., Braunfeld, M. B., Sedat, J. W., Alberts, B. & Agard, D. A. (1995) *Nature (London)* **378**, 638–640.
4. Khodjakov, A. & Rieder, C. L. (1999) *J. Cell Biol.* **146**, 585–596.
5. Dictenberg, J. B., Zimmerman, W., Sparks, C. A., Young, A., Vidair, C., Zheng, Y., Carrington, W., Fay, F. S. & Doxsey, S. J. (1998) *J. Cell Biol.* **141**, 163–174.
6. Purohit, A., Tynan, S. H., Vallee, R. & Doxsey, S. J. (1999) *J. Cell Biol.* **147**, 481–492.
7. Moritz, M., Zheng, Y., Alberts, B. M. & Oegema, K. (1998) *J. Cell Biol.* **142**, 775–786.
8. Schnackenberg, B. J., Khodjakov, A., Rieder, C. L. & Palazzo, R. E. (1998) *Proc. Natl. Acad. Sci. USA* **95**, 9295–9300.
9. Knop, M. & Schiebel, E. (1997) *EMBO J.* **16**, 6985–6995.
10. Nguyen, T., Vinh, D. B. N., Crawford, D. K. & Davis, T. N. (1998) *Mol. Biol. Cell* **9**, 2201–2216.
11. Sundberg, H. A., Goetsch, L., Byers, B. & Davis, T. N. (1996) *J. Cell Biol.* **133**, 111–124.
12. Kilmartin, J. V. & Goh, P. Y. (1996) *EMBO J.* **15**, 4592–4602.
13. Stirling, D. A., Rayner, T. F., Prescott, A. R. & Stark, M. J. (1996) *J. Cell Sci.* **109**, 1297–1310.
14. Kilmartin, J. V., Dyos, S. L., Kershaw, D. & Finch, J. T. (1993) *J. Cell Biol.* **123**, 1175–1184.
15. Willingham, M. C., Wehland, J., Klee, C. B., Richert, N. D., Rutherford, A. V. & Pastan, I. H. (1983) *J. Histochem. Cytochem.* **31**, 445–461.
16. Zavortink, M., Welsh, M. J. & McIntosh, J. R. (1983) *Exp. Cell. Res.* **149**, 375–385.
17. Li, C. J., Heim, R., Lu, P., Pu, Y., Tsien, R. Y. & Chang, D. C. (1999) *J. Cell Sci.* **112**, 1567–1577.
18. Tassin, A. M., Celati, C., Paintrand, M. & Bornens, M. (1997) *J. Cell Sci.* **110**, 2533–2545.
19. Berger, B., Wilson, D. B., Wolf, E., Tonchev, T., Milla, M. & Kim, P. S. (1995) *Proc. Natl. Acad. Sci. USA* **92**, 8259–8263.
20. Stirling, D. A., Petrie, A., Pulford, D. J., Paterson, D. T. & Stark, M. J. (1992) *Mol. Microbiol.* **6**, 703–713.
21. Salisbury, J. L., Baron, A. T. & Sanders, M. A. (1988) *J. Cell Biol.* **107**, 635–641.
22. Rhoads, A. R. & Friedberg, F. (1997) *FASEB J.* **11**, 331–340.
23. Chen, H., Gos, A., Morris, M. A. & Antonarakis, S. E. (1996) *Genomics* **35**, 620–624.
24. Lapenta, V., Sosa, V., Gosset, P., Vaysettes, C., Vitali, T., Rabatel, N., Tassone, F., Blouin, J. L., Scott, H. S., Antonarakis, S. E., *et al.* (1998) *Genomics* **49**, 1–13.
25. Doxsey, S. J., Stein, P., Evans, L., Calarco, P. D. & Kirschner, M. (1994) *Cell* **76**, 639–650.
26. Pihan, G. A., Purohit, A., Wallace, J., Knecht, H., Woda, B., Quesenberry, P. & Doxsey, S. J. (1998) *Cancer Res.* **58**, 3974–3985.
27. Geiser, J. R., Sundberg, H. A., Chang, B. H., Muller, E. G. & Davis, T. N. (1993) *Mol. Cell. Biol.* **13**, 7913–7924.
28. Adams, I. R. & Kilmartin, J. V. (1999) *J. Cell Biol.* **145**, 809–823.
29. Elliott, S., Knop, M., Schlenstedt, G. & Schiebel, E. (1999) *Proc. Natl. Acad. Sci. USA* **96**, 6205–6210.
30. Saunders, R. D., Avides, M. C., Howard, T., Gonzalez, C. & Glover, D. M. (1997) *J. Cell Biol.* **137**, 881–890.
31. do Carmo Avides, M. & Glover, D. M. (1999) *Science* **283**, 1733–1735.

MARK R. FLORY
VITA

EDUCATION

- Ph.D., Program in Molecular and Cellular Biology (December, 2000)
- B.S. Biology, Chemistry minor, *Summa Cum Laude* with Departmental Honors, University of Richmond, VA (May, 1994)

HONORS

- Benjamin Schultz Research Award in Biochemistry (2000)
- Molecular and Cellular Biology Training Grant (1995-1998)
- Developmental Biology Training Grant (1995, declined)
- Phi Beta Kappa, University of Richmond (1994)
- Most Outstanding Student, Natural Sciences, Univ. of Richmond (1994)
- Oldham Scholar, University of Richmond (1990-1994)

PUBLICATIONS

Flory, M.R. and T.N. Davis. 2001. Analysis the relationship between human kendrin and mouse pericentrin, manuscript in preparation.

Flory, M.R., Joseph, J., Morphew, D.M., McIntosh, J.R., Means, A.R. and T.N. Davis. 2001. Pcp1p, a fission yeast centrosomal calmodulin whose overexpression results in spindle defects, DNA missegregation, and extra centrosome-like structures, manuscript submitted.

Flory, M.R., Moser, M.J., Monnat, R.J. and T.N. Davis. 2000. Identification of a human centrosomal calmodulin-binding protein that shares homology with pericentrin. *PNAS* 97(11):5919-23.

Flory, M.R. and T.N. Davis. 1998. Localization of calmodulin in budding yeast and fission yeast using GFP. *Meth. Enzymol.* 302(ch.10):87-102.

Moser, M.J.*, Flory, M.R.*, and T.N. Davis. 1997. Calmodulin localizes to the spindle pole body of *Schizosaccharmocyes pombe* and performs an essential function in chromosome segregation. *J. Cell Sci.* 110(15):1805-12. (*, both authors contributed equally)